Chapter 5

PLANETARY CRUSTS

The terrestrial planets have developed crusts that differ in chemical composition from their interiors, and from their bulk composition. This was remarked upon long ago for the Earth. This process shows remarkable diversity among those planets and satellites of which we have detailed knowledge. When the lunar samples were examined, the crustal composition of the Moon was found to be so highly differentiated that models involving heterogeneous accretion were invoked, plastering on a layer of refractory material as the last episode of forming the Moon. Such models were in direct contrast to earlier views that the Moon might be a primitive object. The surface of Mars, Mercury and Venus likewise turned out to be different from reasonable estimates of their bulk compositions and accordingly the study of planetary crusts received impetus. Crustal development is an expression of planetary differentiation, which in turn is driven by mass, volatile content, radioactive heat sources, initial accretion energy and many other factors. Crusts may develop early or grow slowly through time. In the examples with which we are familiar—Earth, Moon, Mars, Mercury, Venus, Galilean and Saturnian satellites (in decreasing order of knowledge)—their crustal compositions depart, sometimes to an extreme degree, from our concepts of solar nebula compositions.

Models involving the late accretion of differentiated material have fallen into disfavor. It has now become clear that such surficial crusts on planets may arise in two ways, either as a consequence of early melting and differentiation, or by derivation from the planetary mantles by partial melting long after accretion, this time being measured in billions of years. The highland

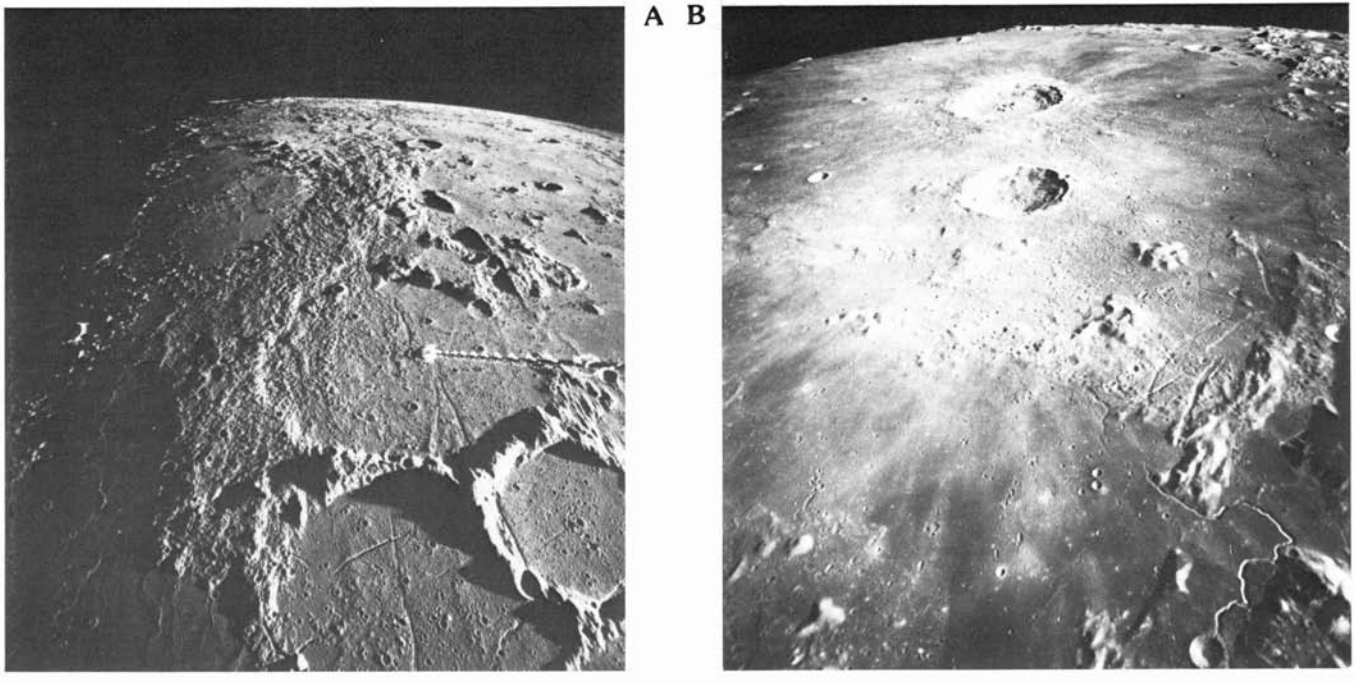

5.1 The four Apollo landing sites where the lunar highland crust was directly sampled. **a.** Apollo 14, on the ejecta blanket from Imbrium. The spacecraft boom points to the center of Fra Mauro crater, 95 km diameter. The landing site was northwest of the crater rim (NASA AS-16-1420). **b.** Apollo 15 site, showing Hadley Rille, 1 km wide, adjacent to the Apennines Mountains. The prominent craters are Autolycus (diameter, 39 km) and Aristillus (55 km diameter)(NASA AS 15–1537).

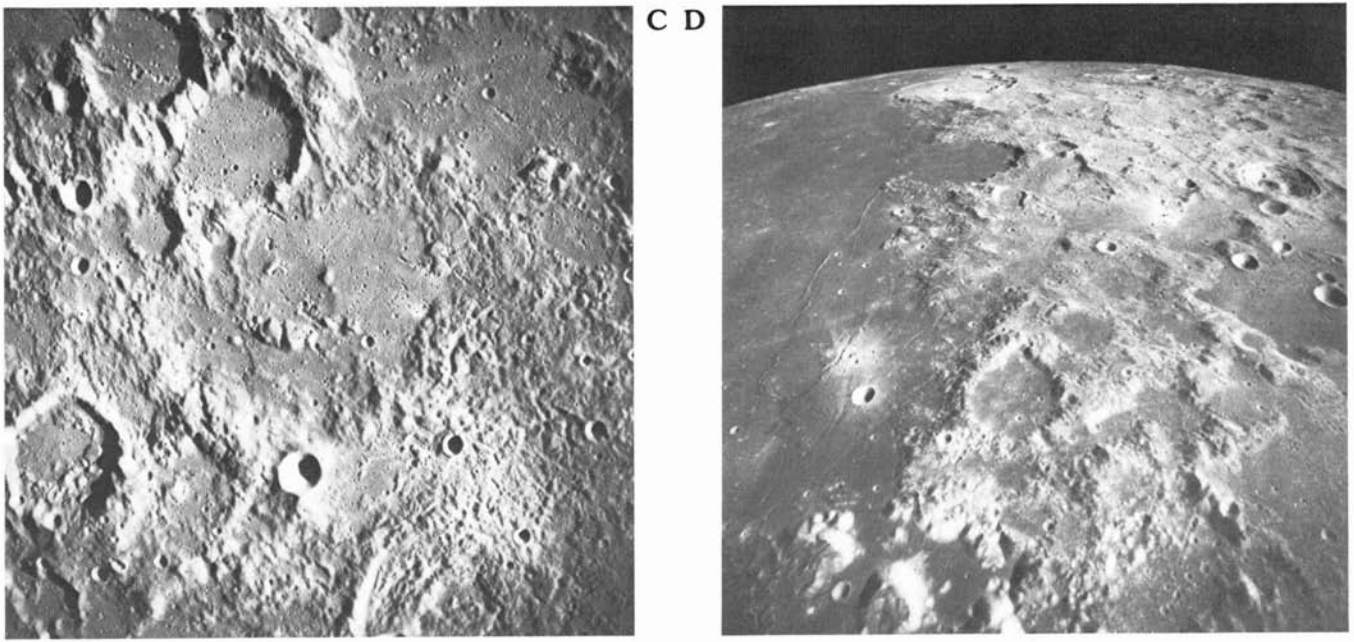

c. The Apollo 16 site showing the smooth plains of the Cayley formation to the left of the landing site and the hilly Descartes formation to the right (east). The bright white dot is South Ray Crater just south of the landing site. The diameter of Dollond B, the large crater floored with Cayley formation, in the northwest quadrant, is 37 km in diameter (NASA A–16 metric 539, 540). **d.** The Apollo 17 landing site in the Taurus-Littrow Valley, bottom left. The landslide from the South Massif is clearly visible. Littrow is the large degraded crater (31 km diameter) north-northeast of the landing site. Mare Serenitatis occupies the left side of the picture. The large crater, north center embayed and flooded with basalt, is Le Monnier, site of Lunokhod 2 mission. The large crater beyond Le Monnier is Posidonius, 95 km in diameter. Note the dark basalts near the Apollo 17 site, and the wrinkle ridges and rilles in the mare.

crust of the Moon represents a well-studied example of the first type, while the continental crust of the Earth is a familiar example of the second process.

The continental crust of the Earth, as distinct from the oceanic crust, is uniquely useful in providing a platform on which the later stages of evolution could occur and from which we can study the development of the planets [1]. Our understanding of the composition and evolution of the Earth's crust is slowly growing. It is an interesting commentary that we understand the formation of the lunar crust to a rather better degree. Accordingly, in this chapter, a large section is devoted to the highland crust of the Moon, both because it differs in nearly all respects from the continental crust of the Earth and because it provides us with a key to understanding the crusts on other planets.

The section on the continental crust of the Earth is brief, since adequate extended accounts are available (e.g., [2]). It would be a disservice to the reader to attempt a summary of these, and only some highlights are noted with an emphasis on chemical composition and crustal evolution which are especially relevant here.

5.1 The Lunar Highland Crust

The highland crust forms the oldest accessible area on the Moon and is saturated with ringed basins and large craters (Chapter 3). All of the original crustal structure has been obliterated. The complexity of the highland samples constitutes a severe test for the scientific method of inductive reasoning, proceeding from the details to construct a general theory. Workers on these samples, which have endured countless meteorite impacts, must guard against the charms of the deductive approach, deriving the details from a general theory in the manner of medieval scholars, before the strength of the inductive approach was realized. "Reality cannot enter . . . as an afterthought. Either it is shown due respect at the start, or it forces its way into the picture later, taking revenge on those who tried to ignore it" [3]. It is possible that the surface which we sampled dates from about 4.2–4.3 aeons (Fig. 5.1), the earliest age at which the growth of a crust solidifying from the magma ocean could outstrip destruction by the intense bombardment. The debate over the question of the ultimate origin of the highland crust, late-accreted refractory addition or derived by differentiation from within the planet, was resolved principally by geochemical data, in favor of the latter alternative.

5.1.1 Thickness and Density

Haines and Metzger [4] have used the orbital geochemical values, the lunar sample and the seismic data, to derive values for highland crustal

thickness and density. Crustal densities are calculated using the new orbital values for Fe and Mg [5]. Knowing the average elevation, and assuming isostatic equilibrium, the densities provide estimates of crustal thickness for thirty-five highland regions.

The average weighted density for the lunar highland crust obtained in this manner is 2.933 ± 0.007 g/cm^3 [4]. The near-side highlands have an average density of 2.95 g/cm^3. The far-side highlands are less dense, averaging 2.92 g/cm^3. The weighted average thickness is 73.4 ± 1.1 km, with the near-side crust averaging 64 km (with a lower Th content) while the far-side highlands average 86 km in thickness. The near-side highlands are thus 22 km thinner than the average far-side highlands. Recent revisions of the seismic data may indicate a thickness of 50 km for the near-side crust (Y. Nakamura, pers. comm., 1981). Accordingly, the average lunar crust may be closer to 60 km in thickness. This comprises 10% of lunar volume and is the conservative value adopted in most geochemical balance calculations (see Sections 5.9 and 8.4). The geochemical data indicate that lunar isostasy is controlled mainly by crustal thickness rather than by density (Fig. 5.2). The iron content is of prime importance due to its abundance (6.5–7.0% FeO) and to its high atomic weight. Haines and Metzger [4] make a number of clearly stated assumptions: (a) The crust is uniform with depth, which is one interpretation of the seismic data, and (b) the composition of the regolith is the same as that of the underlying crust. This implies that meteoritic contamination, lateral transport, and movement of very fine soil particles do not affect this assumption. Metzger noted that any correlation between elevation and chemical composition is evidence that the composition of the regolith, which was sampled by the orbital geochemical experiment, is linked to that of the crust " . . . the correspondence between chemistry, elevation, and crustal thickness provides direct proof that much of the highland surface is representative of the underlying crust" [5]. A striking observation is that all large unfilled highland basins have Fe contents similar to that of the surrounding highlands [6], which confirms crustal uniformity to the depths to which the basins have sampled. It is further assumed that (c) the upper 20 km is fractured and has a density 0.93 times that of solid rock at depth, lunar gravity being too low to compress rock at that depth [7]. P-wave velocities are less than 6 km/sec, down to 25 km, but increase to 6.8 km/sec. over about the next kilometer and then slowly increase to 7 km/sec. at 60 km depth. The reduced seismic velocities in the upper 25 km are ascribed to fracturing and brecciation.

The abrupt velocity increase at 25 km is here interpreted to indicate an absence of microcracks below that depth. The very slow increase in velocity from 25 to 60 km (only about 0.2 km/sec) is evidence of a uniform material; this velocity ($\sim$7 km/sec) is close to the intrinsic velocity of lunar samples. A final assumption that (d) the highlands are isostatically compensated is suggested by elevation and gravity data [7–9], although possibly the crustal mass

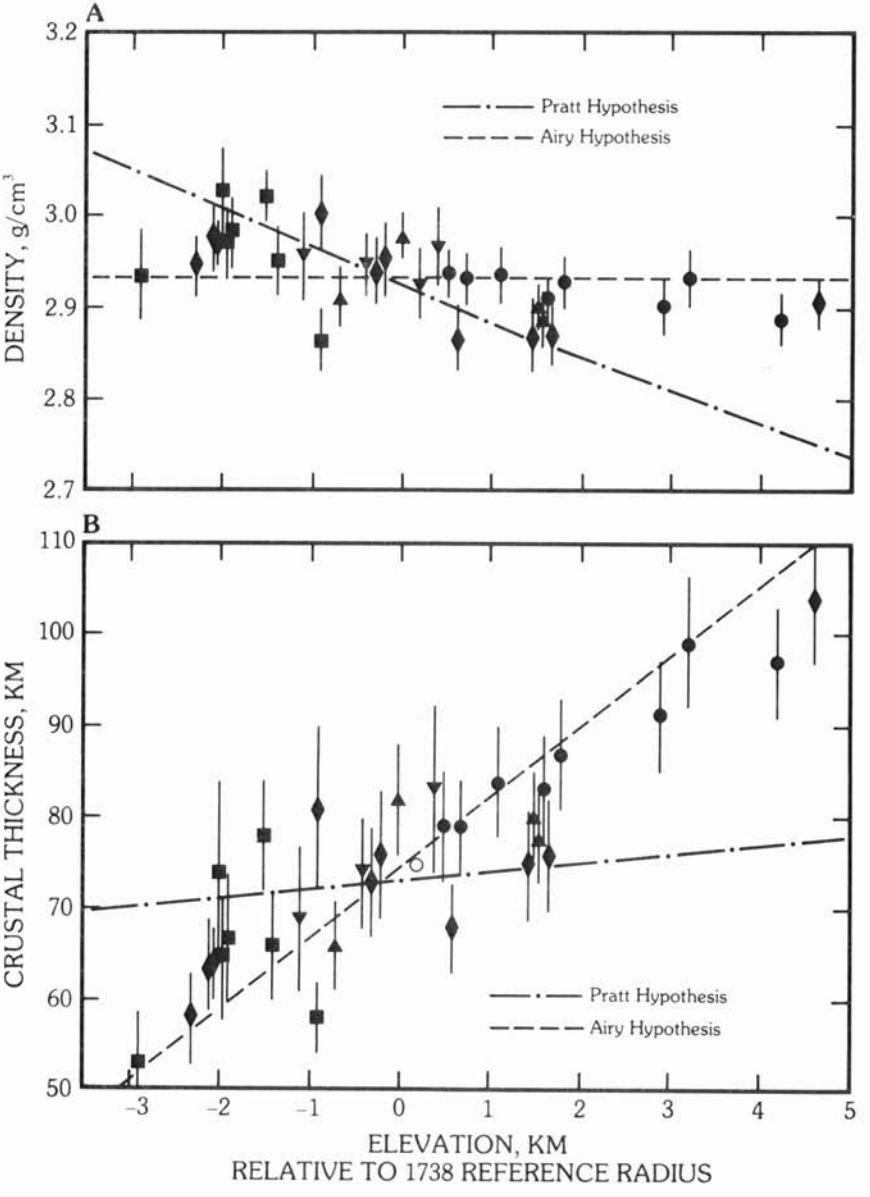

5.2a Plot of crustal density versus elevation for 33 highland regions. Trend lines are shown for the Pratt and Airy theories. Data fit the latter [4]. **b** Plot of crustal thickness versus elevation of 33 highland regions, showing that the data fit the Airy hypothesis better then the Pratt hypothesis [4].

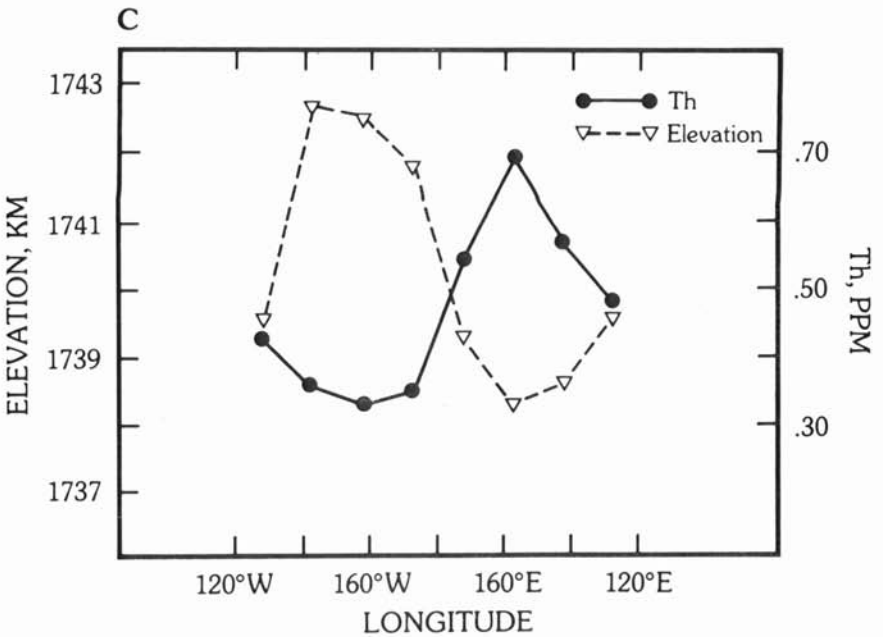

5.2c The lunar thorium concentration from orbital gamma-ray data shows an inverse correlation with elevation [5].

is not fully compensated [10]. If the crust is not compensated fully, then the crustal thickness increases for uncompensated mass deficiencies, or thins for uncompensated mass excesses [10].

Figure 5.2 shows the density and thickness versus elevation relationships for the highlands. Elevation is related to thickness, more than to density, supporting the Airy hypothesis of isostatic adjustment [11]. The alternative Pratt hypothesis [12] states that variations in elevation are due to differences in density of adjacent blocks. The geophysical data for elevation, gravity, or seismic velocity do not distinguish between these two hypotheses, nor do the data require that either hypothesis account for the lunar case. The orbital geochemical data provide a test for the hypotheses and suggest that the difference in crustal thickness is responsible for most of the differences in elevation, with only a minor contribution from the density variations. The variation in highland crustal thickness between near and far-sides is possibly a relic of early convection processes in a cooling and crystallizing magma ocean (see Section 5.11). It is considered generally to be the main contributor to the center of figure-center of mass offset [13] (Section 7.3).

The problems of studying the lunar highland crust and other early planetary surfaces center on the effects of the great bombardment. How has

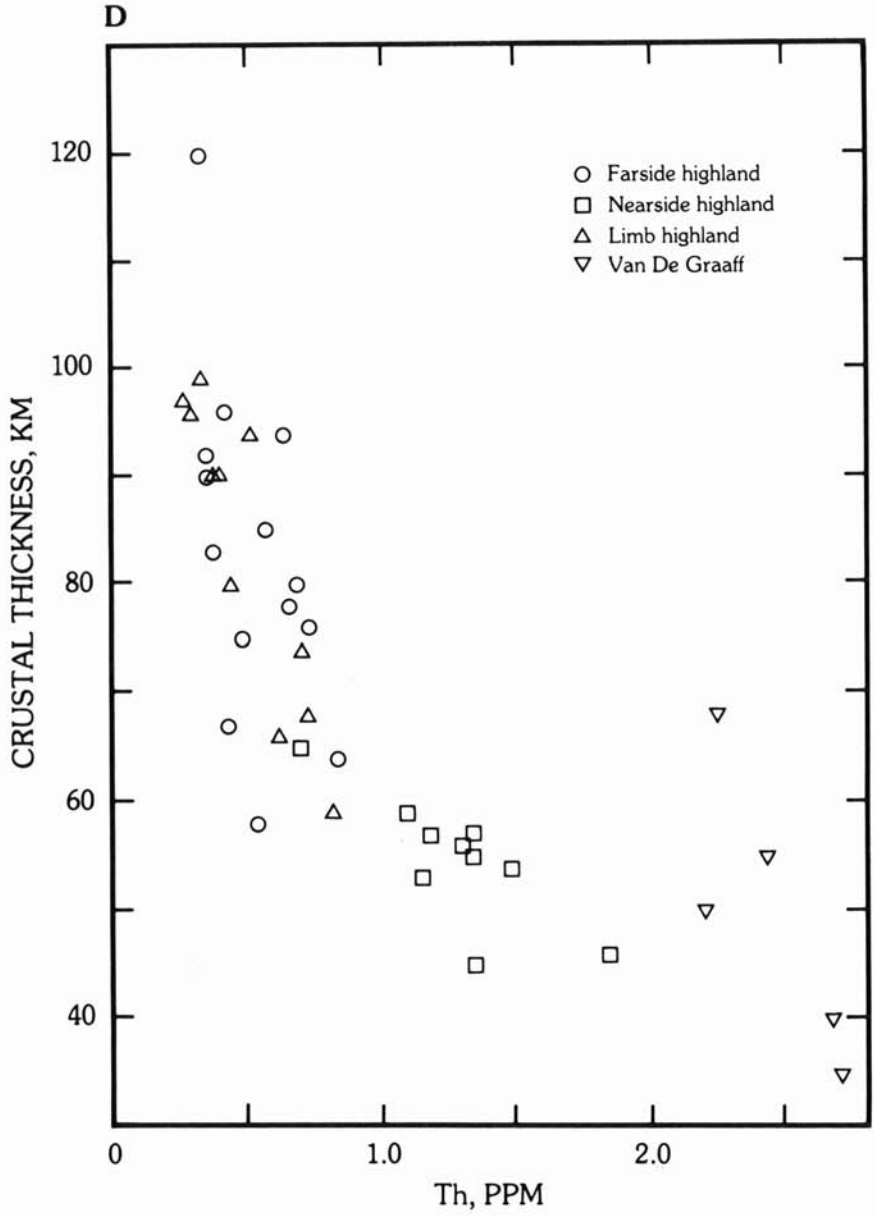

5.2d Thorium concentrations versus crustal thickness for far-side, limb, and near-side highland regions including the regions in and around Van de Graaff [5]. (Courtesy A. L. Metzger.)

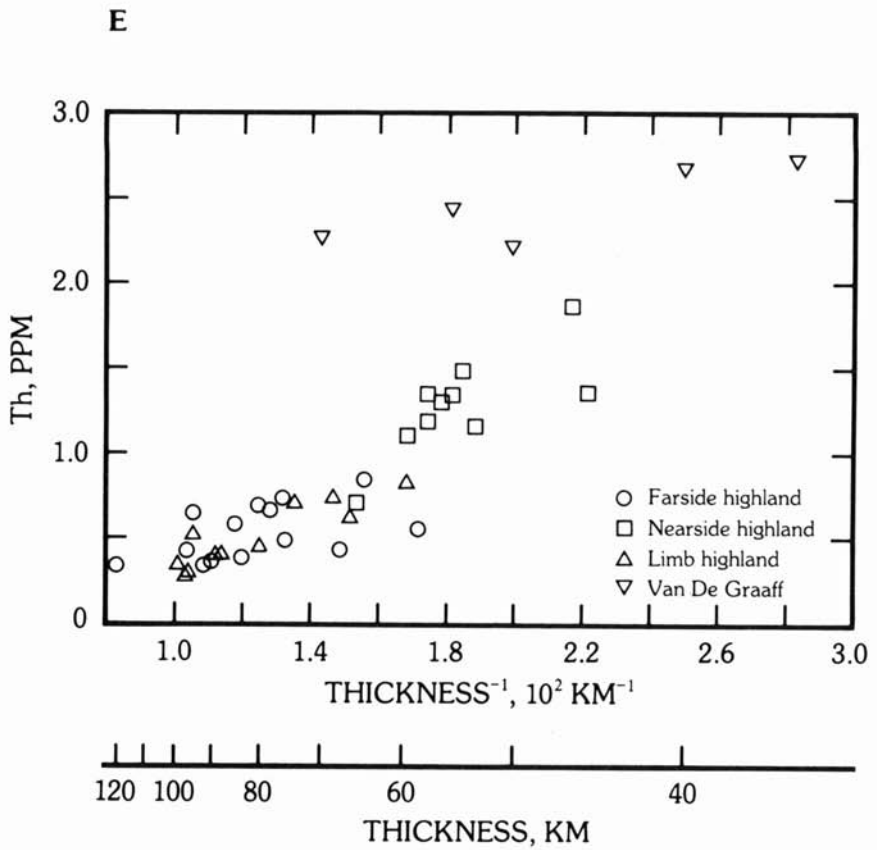

5.2e Data in Fig. 5.2d replotted against the *inverse* of the crustal thickness. If equal amounts of Th were incorporated into each crustal block and were similarly distributed with depth through each block, the relationship would show a straight line with an intercept of zero Th at infinite thickness [5]. The data approximate this theoretical relationship.

this affected the chemistry, mineralogy, petrology and age of the samples? Is any primitive crust left and, if so, can we identify samples from it? A basic question is how deeply is the crust affected by the bombardment, and from what depth do we have samples. This question was discussed in Section 3.17 from which it appears that some samples at least came from depths of from 12–32 km, and that the great basin collisions excavated to depths of 30–60 km, with the latter figure being more likely. Another effect of the formation of multi-ring basins is that mantle plugs may form beneath the centers of the basins. Such a hypothesis is required to account for the mascons (Section

7.4.2). Accordingly, the base of the highland crust may be highly irregular due to this effect, and mantle material may be excavated by subsequent impacts.

5.1.2 The Megaregolith

The present 10-m-thick regolith in the highlands overlies a zone of brecciation and fracturing due to the intense early bombardment of the highland crust. All surfaces older than about 3.8 aeons are saturated with craters 50–100 km in diameter. Most estimates for the thickness of rubble produced during these events fall within the range of 1–3 km. Some of the older mare surfaces also have been affected, and many of the early, now buried, lava flows are probably much broken up by the declining stages of the bombardment. Such fracturing would account for much of the scattering of seismic signals observed in the upper 25 km and concentrated in the upper 2 km.

A detailed model study of the evolution of the megaregolith over the earth-facing side of the Moon [14] predicts an average thickness of about 2 km, although thicknesses are less than 1 km over about 50% of this area. This study has an important corollary in that it provides evidence that the deep megaregolith will affect crater geometry by providing a two-layer structure in the highlands.

A distinct but related question deals with brecciation of the highland crust beneath the multi-ring basins. This possibly extends to depths of 20–25 km, accounting for the seismic velocity data. Additional evidence for a deep megaregolith in the highlands comes from a study of blocky craters. Fresh highland and mare craters exceeding 12 km in diameter have similar infrared and radar signatures [15], but mare craters less than 12 km in diameter exhibit anomalies which are correlated with the presence of fresh rubble ejecta, consistent with the excavation of coherent basaltic rock layers at shallow depths. In contrast, such infrared and radar signatures were less conspicuous on fresh highland craters, consistent with ejecta blankets of previously pulverized material. From the observation that highland craters greater than 12-km diameter have blocky rims, a value of 2-km thickness for the megaregolith results, which is consistent with other estimates.

This ancient megaregolith might be expected to contain some of the oldest accessible fragments of highland crust. The feldspathic fragmental or "light matrix" breccias, excavated by North Ray crater at the Descartes site might represent such material. Indeed, there is support for this view from geochronology. Very old ^{40}Ar–^{39}Ar ages (4.25 aeons) are reported for breccias [16]. The overlapping ejecta blankets probably account for the layering observed in the highlands, such as that exposed at Silver Spur and observed in other areas [17, 18].

5.2 Breccias

The possible complexities in materials subjected to repeated cratering episodes were fully revealed in the samples returned by the Apollo missions. Over 60% of the samples returned from the highlands of the Moon are breccias, most of the remainder being classified as impact melt rocks. Major efforts have been expended by petrologists and geochemists to decipher the record preserved in these breccias. The complexity of the topic, where several generations of breccias may occur within a single hand specimen, frequently accompanied by glass and remelted crystalline fragments, might daunt the most accomplished petrologist. Further problems arise as to the geological location of the material. Which of the Apollo 14 samples from Fra Mauro represent Imbrium basin ejecta and which locally derived material? Is the Apollo 15 Apennine Front composed of Serenitatis ejecta? Are the Taurus-Littrow samples from Apollo 17, on the rim of the Serenitatis basin, ejecta from that event [19] or are they derived from a complex multiple-impact sequence of events? The Apollo 16 Descartes site is located within several old barely recognizable craters, but the surface material is almost certainly younger, related to either the Nectaris or Imbrium collisions. The Cayley Formation could represent Imbrium-derived material, while the Descartes Mountains might be primarily derived from the Nectaris basin [20] or be Imbrium material piled against the Kant Plateau, or be dominated by older material ploughed up by Imbrium, Serenitatis, Crisium, Nectaris (or even Orientale) secondary projectiles.

Were the ejecta blankets hot or cold? The Apollo 14 samples were first interpreted as being derived from a hot ejecta blanket. A current view is that the percentage of Imbrium derived debris at the Apollo 14 landing site is 10–20% [20] but such interpretations are heavily based on terrestrial analogies. Nevertheless, melts from the basin impacts appear to be widespread, and occur, for example, at a distance of 630 km from the Cordillera Scarp of the Orientale basin (Section 3.9). Thus, although most of the ejecta blanket is probably at low temperature, the melted material may be more widely distributed than believed earlier, perhaps as pods or lenses within the cooler mass. As in so many scientific debates where the data are at the limit of resolution, there is some truth on either side. These questions are addressed throughout this chapter in an attempt to reach a consensus.

An important advance has been the creation of a classification system of lunar breccias [21], given in Table 5.1. Soil breccias, which form part of the classification, are discussed in Section 4.3.5. The incredible diversity and complexity of lunar highland breccias is well reflected in the terminology. A list of previous classifications, too long to reproduce, is given by Stöffler et al. ([21], Table 5, p. 62). This useful table correlates the previous terminology with that adopted here [21, 22] (Table 5.1). The production of breccias in

Table 5.1a Highland breccia classification.[†]

Breccia Group	Breccia Class	Main Textural Characteristics	Typical Examples
Monomict	Cataclastic rock	intergranular in-situ brecciation of a single lithology	60225, 65015, 67955, 72415, 78527
	Metamorphic (recrystallized) Cataclastic rock	intergranular in-situ brecciation of a single lithology and partial recrystallization	67955
Dimict	Dimict breccia	intrusive-like, veined texture of very fine-grained crystallized melt breccia within coarse-grained plutonic or metamorphic rock types	61015, 62255, 64475
Polymict	Regolith breccia or soil breccia	clastic regolith constituents including glass spherules with brown vesiculated matrix glass	10018, 14313, 15205
	Fragmental breccia	rock clasts in a porous clastic matrix of fine-grained rock debris (mineral clasts) with or without melt particles	14063, 14082, 67115, 67455, 67475
	(Crystalline) melt breccia or impact melt breccia	rock and mineral clasts in an igneous-textured matrix (granular, ophitic, subophitic, porphyritic, poikilitic, dendritic, fibrous, sheaf-like etc.); may be clast-rich or clast-poor	14310, 14312, 15455, 62235, 62295, 68415, 78235
	(Impact) glass or glassy melt breccia	rock and mineral clasts in a coherent glassy or partially devitrified matrix, with or without clasts	60095, 61016, 72215, 77135
	Granulitic breccia	rock and mineral clasts in a granoblastic to poikiloblastic matrix	15418, 67955, 73215, 77017, 78155, 79215

[†]Adapted from Stöffler, D., et al. (1980) *Lunar Highlands Crust,* p. 54, 57 (Tables 1 and 2).

Table 5.1b Shock metamorphic characteristics of lunar highland breccias.[†]

Rock Type	Degree of Shock	Estimated Peak Pressure (kbars)	Textural Characteristics
Non-porous rocks (igneous and metamorphic rocks, monomict breccias, dimict breccias, crystalline melt breccias, impact glass, granulitic breccias)	unshocked	50	primary rock texture and intragranular texture of mineral grains unchanged
	weakly shocked	5–300	intragranular fracturing and mosaic texture in all mineral constituents; planar deformation structures in feldspar pyroxene and olivine; primary rock texture unchanged
	strongly shocked	300–450	mosaic texture and planar deformation structures in mafic minerals; plagioclase changed to maskelynite, diaplectic or thetomorphic glass; primary rock texture unchanged
Porous rocks (regolith breccias, fragmental breccias)	unshocked (friable)	0–30	highly porous aggregation of breccia constituents
	shocked (coherent)	>30 mostly >100	moderate, small or lacking porosity in the matrix; mosaicism and fracturing of minerals; intergranular melt

[†]Adapted from Stöffler, D., et al. (1980) *Lunar Highlands Crust,* p. 59 (Table 4).

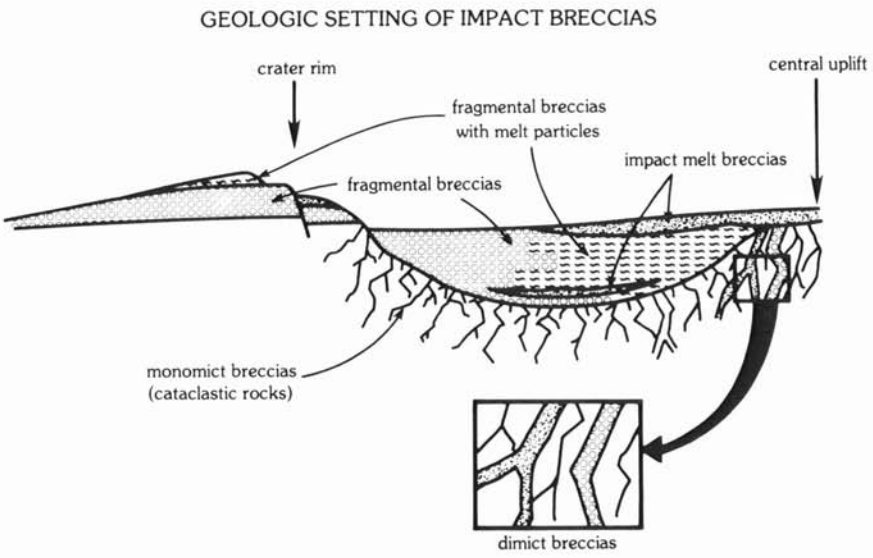

5.3 Schematic cross-section through a complex central peak crater after the crater modification stage. (Courtesy D. Stöffler, *Workshop on Apollo 16*. LPI Tech. Report No. 81-01.)

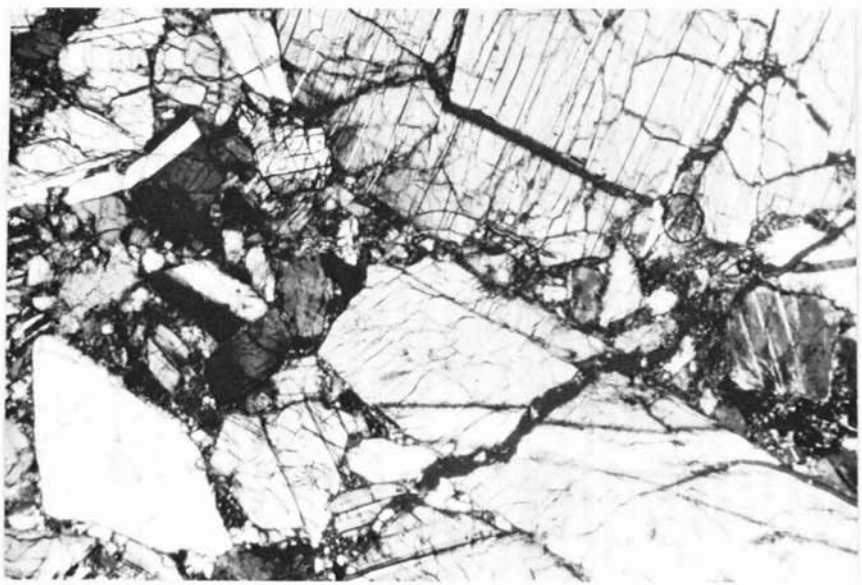

5.4a Monomict cataclastic anorthosite (lunar sample 65015,16; crossed polarizers, width of field: 0.20 mm); note intergranular brecciation [22] (Courtesy D. Stöffler.)

relation to a single impact event is shown in Fig. 5.3 [22] (see also Fig. 3.3); this work owes much to the study of terrestrial impact craters. On the Moon, the complexity of the breccias can be simulated by superimposing the situation shown in Fig. 5.3 many times at many different scales. All possible variations exist, but several distinct types may be recognized.

5.2.1 Monomict Breccias

These are composed dominantly of one rock type and are characterized by intergranular brecciation, resulting from *in situ* brecciation of single rock

5.4b Monomict cataclastic anorthosite, 15415,29 (Genesis Rock), crossed polarizers, 3 × 4 mm. (Courtesy G. Ryder.)

types, probably in the basal regions of impact events (Fig. 5.3). They are best developed in coarse grained rocks, and frequently have been referred to as cataclastic rocks (Figs. 5.4 and 5.5). These breccias probably form in craters larger than about 100 m in diameter [22] and commonly occur as clasts in breccias, lenses, and ejecta blankets. Some have been affected by later thermal metamorphism which has caused some recrystallization. This is inferred to have occurred by subsequent heating when the clasts are incorporated in hot impact melts, either in the initial, or subsequent impact events. Examples of monomict breccias include samples 65015 (anorthosite), 67955, 72415 (dunite) and 78527.

5.2.2 Dimict Breccias

As the name implies, these breccias consist dominantly of two distinct components. The most impressive examples are formed of white anorthosites and dark melt rocks. The resulting breccias, often called "black and white" rocks, are among the most striking of the large samples returned from the Moon (Figs. 5.6 and 5.7).

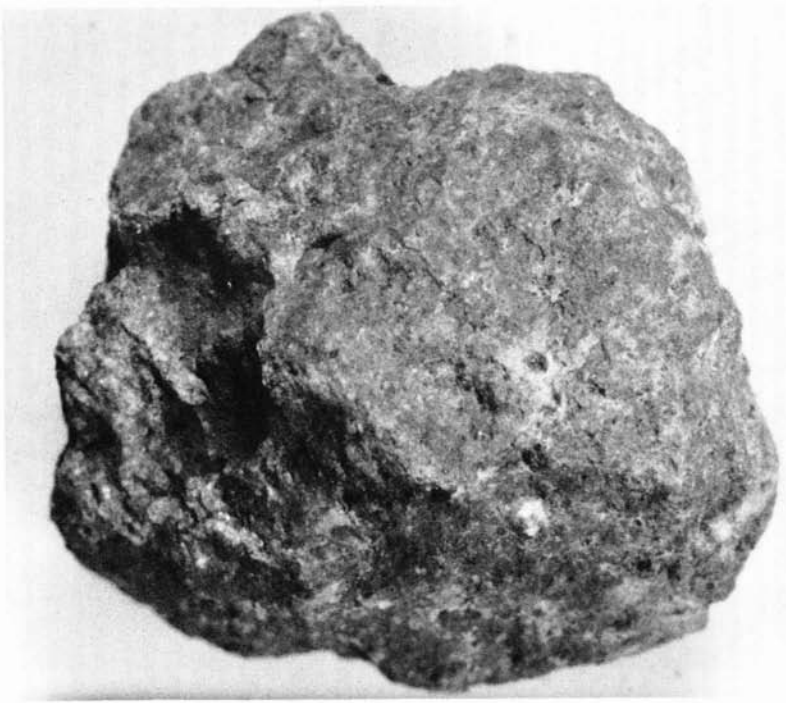

5.5 The Apollo 17 troctolite 76535, a monomict breccia (NASA S 73-19640).

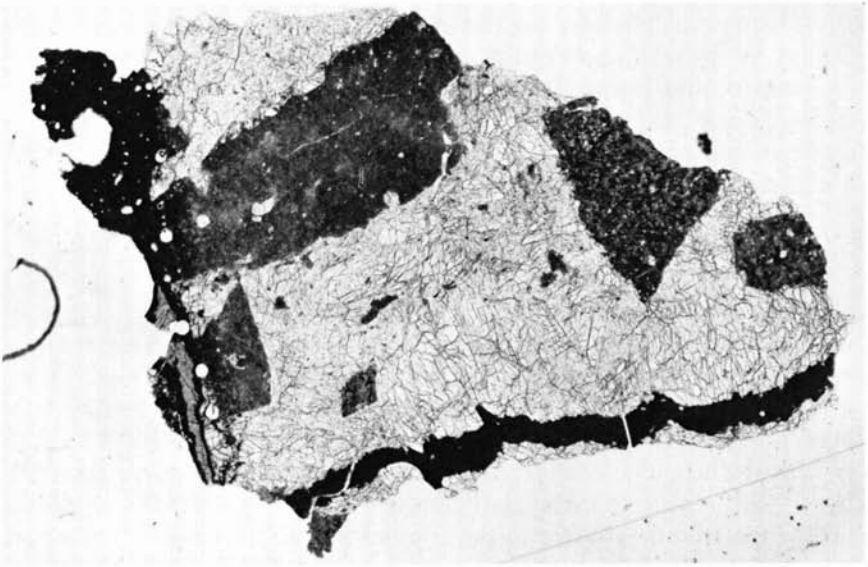

5.6 Dimict breccia 61015, with grey, intrusive material of aphanitic, crystalline matrix texture and white brecciated anorthositic "country rock." Younger "pseudotachylite" veins (black and grey with black rim) occur on two sides of the sample. Width of field = 12.5 mm [22]. (Courtesy D. Stöffler.)

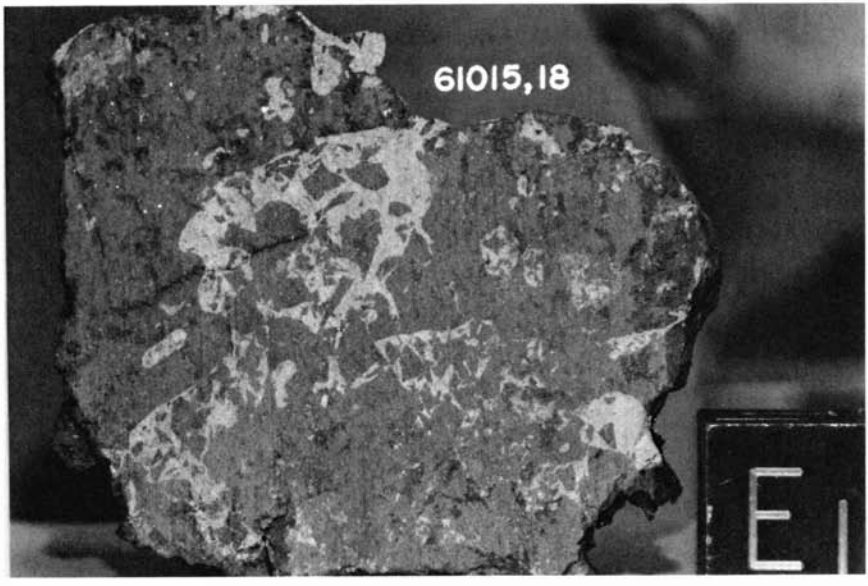

5.7 Dimict breccia 61015,18. Cube is 1 cm on side (NASA S.75 20878).

These rocks have also been referred to as "dike breccias," and probably formed by the intrusion of melt rocks into weakly shocked solid rocks. A probable location is within or near the central uplift regions of large complex craters (Fig. 5.3). The melt portions of dimict breccias appear to be rather uniform, at least for the Apollo 16 examples [23], possibly indicating formation in a single impact.

5.2.3 Feldspathic Fragmental Breccias

These lunar rocks are polymict, with several different types of clasts, set in a friable porous white feldspathic matrix. Dark melt rocks are common among the clasts, along with fragments of minerals and glass (Figs. 5.8 and 5.9). These breccias tend to be rather weakly coherent, due to the clastic matrix.

The melt-free varieties are inferred to form as shocked crater ejecta in the upper portions of the target stratigraphy, while those examples containing melted material (equivalent to the Ries crater suevite which is an impact-produced breccia containing both shock-metamorphosed rock fragments and

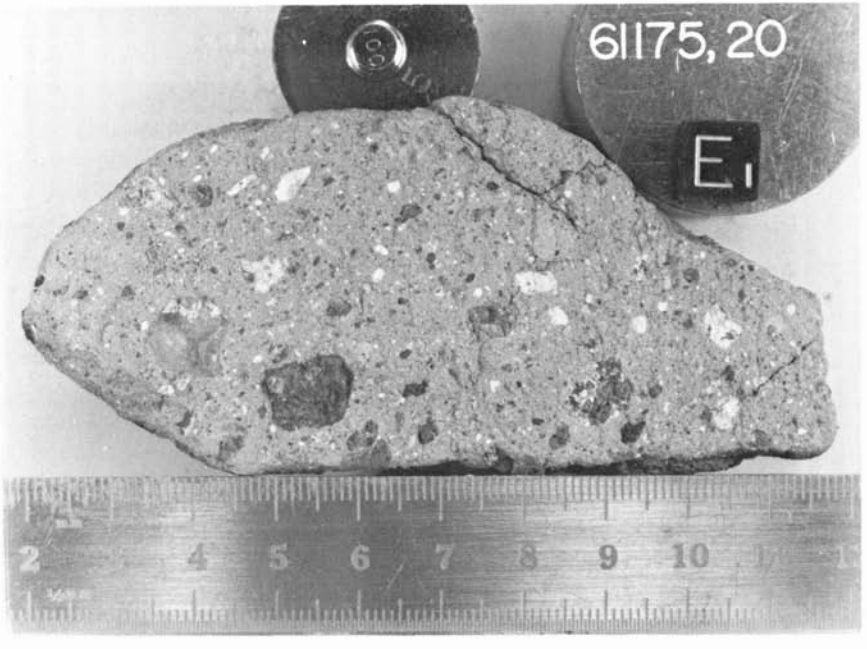

5.8 Feldspathic fragmental breccia 61175, showing a wide variety of clast types (NASA S78-31342).

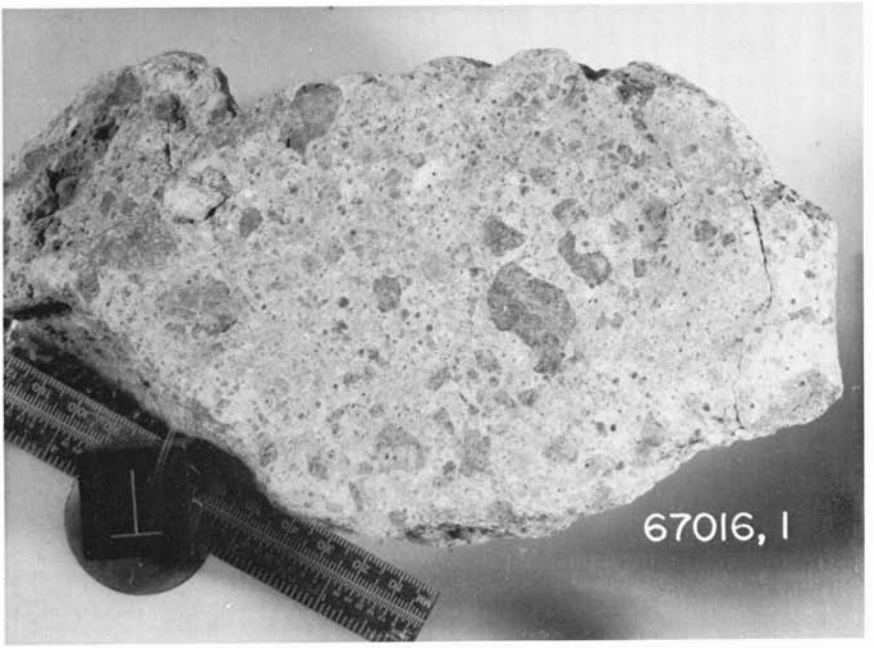

5.9 Feldspathic fragmental breccia 67016 (NASA S.81-26051).

glass bombs) come from the lower portions of the pre-crater stratigraphy. They occur in simple craters mainly as ejecta sheets outside the crater rim, or as fall-back breccia within the crater (Fig. 5.3) and form in craters larger than a few hundred meters in diameter. Examples of these include the white breccia boulders from the North Ray crater (Apollo 16: 67455, 67475). The "white rocks" at Cone crater (Apollo 14: 14063, 14082) are examples of breccias with some admixed melt material, while the Apollo 16 sample 67016 is a particularly good analogy to terrestrial suevite [24]. There is a very large compositional and textural variation in the clast populations of these breccias, indicative of rather low energy conditions during their formation.

5.2.4 Impact Melt Breccias

This class comprises the most abundant type of samples returned from the lunar highlands. Typically they consist of rock and mineral fragments set in a crystalline matrix, which has the texture of an igneous rock (Figs. 5.10 and 5.11). These rocks result from the crystallization of an impact melt laden with rock fragments resembling some of the melt-rich suevites, being transitional between the feldspathic fragmental breccias and the true impact glasses. The

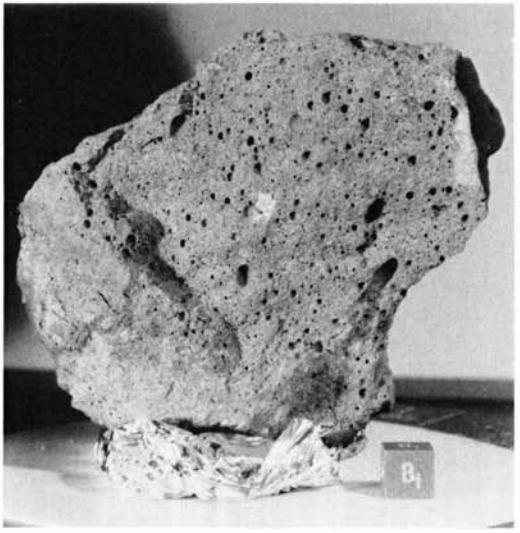

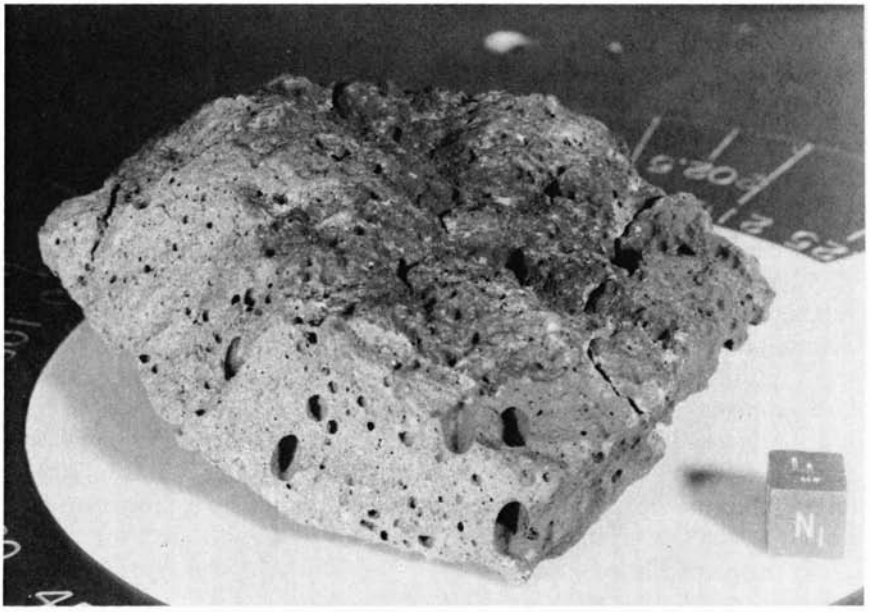

5.10a, b Highland impact melt rock 77135 showing vesicular structure (NASA S.72-56387, S.72-56391).

melt breccias are inferred to form in the deeper central part of large craters (greater than 1–5 km diameter) by shock melting, more or less below the impact point (Fig. 5.3). Various textural subtypes are recognized [25] (e.g., granular: 72215; ophitic: 61016, 62295; poikilitic: 77135).

5.11a Thin section of impact melt 68415,126. Field of view 4 × 3 mm crossed polarizers. (Courtesy G. Ryder.)

The further class of impact melts and glassy melt breccias is dealt with in Sections 3.8, 4.4.2 and 5.3. These samples comprise clast-free glasses generally occurring as clasts or coatings of breccias, in addition to their occurrence in the regolith as glasses and agglutinates (Sections 4.4.1, 4.4.2). The impact melt breccias grade into the true clast-free melt rocks (Section 5.3) and the separation of these classes is partly semantic.

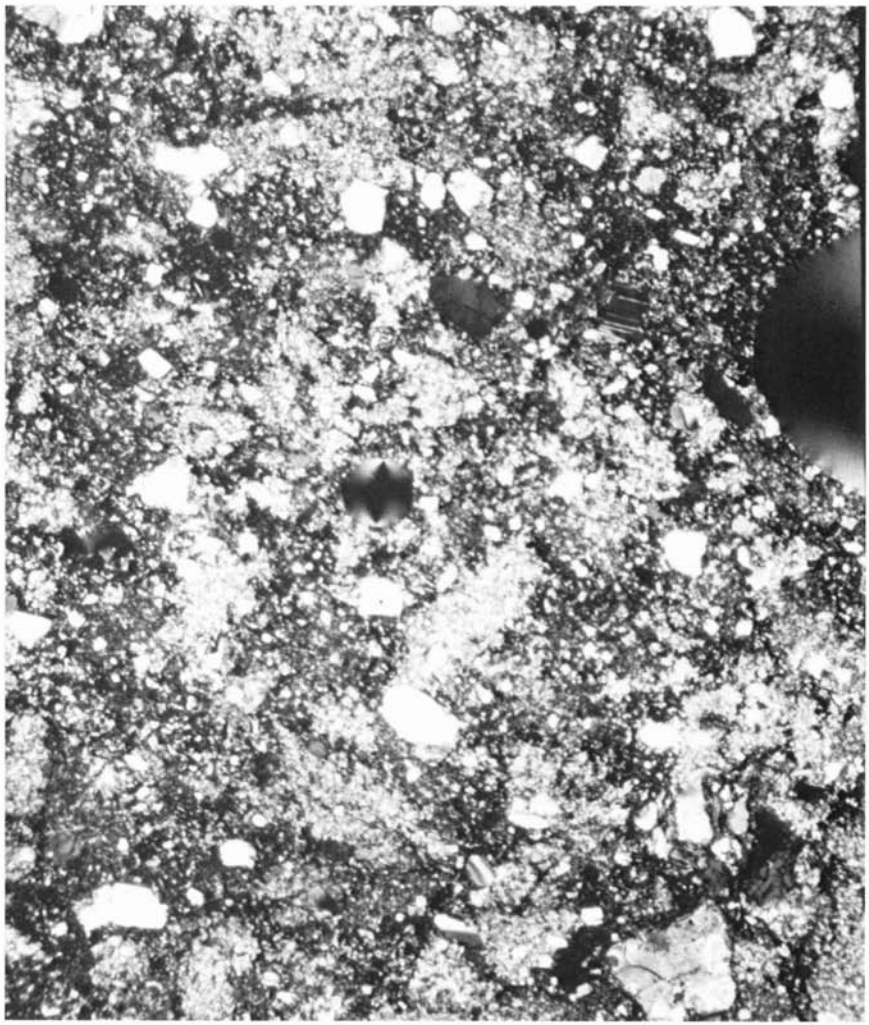

5.11b This section of impact melt rock 77135, 7 showing vesicle. Field of view 3 × 4 mm, crossed polarizers. (Courtesy G. Ryder.)

5.2.5 Granulitic Breccias

Granulitic breccias are abundant in the sample collections. They have been heated to near-melting temperatures; some are partly melted and all have recrystallized, but retain rock fragments or relics to indicate their original formation as breccias of various classes. The clasts are usually

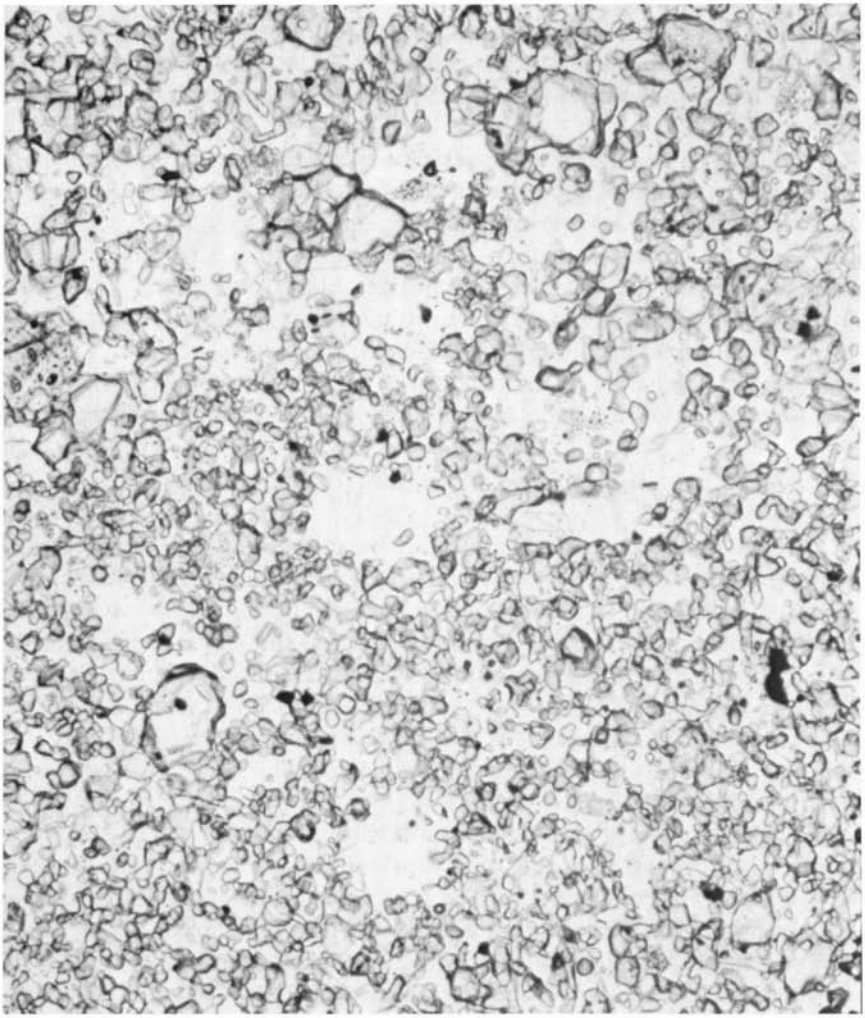

5.12 Granulitic breccia 79215,98 showing typical granoblastic or mosaic texture. Width of field 1 mm (plane polarized light). (Courtesy G. Ryder.)

recrystallized along with the matrix, which is commonly feldspathic (Fig. 5.12). These breccias have formed by thermally induced recrystallization of earlier-formed breccias at temperatures up to 900°C [26]. Many have been granulated and recrystallized several times, so that they contain breccias within breccias. Some of their compositions may approach that of the bulk composition of the crust due to this extensive reworking. Examples include

15418, 67955, 73215, 77017, 78155 and 79215. Two sources for the heat necessary to cause the metamorphic recrystallization have been suggested: (1) global metamorphism (the so-called Apollonian metamorphism) [27, 28] and (2) high temperatures from nearby lenses of impact melt trapped within the breccias [29].

Judging by terrestrial analogies, hot ejecta blankets are rare [30]. The Bunte breccia does not appear to have exceeded temperatures of 500–600° C [31]. The granulitic breccias, in contrast, appear to have been at 1000° C for an extended period, estimated by Stewart as 1–10 m.y. [27]. The implications for a crustal thermal event are considerable. It must be early, and if this hypothesis is correct, these rocks are probably the earliest fragments of crust to survive the great meteorite bombardment, and may date back to 4.2 aeons or earlier. The alternative explanation of slow cooling of local patches of impact melt avoids the global connotations of Apollonian metamorphism.

5.2.6 Basalts in Highland Breccias

Occasional fragments of basaltic composition have been returned from the highlands. Their presence has raised the question of the existence and duration of basaltic volcanism before the termination of the catastrophic bombardment at 3.8 aeons. The composition of these basalts is somewhat different from most of the common species returned from the maria proper. They are higher in Al_2O_3 (11–14%) and have lower iron contents. Their REE patterns resemble those of the VLT basalts from Luna 24 [32], and they exhibit variable Eu anomalies. Examples include 14053, 14072 and clasts from breccias 14063, 14321 and 73255 [33].

The ages of these basalts appear to be in the range of about 3.9–4.0 aeons, more or less contemporaneous with the final great meteoritic collisions (see Section 6.4.1). If volcanism had been as widespread in pre-Imbrian as in post-Imbrian time, then basaltic clasts might be expected to constitute at least one percent of the highland sample return. Their scarcity, as well as the geochemical evidence, argues against extensive pre-3.8 aeon basaltic volcanism.

Since the volcanic activity is concentrated at the surface, this estimate of the likely frequency of basaltic clasts is a minimum value. Extensive subcrustal sill and dike formation might be expected also to contribute clasts to breccias. Scenarios which call for increased early basaltic volcanism, of which the visible mare basalts constitute the declining phase [34], should contribute even more basaltic clasts.

If the present visible amount of mare basalt were mixed by cratering into the highland crust, it would not produce a distinctive geochemical signature. The highland crust contains Mg, Cr, V and other elements which are enriched in mare basalts. One scenario would be to account entirely for these mafic components by admixture, through cratering, of appropriate amounts of

mare basalt. Various constraints have been noted which make this scenario unlikely [34, 35] and a vast amount of very early (pre-4.2 aeons) basaltic volcanism, comprising about 20% of the volume of the highland crust would be needed. Isotopic evidence for this event is lacking.

5.3 Melt Rocks

A distinctive suite of igneous-appearing rocks is also present in the Apollo collections from the highlands. These may be chemically distinguished from the mare basalts, principally Al_2O_3/CaO ratios, which are a factor of two higher in the highland samples. A suite of these has been selected as a "reference suite" as part of the NASA Basaltic Volcanism Study Project [36, 37], which covers the whole range of lunar highland compositions. A debate ensued over whether these rocks were of primary igneous origin or crystallized from melts generated by meteorite impact. The presence of clasts, the frequent evidence of high concentrations of siderophile elements, and the bulk compositions all tended to favor the latter view. They are, in general, medium to dark grey in color, usually fine-grained and occasionally vesicular. They may be glassy or wholly crystalline (e.g., sample 14310). Some are clast-laden microbreccias and hence would be classified as impact melt breccias (Section 5.2.4). The fragment-laden melt rocks appear to have formed mainly between about 4.05 and 3.85 aeons, and, therefore, appear to be younger than the granulitic breccias. Examples of rocks with true igneous textures (clast-free impact melt rocks) include 14310, 68415 and 78235 [38–42]. (See Section 5.4.4 for a discussion of "KREEP basalts.")

5.4 Highland Crustal Components

The previous sections classify the physical nature of the rocks sampled by the Apollo missions. Before going on to specify the compositions and discuss petrogenesis, it is necessary to consider the broader aspects of the problem. The Moon, as a planet, is simple enough to make broad scale overviews more profitable than on complex planets, a view with much historical truth. A basic premise in this approach is that the major element chemistry is not seriously affected by the impact process and that the dominant effect is not partial melting, but rather is impact-induced melting and mixing.

A major controversy has centered around questions of the components making up the highland crust. It was clear from the time of the Apollo 14 and 15 missions that many of the breccia compositions could be resolved into mixtures of two or three components. The Apollo 16 sample return aided greatly in this interpretation. The most useful key in unravelling the composi-

tion of the battered lunar highland crust has been the fact that the chemistry of the samples has survived the impact process, whereas most information on texture and other petrological and mineralogical indexes has been destroyed by the bombardment. A trap awaited the too-ready use of chemical composition of glasses as indicative of "primary" rock types. Impacts produce glasses. Chemical fractionation or partial melting mostly does not occur, so that the frequency of glass compositions can provide an index of the relative abundance of rock types. This approach was used by the "Apollo Soil Survey." However, the impact process is an extraordinarily efficient mixer, as shown, for example, at large terrestrial impact sites such as Manicougan [43, 44]. The effect of this process on the Moon has been to produce some average crustal compositions which have been mistaken for primary rock types; e.g., highland basalt, with about 26% Al_2O_3, is close in composition to the average highland crust (Section 5.9) [45]. Thus, the compositions due to mixing must be carefully disentangled from the original or pristine highland crustal compositions. An additional artifact of this sort has been the identification of "low-K Fra Mauro basalt" (LKFM) as a primary rock type. No unambiguous rock of this composition has been returned [46]. Once this complicating factor was understood, lunar highland crustal rock types became simpler and easier to fit into a rational petrologic scheme. A primary piece of evidence comes from the REE abundances and distribution patterns in highland breccias.

The REE patterns for most lunar highland samples are sub-parallel [47–50]. La/Yb ranges from 1.3 to 3.4. Strong negative and positive Eu anomalies are superimposed on these otherwise very regular patterns. As Haskin [50] comments, "So little change suggests a relatively simple genetic relationship among highland rocks." The range in the absolute abundances of the LIL elements is very large (>4000). As with many other lunar problems, the geochemistry of the samples provides the decisive clues. The two basic REE patterns which dominate highland crustal REE geochemistry are: (a) the anorthosite pattern, with La/Yb about 3 and Eu/Eu* about 20 [51], and the so-called KREEP pattern with La/Yb about 2 and Eu/Eu* about 0.10. Mixing of these two patterns accounts for nearly all the intermediate patterns.

A third component is required to provide the concentrations of Mg, Cr, etc., observed in the highland breccias. This is variously considered to be derived from an initial frozen crust, from infalling late accreting planetesimals or from trapped liquids within the crystallizing crust. Mare basalts cannot account for it, and are "probably only a minor component" [52]. Wänke et al. [53] considered that it was a primary chondritic component, but Ryder [52] examined the evidence and stated that "There is no basis for believing that the Mg-component is a primary chondrite-related non-lunar material." Taylor and co-workers considered it to be either a frozen crust or due to infalling planetesimals of lunar composition [47]. Plots of Ti/Sm [54] serve to distin-

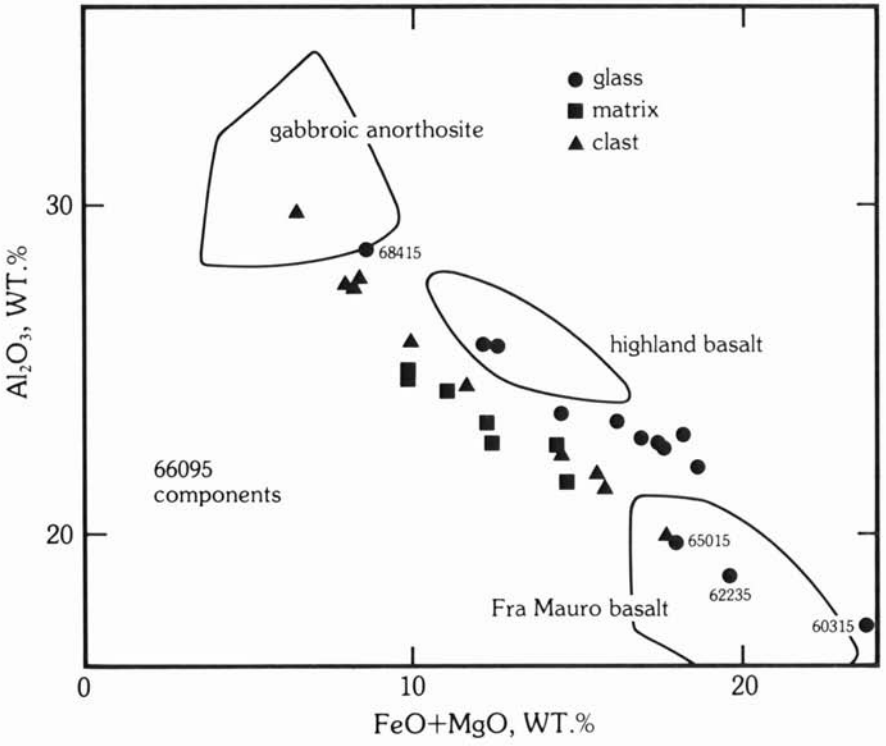

5.13 Plot of Al_2O_3 versus FeO + MgO showing the compositions of 66095 matrix, vein glass, and clasts relative to the compositions of rocks and glasses of Fra Mauro basalts, highland basalts, and gabbroic anorthosites [55]. (Courtesy L. A. Taylor.)

guish it clearly from chondritic material, thus removing the possibility of deriving the high Mg content from that source. The nickel and other siderophile element abundances are too low to make chondritic meteorites more than a trivial contributor.

Further insight into the difficult problem of the nature of the highland crustal components has been provided by a study of the "rusty" rock 66095, which is a polymict breccia. It provides within its mass of 1185 g a reasonable representative sampling of the highland crust. Bulk compositions approximate that of the soil at the Descartes site. On an Al_2O_3 versus FeO + MgO diagram, individual clasts, glasses, and matrix correspond to gabbroic anorthosite, "highland basalt," and Fra Mauro basalts (Fig. 5.13). The REE patterns range from less than 10 times chondritic, with Eu enrichment, through patterns at about 20 times chondritic, with no Eu anomaly, up to patterns about 200 times chondritic with deep Eu depletion. These character-

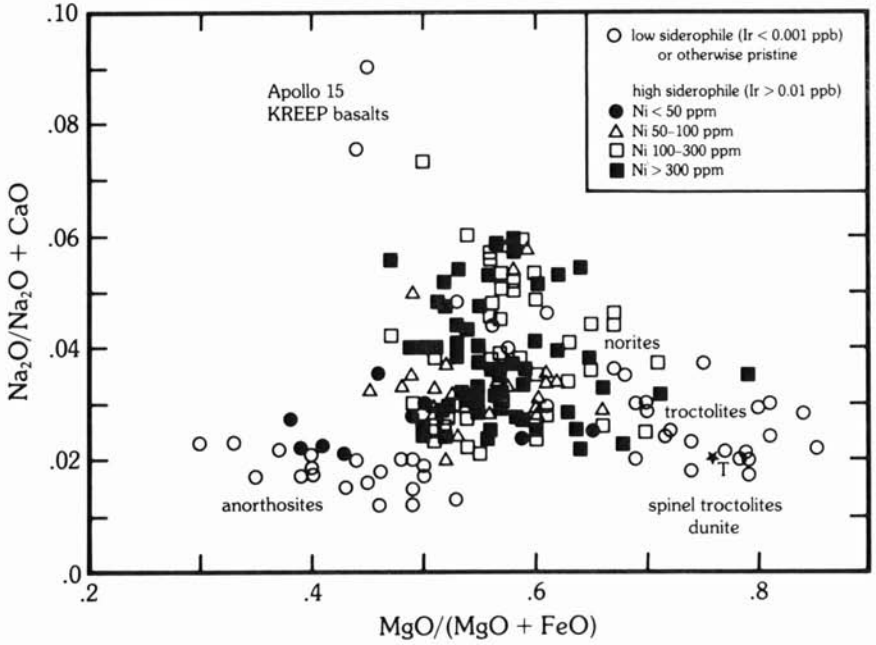

5.14 Highland rock compositions showing that high siderophile element abundances tend to fall within the boundaries created by samples with low siderophile element abundances [35]. (Courtesy G. Ryder.)

istics encompass most of the chemical variations observed in highland breccias. Garrison and Taylor [55] caution against attempts to over-refine the end-members of the highland crust by introducing additional elusive components. "Highland basalt" is almost certainly a mixture. They propose a three-component mixing model comprising ANT, KREEP and a small meteoritic component. This avoids the question of the origin of the Mg component.

Plots of $MgO/(MgO + FeO)$ versus $Na_2O/(Na_2O + CaO)$ [49] indicate a triangular range of highland compositions, outlined by anorthosite, KREEP and troctolites, very close to the Taylor and Bence [47] components. The siderophile-rich samples cluster within the triangle, while the pristine components fall toward the outer boundaries [56] (Fig. 5.14). This result, like the REE patterns, is good evidence for mixing models. Garrison and Taylor [55] note that "recent modelings of lunar highland rocks have fallen prey to the over-interpretation of the chemical data" and continue that "we do not feel that any model can be totally quantified and realistically explain the highland breccias" [55, p. 411], particularly in view of their history of multiple brecciation.

One problem encountered in mixing models is the identification of end-members precisely defined to explain all the trace element chemistry of the breccias. Clearly the end-member components should be reasonably abundant and "The use of dunite (74215) as an end-member is unwarranted because of its scarcity" [55]. Most of the elements in the norite component used by Ryder [50] are really those of the KREEP component. Wasson et al. [56] have introduced SCCRV, an Mg-rich rock type characterized by high Sc, Cr and V contents and representing yet another addition to the collection of lunar acronyms. Garrison and Taylor [55] complain that it is "an elusive n+1 component" and that "even dunite is more realistic than SCCRV" as a possible end-member component for highlands breccias [55, p. 411]. Clearly there is little agreement on the nature of the Mg component, except that it is not chondritic, but some resolution of these questions will become apparent.

The view is taken here that too much fine-tuning of the components is not possible, but that the overall chemistry of the highland crust is consistent with a minimum of three initial components, together with the meteoritic addition. The later complexities have arisen as a consequence of the meteoritic bombardment of a crystallizing crust.

5.4.1 Anorthosites

This significant and widespread component [57] in the lunar highlands is principally responsible for the light color of the highlands, in contrast to the darker basalts of the maria, familiar as the features of the "man in the moon." Plagioclase feldspar constitutes the bulk (95%) of these pale rocks; they are very calcium-rich, with compositions typically in the range An_{95-97}. This uniformity of anorthosite composition indicates that the parent magma body was very large, probably moon-wide. The distinction between a single "magma ocean" and many smaller bodies of melt is in part semantic. The evidence for moon-wide crystal fractionation processes cannot easily distinguish between these alternatives. Low-calcium pyroxene is the next most abundant constituent, but olivine and clinopyroxenes may also be present, although the mafic minerals are only present as minor components.

Full details of the mineralogy are given by James [58] and Norman and Ryder [59]. Examples include 15415 (the genesis rock), 15437, 60025, 60055, 60215, 61015, 61016, 62255, 64475, 65035, 65315, and 67075. These rocks have been mostly granulated by impact. The chemical compositions of some selected rocks are given in Table 5.2.

The REE abundances (Fig. 5.15) are all low, with a pronounced positive Eu anomaly. The La/Yb ratios become steeper as the total REE fall, typical of plagioclase patterns. Europium is nearly constant at 0.6–0.9 ppm. The $^{87}Sr/^{86}Sr$ ratios of the anorthosites are very low. This constitutes primary evidence that they are relics of the early crust [60]. Sample 60025, for example,

Table 5.2a Major element compositions of typical highland samples.†

	Anorthosites				Gabbroic Anorthosites		Anorthositic Gabbros		
	15415 (1)	65315 (2)	60055 (3)	61016 (4)	68415 (5)	65055 (6)	15455 (7)	60335 (8)	66095 (9)
SiO_2	44.1	44.3	44.3	45.0	45.5	45.5	44.5	46.2	44.5
TiO_2	0.02	0.012	—	0.02	0.32	0.28	0.39	0.58	0.71
Al_2O_3	35.5	34.9	34.0	34.6	28.6	28.5	26.0	25.3	23.6
FeO	0.23	0.31	0.34	0.30	4.25	3.90	5.77	4.51	7.16
MnO	—	0.006	0.10	—	0.06	0.05	—	0.07	0.08
MgO	0.09	0.25	0.33	0.20	4.38	4.81	8.05	8.14	8.75
CaO	19.7	19.1	19.0	19.6	16.4	16.1	14.9	14.4	13.7
Na_2O	0.34	0.30	0.34	0.40	0.41	0.44	0.25	0.52	0.42
K_2O	—	0.007	0.01	0.01	0.06	0.13	0.10	0.23	0.15
Cr_2O_3	—	0.003	0.005	0.01	0.10	0.08	0.06	0.13	0.15
P_2O_5	0.01	0.001	—	0.05	0.07	0.13	—	0.19	0.24
Σ	99.99	99.2	98.4	100.2	100.1	99.8	100.0	100.3	99.4

†Values given in wt.%.

Sources of data (also for Tables 5.3a and 5.4):

Apollo 15 PET NASA SP-289, 6–6 (1);
Hubbard, N. J., et al. (1971) *EPSL.* 13: 73 (1);
Hubbard, N. J, et al. (1974) *PLC 5*: 1234 (4);
Taylor, S. R., et al. (1973) *PLC 4*: 1454 (7);
Vaniman, D. T., and Papike, J. J. (1980) *Lunar Highlands Crust,* p. 276 (5,6,8,9);
Wänke, H. (1974) *PLC 5*: 1307 (2);
Warren, P. H., and Wasson, J. T. (1978) *PLC 9*: 188 (3);
Wolf, R., et al. (1979) *PLC 10*: 2112 (1,4,5).

has an $^{40}Ar/^{39}Ar$ age of 4.13 aeons [61]. Some anorthosites (so-called troctolitic anorthosites) contain 15-20% olivine or pyroxene, without appreciable differences in the REE patterns. Sample 76535 is one example. It has an initial $^{87}Sr/^{86}Sr$ of 0.6990, but the Sm-Nd age is 4.25 aeons [62, 63]. (See [41, 56, 64, 65] for further data on anorthosites.)

5.4.2 The Mg Suite

Norites, troctolites, dunite, spinel troctolite, and gabbroic anorthosites are collectively designated as the Mg-rich plutonic rock suite (Fig. 5.16). Typical compositions are given in Table 5.3 [42]. Norites do not contain olivine and have flat REE patterns, with about the same abundance of Eu, and either small negative or positive anomalies (Figs. 5.17 and 5.18). Examples include 15445c, the civet cat clast from 72255 and large samples from Apollo

Table 5.2b Major element compositions of typical lunar highland samples.†

	Anorthositic norite	Norites		Spinel troctolite	Tracto-lite	Dunite	LKFM		MKFM
	78255	77075	78235	73215, 32	76535	72417	14310	65015	15386
	(1)	(2)	(3)	(4)	(5)	(6)	(7)	(8)	(9)
SiO_2	47.3	51.2	49.5	44.7	42.9	39.8	47.2	47.0	50.8
TiO_2	0.67	0.33	0.16	—	0.05	0.03	1.24	1.26	2.23
Al_2O_3	27.4	15.0	20.9	31.2	20.7	1.3	20.1	19.7	14.8
FeO	2.64	10.7	5.05	3.05	5.0	11.9	8.38	8.59	10.6
MnO	0.046	0.17	0.08	—	0.07	0.11	0.11	0.11	0.16
MgO	5.97	12.9	11.8	3.42	19.1	45.4	7.87	9.31	8.17
CaO	15.0	8.82	11.7	17.2	11.4	1.1	12.3	11.9	9.71
Na_2O	0.45	0.38	0.35	0.47	0.20	0.013	0.63	0.55	0.73
K_2O	0.084	0.18	0.061	0.075	0.03	0.002	0.49	0.36	0.67
Cr_2O_3	0.14	0.39	0.23	—	0.11	0.34	0.18	0.19	0.35
P_2O_5	—	—	0.04	—	0.03	—	0.34	0.41	0.70
Σ	99.7	100.1	99.8	100.2	99.6	100.0	98.8	99.4	99.0

†Values given in wt.%.

Sources of data (also for Tables 5.3b and 5.4):

Bence, A. E., et al. (1975) LS VI: 38 (4);
Higuchi, H., and Morgan, J. W. (1975) *PLC 6*: 1628 (3, 4, 6);
Haskin, L. A., et al. (1974) *PLC 5*: 1213 (5);
Keith, J. E. (1974) *PLC 5*: 2122 (3);
Laul, J. C., and Schmitt, R. A. (1975) *PLC 6*: 1234 (6);
Vaniman, D. T., and Papike, J. J. (1980) *Lunar Highlands Crust*, p. 276 (7, 8, 9);
Warren, P. H., and Wasson, J. T. (1978) *PLC 9*: 188 (1, 2);
Wolf, R., et al. (1979) *PLC 10*: 2112 (1).

17 (stations 7 and 8). Spinel troctolites (e.g., 67435c) consist of olivine and pleonaste enclosed in plagioclase and appear to be of deep-seated origin, as indicated by the presence of Al-enstatite and Mg-Al spinel. One of the most interesting samples which possibly belongs to the Mg suite is the well-known dunite 72415-8, which is mainly crushed olivine [66, 67]. There is much variation among the REE in different samples of this rock (Fig. 5.18). It contains only 160 ppm Ni, and 2500 ppm Cr, typical lunar ratios for these elements. The Rb-Sr internal isochron age is 4.45 aeons with an initial $^{87}Sr/^{86}Sr$ of 0.69900 ± 7 [60].

The plagioclase and ferromagnesian minerals in the Mg suite show wide ranges in composition, and these are correlated in a manner simply related to fractional crystallization. The relationships of this suite of rocks to the anorthosites on the one hand and the KREEP components on the other are the subject of much current debate (see also [41, 56].)

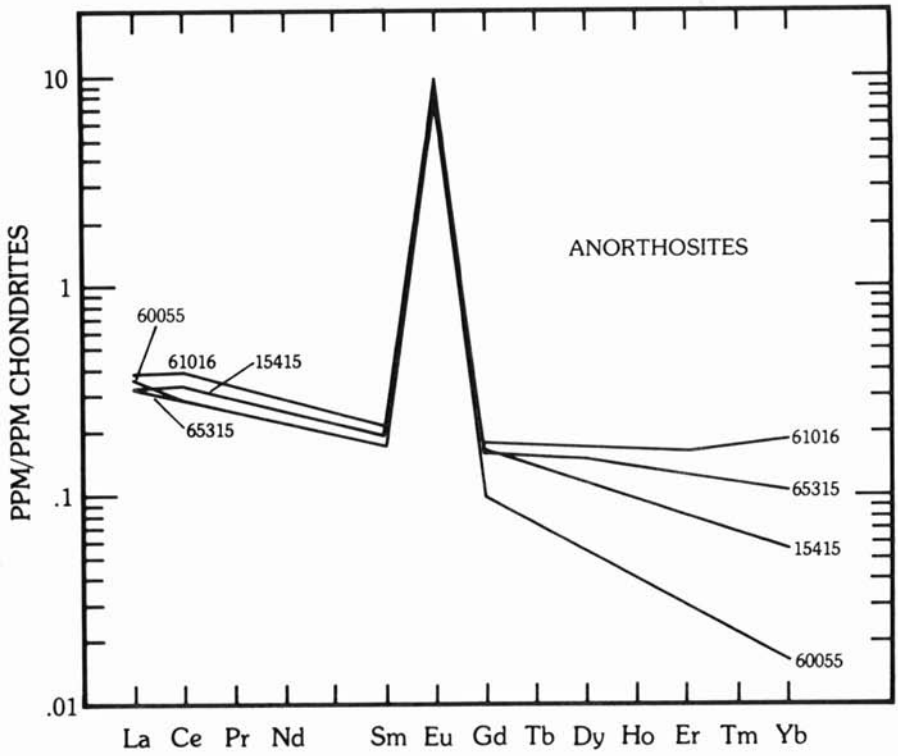

5.15 Chondrite-normalized rare-earth element abundances in lunar anorthosites. Data from Table 5.3. Note the low overall abundances and the high enrichment of europium, due to the selective uptake of Eu^{2+}. See Appendix VIII for rare-earth element chondritic normalizing factors.

5.4.3 KREEP

The existence of high concentrations of KREEP has beguiled the lunar community since the first discovery during the Apollo 12 mission of a layer in the regolith of "light gray fines" and of rock 12013, picked up by Astronaut Pete Conrad on an unscheduled traverse. The surprise in finding extreme concentrations of elements typical of the residual liquids produced by fractional crystallization, on a Moon which many considered to be a primitive unfractionated body, was compounded by the widespread occurrence of such a component. This contrasts with the so-called lunar granites, which are of trivial extent in the whole lunar picture [68–71]. Mostly they appear to be fragments of interstitial glass from mare basalts. Such interstitial glasses (up to 150 microns) are reported by many authors studying mare basalts. High

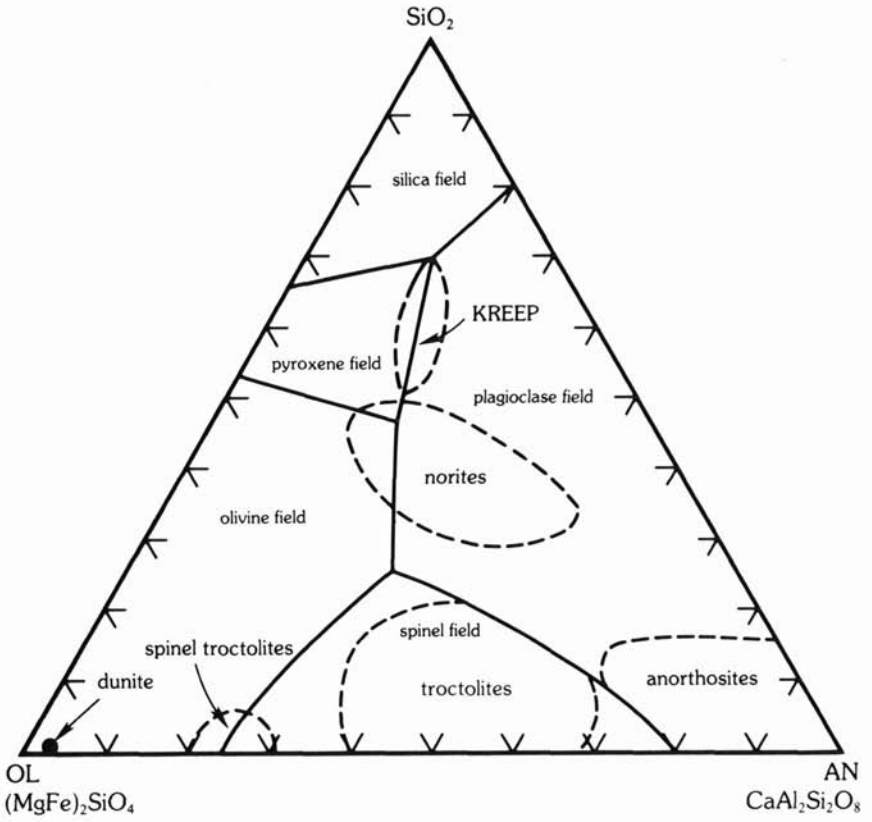

5.16 Compositions of apparently pristine lunar highland samples plotted on the olivine-anorthite-silica pseudoternary diagram. (Adapted from [42].)

silica glass fragments have not been reported from the Apollo 16 highland soils with one exception (see Section 4.4.2).

Although KREEP was thought at one time to be rather restricted in areal extent, and perhaps even confined to be the Imbrium basin [71, 72], the consensus emerges that it is in fact widely distributed on the Moon [73], although it does appear to be restricted to regions where the highland crust thickness is 60 km or less. Because KREEP is so widespread, it cannot be dismissed as a small or trivial volume of residual melt produced from crystallization of a local intrusion. In magma ocean models, it represents perhaps the final 2% residue. Studies of Sm/Nd isotopic systematics indicate that the samples measured come from a common source [73]. Sm/Nd ratios and $^{143}Nd/^{144}Nd$ ratios are very close for samples from Apollos 12, 14, 15 and 16. The idea that KREEP was derived as the final residual liquid from the

Table 5.3a Trace element compositions of lunar highland samples.†

	Anorthosites				Gabbroic Anorthosites		Anorthositic Gabbros		
	15415	65315	60055	61016	68415	65055	15455	60335	66095
I. Large cations									
Cs	0.02	0.015	—	0.0003	—	—	0.12	0.28	0.40
Rb	0.22	0.17	—	0.02	1.7	—	1.1	6.2	4.2
K	151	58	85	80	650	1100	830	1900	1200
Ba	6.3	5	11	7	76	80	42	190	240
Sr	173	170	—	180	182	140	220	163	154
Pb	0.27	—	—	—	0.78	—	1.0	2.0	15
K/Rb	690	340	—	4000	380	—	750	300	290
Rb/Sr	0.001	0.001	—	0.0001	0.009	—	0.005	0.038	0.027
K/Ba	24	11.6	7.7	11	8.5	14	20	10	5
II. Rare earth elements									
La	0.12	0.12	0.13	0.14	6.8	6.2	3.0	20.0	18.5
Ce	0.33	—	0.27	0.37	18.3	16.0	6.7	52	50
Nd	0.18	—	—	0.21	10.9	—	3.73	32	—
Sm	0.046	0.04	0.040	0.058	3.09	2.6	0.88	9.1	8.8
Eu	0.81	0.74	0.76	0.77	1.11	1.0	1.67	1.28	1.63
Gd	0.05	—	—	0.054	3.78	—	0.95	10.6	—
Tb	—	—	—	—	—	0.55	0.14	1.9	—
Dy	0.044	0.056	—	0.065	4.18	—	0.84	11.5	9.4
Ho	—	—	—	—	—	—	0.17	2.5	—
Er	0.019	—	—	0.040	2.57	—	0.46	6.77	—
Yb	—	0.026	0.035	0.045	2.29	2.1	0.36	6.23	4.9
Lu	—	0.004	0.004	0.01	0.34	0.29	0.06	0.68	0.90
Y	—	—	—	—	22	19	4.8	57	70
La/Yb	3.4	4.6	3.7	3.1	3.0	3.0	3.0	3.2	3.0
Eu/Eu*	51.6	51.6	64.7	45.2	0.99	1.08	5.58	0.40	0.54
III. Large high valence cations									
U	0.0017	—	—	0.0015	0.32	0.31	0.05	0.92	1.0
Th	0.0036	—	—	—	1.26	1.18	0.23	2.75	2.2
Zr	—	15	—	2.4	100	72	11	290	320
Hf	—	0.49	—	—	2.4	2.1	0.17	6.9	5.0
Nb	—	—	—	—	5.6	—	0.95	10	21
Th/U	2.1	—	—	—	3.94	3.79	4.6	3.0	2.2
Zr/Hf	—	31	—	—	42	34	65	43	64
Zr/Nb	—	—	—	—	18	—	11.5	29	16
IV. Ferromagnesian elements									
Cr	—	—	33	21	700	500	440	910	1000
V	—	—	—	—	20	35	16	26	110
Sc	—	0.39	0.55	0.5	8.2	7.2	—	8.5	6.8
Ni	1.0	1.4	1.9	1.0	180	390	12	720	710
Co	—	0.058	0.84	1.0	11	29	10	37	44
Cu	—	2.1	—	—	12	2.4	1.3	7.4	3.9
Fe, %	0.18	0.24	0.26	0.23	3.30	3.03	4.49	3.50	5.56
Mn	—	47	75	—	470	390	—	540	620
Zn	0.26	—	0.60	1.6	4.8	0.56	1.9	4.3	92
Mg, %	0.05	0.15	0.20	0.12	2.54	2.90	4.86	4.91	5.28
Ga	—	—	3.8	—	2.0	3.0	2.6	3.1	3.8
Li	—	—	—	—	5	2.2	—	13	11
V/Ni	—	—	—	—	0.11	0.09	1.3	0.04	0.15
Cr/V	—	—	—	—	35	14	28	35	9

†Data in ppm.

Table 5.3b Trace element composition of lunar highland samples.†

	Anorthositic norite	Norites		Spinel troctolite	Troctolite	Dunite	LKFM		MKFM
	78255	77075	78235	73215, 32	76535	72417	14310	65015	15386
I. Large cations									
Cs	—	—	0.064	0.007	0.001	0.014	0.54	0.42	—
Rb	—	—	0.92	0.30	0.24	0.045	12.8	10.2	18.5
K	700	1500	510	620	220	16	4080	3000	5600
Ba	86	160	80	61	33	4.1	630	570	840
Sr	—	—	—	—	115	8.2	250	145	190
Pb	—	—	—	1.9	—	—	6.2	4.7	—
K/Rb	—	—	550	2070	920	360	320	300	300
Rb/Sr	—	—	—	—	0.002	0.005	0.05	0.07	0.10
K/Ba	8.1	9.4	6.4	10.2	6.7	3.9	6.5	5.3	6.7
II. Rare earth elements									
La	3.3	7.2	—	4.2	1.51	0.15	56	66	84
Ce	7.8	—	9.2	12	3.8	0.37	144	185	210
Pr	—	—	—	1.54	—	—	17	26	—
Nd	5.0	8.5	5.4	6.3	2.3	—	87	120	130
Sm	1.20	3.0	1.49	1.82	0.61	0.080	24	27	38
Eu	1.21	0.98	1.03	0.50	0.73	0.061	2.15	1.97	2.72
Gd	—	—	—	2.05	0.73	—	28	36	45
Tb	0.23	0.74	—	0.42	—	0.017	5.1	6.3	7.9
Dy	—	—	2.26	2.71	0.80	0.11	33	38	46
Ho	—	—	—	0.57	—	0.023	6.5	8.3	—
Er	—	—	1.47	1.62	0.53	—	20	24	27
Yb	0.98	3.9	1.64	1.66	0.56	0.074	18	21	24
Lu	0.14	0.59	0.24	0.26	0.08	0.012	2.5	2.8	3.4
Y	—	—	—	20	—	—	175	174	—
La/Yb	3.4	1.8	—	2.5	2.7	1.9	3.1	3.1	3.4
Eu/Eu*	2.93	0.87	1.97	0.80	3.34	2.1	0.25	0.19	0.20
III. Large high valence cations									
U	0.19	0.5	0.19	0.23	0.020	0.006	3.10	2.2	2.8
Th	0.44	1.57	0.59	0.80	—	—	10.4	8.9	10.0
Zr	49	210	—	79	24	—	840	940	970
Hf	0.67	3.5	—	2.0	0.52	0.10	21	22	32
Nb	—	—	—	6.3	—	—	52	48	—
Th/U	2.3	3.1	3.1	3.5	—	—	3.4	4.0	3.6
Zr/Hf	73	60	—	40	46	—	40	44	31
Zr/Nb	—	—	—	12.5	—	—	16	20	—
IV. Ferromagnesian elements									
Cr	990	2650	—	—	—	—	1250	1280	2400
V	—	—	—	—	—	50	36	—	—
Sc	4.6	17	—	—	—	4.3	20	17	24
Ni	22	6	12	247	44	160	270	490	13
Co	23	33	—	—	—	55	17	43	18
Cu	—	—	—	—	—	—	5.0	5.1	—
Fe, %	2.05	8.31	3.93	2.37	3.89	9.25	6.51	6.67	8.24
Mn	335	1320	600	—	540	850	850	850	1240
Zn	0.095	3.3	1.5	6.2	1.2	2	1.8	1.5	—
Mg, %	3.60	7.78	7.12	2.06	11.5	27.4	4.75	5.62	4.93
Ga	5.1	4.0	—	—	—	—	3.2	3.8	3.5
Li	—	—	—	—	3.0	—	22	21	27
N/Ni	—	—	—	—	—	—	0.13	—	—
Cr/V	—	—	—	—	—	—	35	—	—

†Data in ppm.

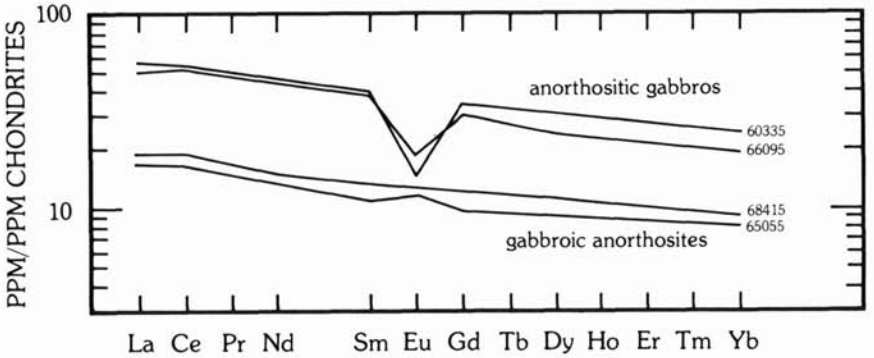

5.17 Rare-earth element abundances in lunar gabbroic anorthosites and anorthositic gabbros. Data from Table 5.3. Note that in comparison with Fig. 5.15, the Eu anomaly ranges from slightly positive to negative, and that the total REE abundances are higher.

crystallization of a magma ocean was stated by Taylor and Jakeš [74] and Taylor [75]. Major reviews have been undertaken by Warren and Wasson [76] and Meyer [77] to which the reader is referred for much valuable material.

KREEP is elusive as a rock type [46]. Some so-called pristine fragments (i.e., lacking in siderophile elements) exist (15382, 15386) and various clasts in

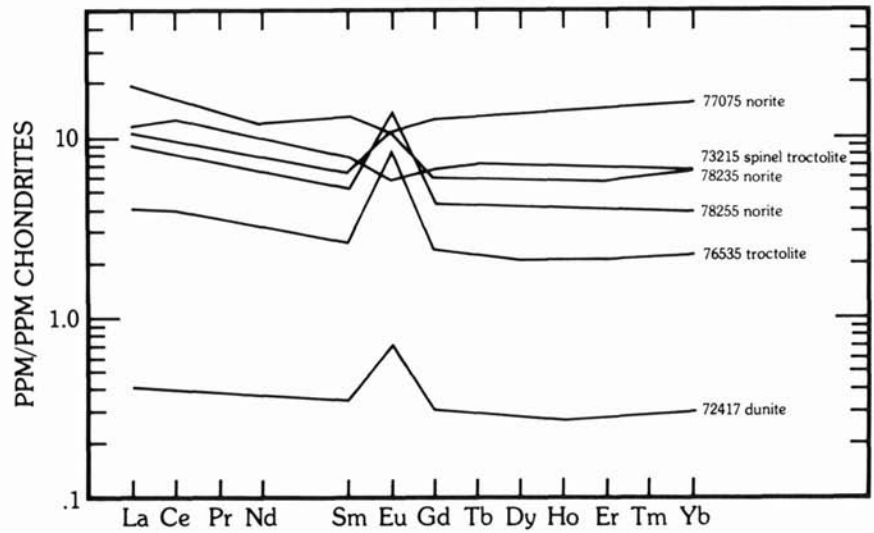

5.18 Rare-earth element abundances for norites, troctolites and the dunite. Data from Table 5.3.

Table 5.4 Volatile and siderophile trace elements in highland samples.†

	Anorthosites				Gabbroic anorthosites		Anorthositic gabbros		
	15415	65315	60055	61016	68415	65055	15455	60335	66095
Ir	—	—	0.013	0.01	4.6	10	0.024	—	—
Re	0.0008	—	—	0.0022	0.43	—	0.006	—	—
Ni, ppm	1.0	1.4	1.9	1.0	180	390	12	720	710
Au	—	1.0	0.014	0.02	2.7	5.0	0.042	—	18*
Sb	0.70	—	—	—	530	—	0.22	—	—
Ge	1.2	—	17	—	73	240	9.4	—	—
Se	0.23	—	—	0.4	98	—	8.3	230	—
Te	—	—	—	—	—	—	2.6	—	—
Ag	1.7	—	—	0.29	—	—	1.7	—	—
Zn, ppm	0.26	—	0.60	1.6	4.8	0.56	1.9	4.3	92*
In	0.18	—	3.6	—	—	6.4	0.05	—	680*
Cd	0.57	—	0.57	—	2.8	—	1.0	—	—
Bi	0.1	—	—	—	—	—	0.14	—	—
Tl	0.09	—	—	—	—	—	0.054	—	—
Br	2.3	—	—	—	—	—	35	—	—

†Data in ppb except where noted.
*Rusty rock sample.

Table 5.4 *(Continued).*

	Anorthositic norite	Norites		Spinel troctolite	Trocto-lite	Dunite	Fra Mauro		
							LKFM	MKFM	
	78255	77075	78235	73215, 170	76535	72417	14310	65015	15386
Os	—	—	—	—	—	—	10.5	—	—
Ir	0.43	0.25	0.14	1.0	0.005	0.005	10.5	17	0.06
Re	0.021	0.022	0.012	0.04	0.0012	0.005	1.0	1.8	—
Ni, ppm	22	6	12	247	44	160	270	490	—
Au	0.11	0.026	0.42	2.6	0.0025	0.25	4.3	11	0.22
Sb	—	—	0.08	0.71	0.01	0.47	4	14	—
Ge	58	11	19	110	1.7	30	110	—	60
Se	—	—	7.5	4	4.1	5	120	290	—
Te	—	—	—	—	0.28	—	—	—	—
Ag	—	—	0.40	130	0.12	0.3	—	—	—
Zn, ppm	0.095	3.3	1.5	6.2	1.2	2	1.8	1.5	—
In	0.05	—	—	—	—	—	30	—	—
Cd	4.2	5.4	2.9	3.1	0.6	0.4	8.4	9.3	10
Bi	—	—	0.05	0.49	0.04	0.4	—	—	—
Tl	—	—	0.02	1.0	0.012	0.05	—	—	—
Br	—	—	6	14	3.2	8.4	—	—	—

breccias have been so identified (15405c, 72275c, 77115c) (Table 5.4). It is probably fair to say that no topic has caused more confusion in our understanding of lunar petrogenesis than has KREEP; this emphasizes the hazards of attaching labels. However, some resolution of these problems appears possible. The chemical relationships are relatively simple. A dominating characteristic is the simplicity of the REE patterns (Fig. 5.19), possibly best illustrated by "Super-KREEP" (15405, 85) which has an La content 700 times the chondritic abundance [78]. The absence of unambiguous primary examples of KREEP rocks makes a discussion of their mineralogy somewhat ambiguous. The major element chemistry of KREEP-dominated samples is close to that of the olivine-plagioclase-pyroxene peritectic point in the experimental system silica-anorthosite-olivine [for $Mg/(Mg + Fe) = 0.7$] [79]. This fact has led to the popularity of traditional style igneous models, such as derivation by partial melting in the shallow lunar interior (about 120 km depth). This partial melting model is difficult to reconcile with the Rb-Sr isotopic evidence, since the Apollo 15 KREEP basalts have high initial ratios; further, it is not possible to generate Apollo 15 KREEP basalts by partial melting at 3.9 aeons, but this can be done at about 4.3 aeons, the average model age. These and other models involve large-scale lunar volcanism and the eruption of a primary magma of KREEP composition. The widespread use of the term KREEP basalt has exacerbated the problem. The basic question in KREEP genesis is how to reconcile the high concentrations of the incompatible elements with the major element chemistry and the high $Mg/(Mg + Fe)$ values. The view adopted here is that mixing of primitive and late stage liquids provides an explanation for the puzzling chemistry. The question of KREEP "volcanism" is addressed in the next section.

5.4.4 KREEP Volcanism in the Lunar Highlands?

Among the many questions which revolve around the question of KREEP, and of possible pre-mare volcanic activity in the lunar highlands, the occurrence of so-called KREEP basaltic volcanism has often been raised [80, 81, 82]. There is no doubt about the existence of high-Al basalts in the highlands breccias (see Section 5.2.6). These are similar to the familiar mare basalts and do not present a special problem. The "KREEP basalts" are different. Their high content of REE, Th, U, K, etc., together with their high $Mg/(Mg + Fe)$ ratios call for a special petrogenesis, distinct from that of other basalts of undoubted volcanic origin. Accordingly, the evidence for their existence as a "volcanic" rock needs to be carefully examined, because of the problems which they present for lunar petrology. KREEP components are widespread and LKFM appears to be moon-wide [83]. As is argued elsewhere, KREEP is not just restricted to the Imbrium basin and its surrounding terrain. In this context, we note the orbital thorium data, which shows that the

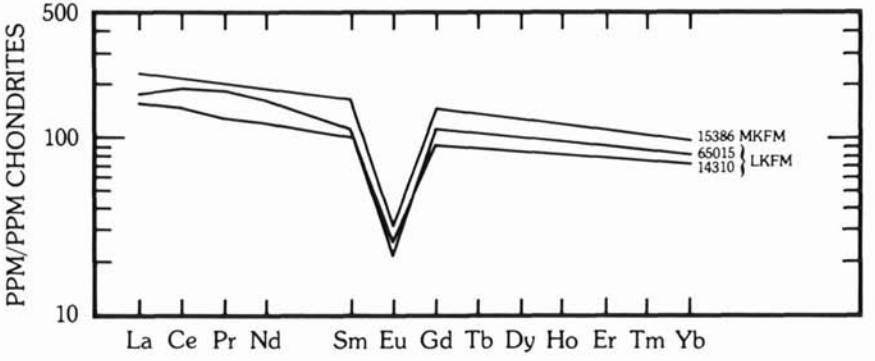

5.19 Rare-earth element abundances in Fra Mauro basalts. Note the extreme enrichment of the total REE and the deep depletion in europium, forming a pattern reciprocal to that of the anorthosites in Fig. 5.15.

Apennine Mountains, as well as the Apennine Bench Formation, have high Th concentrations (~11 ppm) [84]. Thus, popular interpretations of the Apennine Bench Formation as volcanic KREEP flows, extruded after the Imbrium collision but before the mare basalts, are not really supported by the orbital thorium data.

Great petrogenetic problems arise. Mare basalts were being erupted at 3.85 aeons (10003), and basaltic-style volcanism predated the Imbrium collision (Section 5.2.6). If the interpretation of the Apennine Bench Formation as volcanic flows is correct, then two contrasting styles of lunar volcanism were occurring at the same time. This occurs, of course, on the Earth in a complex tectonic environment, but raises many problems on the Moon. If KREEP is volcanic, it is fair to ask where all the flows are. Is the Apennine Bench the only demonstrable example? In view of the widespread nature and high concentrations of K, U, Th, etc., observed in the highland crust, it is remarkable that KREEP basalts so rarely appear. It seems more credible to account for the Apennine Bench Formation as an impact-derived melt sheet or debris flow from the Imbrium basin collision ponded against the Apennine Mountain scarp. The two primary examples of volcanic KREEP basalts usually quoted are samples 15382 and 15386. The evidence that these are "igneous" depends in part on texture and in part on their absence of siderophile elements. This recalls the argument over 14310 (Section 5.7) which was considered truly igneous on the basis of petrological evidence, until the high contents of Ni and other siderophile elements testified to its impact origin. The absence of siderophile elements does not constitute decisive evidence for pristinity (see Section 5.7). Many impact melts at terrestrial craters do not have a siderophile element signature [30]. The position is taken here that the case for KREEP volcanism is not proven, despite some suggestive evidence and many opinions

to the contrary [see for example *Basaltic Volcanism* (1981) Section 1.2.10.5]. The widespread occurrence of impact melt sheets associated with large basins may provide terrains that are very difficult to distinguish, by photogeological techniques, from volcanic flows. The isotopic data lend support to this interpretation. Model ages for KREEP point back to the initial differentiation of the Moon, not to more recent volcanic events, and the view is adopted here that large-scale fractional crystallization of the magma ocean is the ultimate source of KREEP [50, 74, 75]. Small scale partial melting events may have occurred locally during meteoritic bombardment of the growing crust.

An important observation is that there is a good correlation between high abundances of the REE (KREEP component) and position on the SiO_2-Ol-An diagram [85]. Samples with less lthan 15 ppm Sm (65 times chondritic abundances) show scatter, consistent with an origin by mixing. Those with higher abundances of REE tend to lie close to the cotectic line. This may be a consequence of partial melting, or it may simply reflect the dominating influence of the KREEP end member in a mixing model.

5.5 Volatile Components in the Highland Crust

The nature and origin of the volatile elements that are present in minor amounts in the highland breccias are important since the bulk moon composition is highly depleted in these elements. Some rocks (e.g., 66095) have high concentrations of Cl, Pb, Br, Zn, Rb, Ag and Tl. Various sources for these elements may be suggested:

(a) They may be added during meteoritic or cometary impact. Either comets or C1 chondrites possess appropriate levels of volatile elements.

(b) These elements, although low in abundance in the Moon, will be concentrated into the residual melt following crystallization of the magma ocean. They will thus be associated with the KREEP component. They do not enter many common silicate lattice sites and mostly are extreme examples of incompatible elements.

(c) They will be readily remobilized during impact events, or by "impact-induced metamorphism" and so concentrated near the surface. This volatilization model has useful predictive capabilities. For example, volatile trace elements in breccias may be expected to have anomalous abundances, although the major and refractory trace elements will be unaffected. This model, which involves migration of volatile elements from their original source in KREEP, explains many of the effects ascribed to "fumarolic" activity on the Moon.

(d) They may be due to "fumarolic" activity. Fumaroles imply volcanic activity and call for complicated models of igneous activity; the alternative model of secondary mobilization is much more realistic.

For the most part, these elements in lunar samples are easily leachable [86] by water and hence probably reside along grain boundaries, in lattice dislocations and along cracks. Sample 66095 has highly water-leachable and low residual chlorine. Hence, most of the Cl_2 is probably introduced at a late stage. Garrison and Taylor [55] consider that this chlorine attacks native Fe-Ni metal grains, forming $FeCl_2$. "This delinquescent $FeCl_2$ undergoes oxyhydration [in the terrestrial atmosphere] to β FeOOH (akaganéite) resulting in the notorious rust" ([55], p. 313).

Sample 66095 is a complex breccia with components ranging all the way from gabbroic anorthosite (e.g., 68415) to Fra Mauro basalts (e.g., 65015) (Fig. 5.13). It is the most volatile-rich of the lunar samples, containing Br, Cl, F, Bi, Cd, Pb, Tl and Zn. These volatiles will appear mainly as surface coatings and will easily be redistributed and flushed out during the metamorphic effects accompanying meteorite impacts. The water-bearing phase in 66095 is FeOOH (akaganéite) [87] (Figs. 5.20 and 5.21).

Various sources for the water are:

(a) fumarolic activity;
(b) cometary impact;
(c) oxyhydration of $FeCl_2$ (Lawrencite) due to contamination with terrestrial water vapor.

FeOOH cannot exist for any length of time under lunar vacuum (10^{-7} torr) conditions and high lunar daytime temperatures (140° C), and it is concluded that the water is terrestrial [88].

Sample 66095 contains 15 ppm Pb, 85% of which is not supported by U and Th [88]. The most reasonable hypothesis is that the Pb is indigenous to the Moon. Excess Pb in 66095 was evolved in a U rich (high μ) reservoir from 4.47 to 4.01 aeons, when it migrated into 66095. Nunes and Tatsumoto [89] conclude from these data that 4.47 aeons is the best estimate for the time of the early differentiation of the Moon. From this it appears this KREEP will generate highly radiogenic lead, and will probably also concentrate most of the lunar ^{204}Pb that does not get into sulfide phases. Since the volatiles are readily moved around during impact processes, parentless lead should be fairly common in lunar breccias.

Further insights into the occurrence of lunar volatiles in lunar highlands breccias have been gained by experimental investigations [90, 91] (see Section 4.5.2). In thermal release studies, the major fractions of Pb, Zn and Cd in rusty rock 66095 were released below 1000° C, which suggests that they are present mainly on grain surfaces. Experimental studies involving native iron chlorapatite [$Ca_5Cl(PO_4)_3$] and synthetic lunar basalts demonstrated vapor deposition including $FeCl_2$, iron phosphides (Fe_3P) and P. These, including high P metal, could form by disequilibrium thermal metamorphism during impact, which may therefore be an important vapor transport mechanism. Accordingly, there is no requirement to introduce volatiles by either volcanism or by

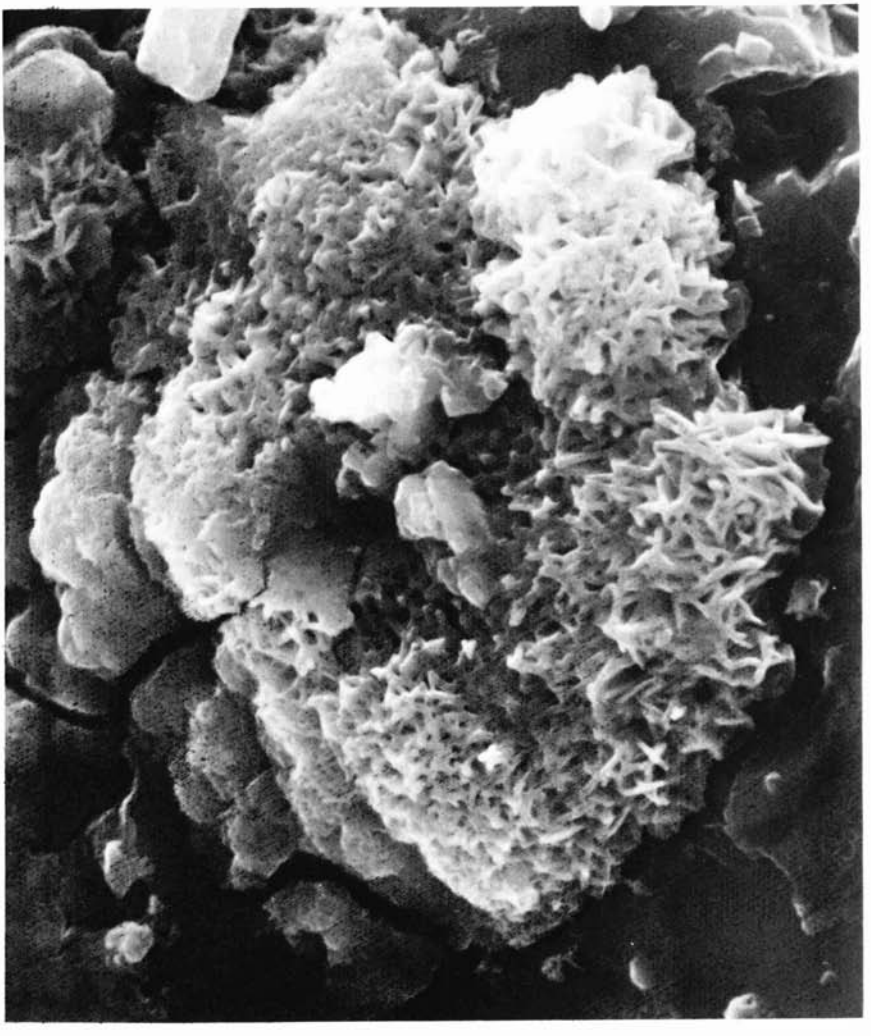

5.20 Rosettes of akaganéite in the rusty rock 66095. Magnification 6000 ×. (NASA S-73-37369. Courtesy D. S. McKay.)

addition from meteorites. Redistribution by impact processes appears adequate [55]. Note that lead, but not uranium or thorium, will be so affected; therefore, excess Pb, unsupported by Th and U, may be frequently mobilized by this mechanism.

In summary, it seems possible to account for the high concentrations of volatiles in samples such as 66095 and 61016 by two causes: (a) they contain

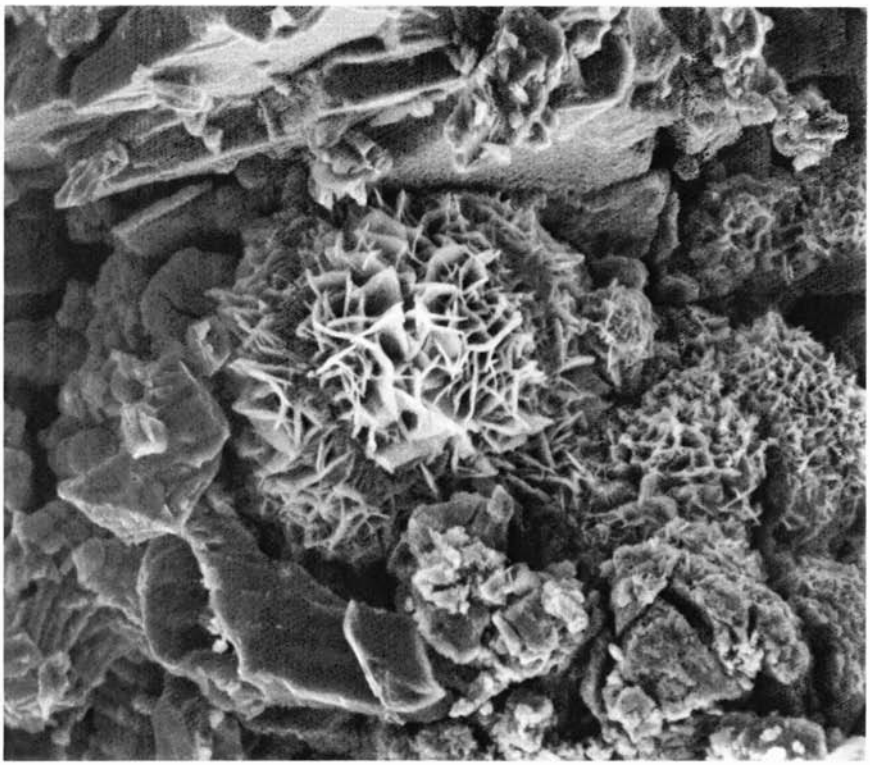

5.21 SEM photograph of one of the three morphologies of "rust" on lunar sample 66095. Compositionally the rosettes contain iron, chlorine, and occasionally up to 5% Ni. The central rosette is 7 microns in diameter. (NASA S-73-17705. Courtesy D. S. McKay.)

a large KREEP component and (b) volatiles have been added by redistribution from other KREEP-rich samples during large impacts [92].

5.6 The Ancient Meteorite Component

It was clear to many early observers that the lunar highlands had been subjected to a massive early bombardment. Once the dispute over the volcanic versus impact origin of the large craters was resolved, then a predictable consequence of the meteorite impact hypothesis was that some chemical signatures derived from the colliding bodies should be found on the surface. Experience at terrestrial impact craters, however, showed that traces of the

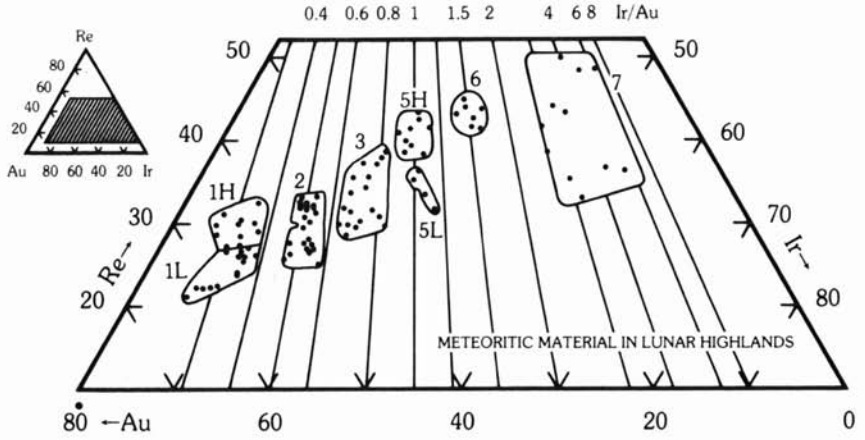

5.22 Ancient meteoritic components in lunar highland samples can be divided into about 8 groups, according to the proportions of siderophile elements Au, Re, and Ir. Reality of groups has been confirmed by objective statistical tests, such as cluster, factor, and discriminant analysis. Some groups are heavily represented at one landing site, e.g., Groups 1H and 7 at Apollo 16 and Groups 2, 3 at Apollo 17 [95]. (Courtesy E. Anders.)

impacting meteorite were often difficult to find, since the size of the crater and the volume of ejected country rock are about an order of magnitude larger than the meteorite. The most reliable chemical indexes are the siderophile trace elements. These are heavily depleted both in the terrestrial and in the lunar crusts. The determination of Ir, Re, Os, Pt, Pd, and Au at the parts per billion level is a task for neutron activation methods of analysis. These elements are abundant in the native iron of many classes of meteorites, so that they form the best index and signature of the meteoritic contribution. They can also be used in a contrary sense, so that their absence may identify "pristine" samples which have apparently escaped the bombardment. It has already been shown (Section 5.4) that the post-mare meteorite component present in the regolith is due principally to C1 carbonaceous chondrites.

Ir/Au ratios are particularly diagnostic, and have been used to identify eight groups of projectiles of differing composition, which have impacted the Moon [93–95]. From the distribution of these groups at various landing sites, it is tentatively concluded that seven of the groups are associated with basin-forming impacts rather than craters (Figs. 5.22, 5.23). One group (1H) appears to be associated with a local crater at the Apollo 16 site. There also appears to be some temporal correlation, with the more refractory "moon-like" compositions falling first. If this interpretation is correct, then it provides good evidence for heterogeneous accretion models for planetary growth (see Section 9.6).

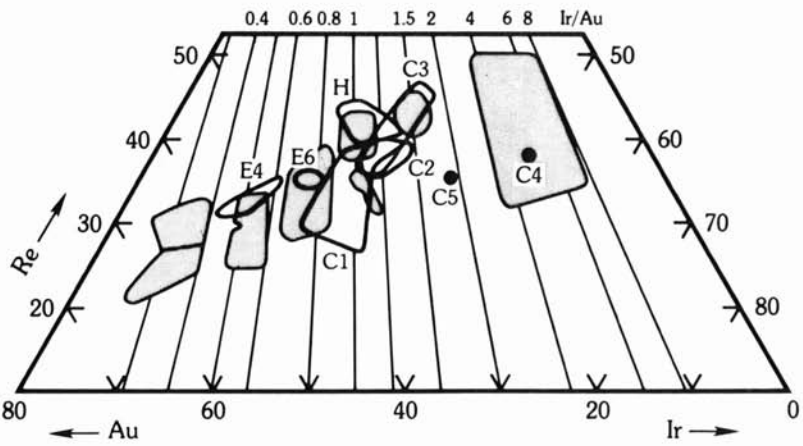

5.23 The ancient lunar highland meteorite components compared with the abundances for Au, Re and Ir in the various chondrite groups. Ancient meteoritic groups cover wider compositional range than do present-day chondrites. Except for Group 7 (where the low Au content causes scatter), they are no more distended than are some chondrite classes, e.g., C1's. However, since the Ir-Au-Re diagram does not fully resolve C1, C2, and C3 chondrites, one cannot rule out the possibility that some lunar groups are composite [94].

Many uncertainties beset this approach. If the highlands have undergone a saturation bombardment [30, 96], then the preservation of chemical evidence for a particular impact becomes more difficult and requires much selenodetective work.

5.7 Pristine Rocks in the Lunar Highlands

The widescale destruction of original textures and petrological and mineralogical relationships among the highland crustal rocks, by the raining meteoritic bombardment, has led to a search for those samples which might have escaped this fate. Pristine highland rocks are generally considered to be those produced by primary igneous activity, and which have subsequently retained their original chemical identity [97, 98]. Four characteristics may be used in assessing pristinity: (a) a low abundance of siderophile elements is essential. Since the bulk moon appears to be depleted in siderophile elements, this is a key parameter. The abundance of Ni, Au, Ge, Ir, Os and Re should be less than 3×10^{-4} times C1 chondrite compositions [99]; (b) various textural or mineral compositions that identify a monomict cumulate origin; (c) identifiable regolith components, including high concentrations of KREEP components, may indicate a polymict origin; (d) low $^{87}Sr/^{86}Sr$ initial ratios or old

ages are supportive evidence, since impact will reset the radiometric clocks. It is clear that the unequivocal identification of pristine rocks is not a simple task, but calls for the highest geochemical and petrological skills. Thus, many pristine rocks are brecciated with few remaining vestiges of igneous texture. Basaltic textures can be produced in impact melts (Section 5.3). The compositional fields of the silicate minerals overlap those of the polymict rocks. The most acceptable method is chemical: the controversy over whether rock 14310 was an impact melt or a primary igneous basaltic rock [100] should be a salutary reminder of the difficulties of making these decisions on the basis of petrography.

Possibly the best case for demonstrating that the search for pristine rocks (a lunar equivalent of the holy grail) is useful is shown in Fig. 5.14 where the siderophile element distribution in pristine rocks and polymict rocks is shown. The polymict breccias show high siderophile element signatures, and cluster in the center of the diagram. The rocks with low siderophile elements cluster toward the compositions of postulated primitive highland crustal components (anorthosite, Mg suite and KREEP). This diagram constitutes probably the best evidence for the pristine rock concept [49].

However, the converse that one can calculate the indigenous siderophile element abundances on the Moon from such rocks encounters serious problems [98, 101] since the addition of small amounts of meteoritic contamination, which produce no effect on the other element concentrations, can never be excluded.

It is also clear that most highland rocks have been involved in impact events, and the definitions for pristinity are not exclusive. Thus, many impact melts at terrestrial impact sites have no detectable siderophile element component [30, 102] and so meet the criteria for pristinity [97, 99]. The difficulty of finding a chemical signature of the impacting body is a familiar problem to investigators at terrestrial impact sites. Thus, caution is needed in applying the concept of pristinity. Accordingly, the absence of a siderophile element signature is not a decisive criterion.

The use of Ni/Co ratios in metal grains as an index of pristinity has been proposed [103]. However, projectile metal is usually different in composition to the impacting meteorite and much redistribution may take place with change of composition [104]. The concept that low siderophile rocks were produced in an impact melt, with extraction of the siderophile elements by a metal phase [101], would remove any genetic significance from apparently pristine rocks. There seems however to be no evidence to support this proposal [97, 105, 106].

5.8 The Orbital Chemical Data

A fundamental problem on the Moon is how to relate the information obtained from the individual samples and landing sites with overall surface or bulk moon compositions. This problem is much less difficult than might be supposed from analogies with the Earth, on account of the simpler history of the Moon, the uniformity imposed by cratering, and the excellent photogeological coverage. The question whether the landing sites were in some way atypical was resolved by the two orbital geochemical experiments flown on Apollo 15 and 16. One measured the secondary X-rays produced at the lunar surface by the primary solar X-rays. On this basis, data for Si, Al, Fe, Mg and Ti were obtained. A second experiment (the gamma-ray spectrometer) measured the natural radioactivity of the surface, providing information on Th, K and Ti abundances.

The depth of sampling of the XRF experiment was about 10 microns, the "very surface" layer (see Section 4.2), and the data collection was limited, of course, to those areas in sunlight. The gamma-ray experiment, in contrast, probed somewhat deeper, on the order of a few tens of centimeters. Both of these experiments provided exceedingly valuable geochemical data. Although the data base of 3–4 elements might be thought sparse, it will be shown later that it is possible to extrapolate from these numbers to provide nearly complete trace and major element information about the areas surveyed.

The area of the Moon surveyed was limited to the track of the orbiting spacecraft. This was at a high inclination for the Apollo 15 mission (26°), but nearly equatorial (9°) for the Apollo 16 flight. The agreement, where overlap occurred, between data from the two missions was generally within 10%. Correlation with surface sample chemistry was established by measurements over the landing sites. Full details of the analytical methods and the experimental details are given by Adler [107] and Arnold [108]. (For reviews, see [109, 110].)

The spatial resolution of the data is about 50 km for the XRF data and about 70 km for the gamma-ray values. An important initial observation from the Al/Si data is that the ratio is greater in the highlands than in the maria, consistent with the more aluminous nature of the highlands and reflected by the high content of plagioclase feldspar. The first-order observation from the gamma-ray data is that the distribution is exceedingly inhomogeneous, with large values in the western maria regions around Mare Imbrium. This striking evidence for the lateral heterogeneity of the distribution of thorium across the lunar surface exceeds that predicted from the first-order highlands-maria dichotomy. The absolute abundance of thorium in the highlands is also a matter of great consequence for geochemical theories of lunar evolution.

Refinements of the data set have produced an average highland surface crustal value of 0.9 ppm Th [111, 112].

A basic question is the degree to which this surface sampling is representative of deeper layers in the highland crust. This question is addressed in the next section, but some direct evidence comes from the orbital data itself. Data collected over the Aristarchus Plateau reveal that the crater Aristarchus and its ejecta blanket have Th values as high as any on the Moon. The crater has sampled material to a depth of at least 3 km and the "thorium concentration of 12–13 ppm clearly demonstrates that the plateau material "has high concentrations of the radioactive elements" to at least that depth; it does not consist of gabbroic or anorthositic highland material lightly mantled with radioactive volcanic material" [112, 113], although opinions still persist about the "skin-deep" nature of the Th concentrations [114].

Other high abundances of K and Th are located generally around the Imbrium basin, with abundances of about 2000 ppm K and 10–12 ppm Th being common [113]. The Apennine Bench Formation has about 11 ppm Th; although this is sometimes interpreted as evidence for KREEP volcanism, the occurrence of similar values around the Imbrium basin and at the Aristarchus impact crater are interpreted here to indicate that the Imbrium impact sampled a KREEP-rich stratum in the lunar highland crust.

In another context, the presence of high-Al ejecta blankets around Mare Crisium, the Smythii basin and the crater Langrenus indicate that ejecta are coming from a deep Al-rich (hence, plagioclase-rich) layer, contrary to notions that the anorthosites form also a thin surficial layer.

The Kant Plateau, an elevated region to the east of the Apollo 16 landing site, has higher Al and lower Mg concentrations than the rest of the central highlands, leading to suggestions that it might constitute "primordial terra crust" [115, 116] (Fig. 5.24). The Kant Plateau forms part of the rim of the Nectaris basin and must be comprised of primary ejecta from that basin. If this anorthositic material was sampled at the Apollo 16 Descartes site, it could provide an age for the Nectaris event (see Sections 5.10.4). The existence of any remnants of primordial crust is exceedingly doubtful (see Sections 3.1 and 3.6).

The sharpness of the boundaries between maria and highlands is instructive. The Al/Si values in both highlands and maria reflect rather closely the values in the bedrock samples from these areas (Fig. 5.25). Thus, this primary difference in composition persists to the "very surface." This observation places severe constraints on the lateral movement of fine-grained material from the highlands to the maria by dust transfer mechanisms.

A further consequence of the data has been noted with reference to the problem of the origin of the smooth highland plains of Cayley Formation type. The lack of correlation between the gamma-ray data and the areas mapped as Cayley Formation might preclude their derivation as a uniform

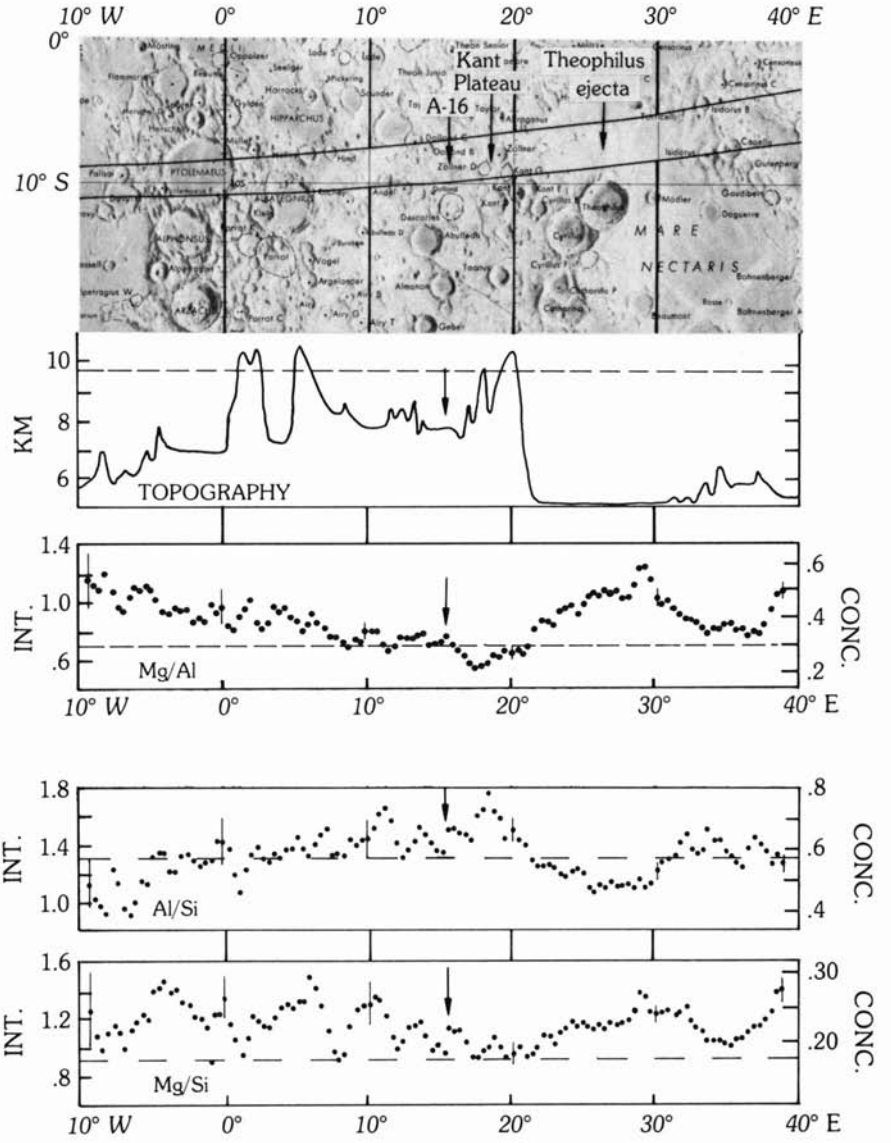

5.24 The variation in topography, Mg/Al, Al/Si and Mg/Si ratios in the vicinity of the Apollo 16 site [115]. (Courtesy C. Andre.)

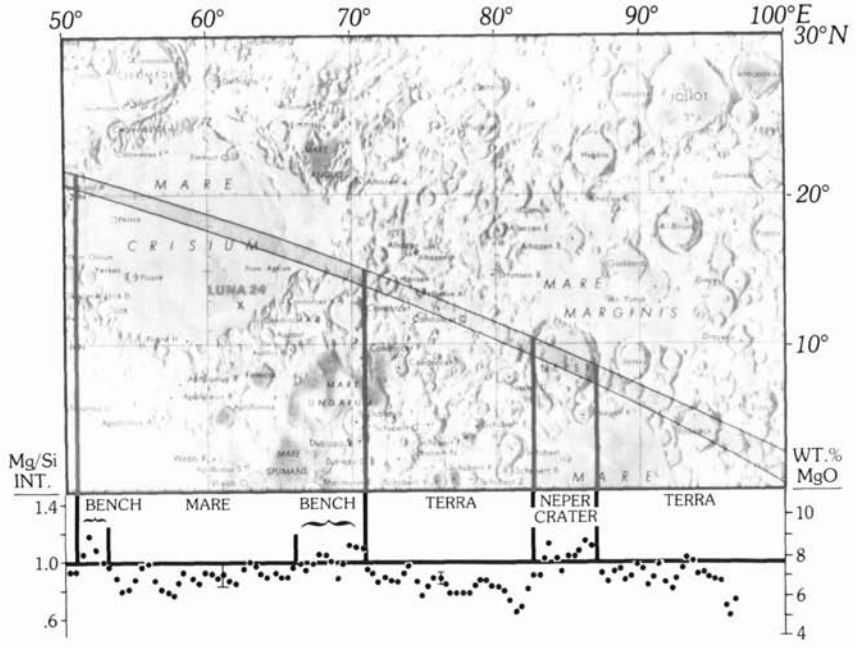

5.25 Highlands-mare contrasts in Mg/Si ratios from orbital data. Note the high-Mg basalts at the edges of Mare Crisium and in the Crater Neper [115]. (Courtesy C. Andre.)

ejecta blanket from a single source but secondary cratering may complicate this picture by excavating older ejecta blankets. The lateral variations in composition indicate that the cratering and ringed-basin formation have not completely homogenized the highland rocks. The belief that the intense cratering might produce an exceedingly uniform highland crustal composition appears unfounded, although the common occurrence of "highland basalt" compositions indicates that mixing is an important process. If terrestrial experience is a guide, this occurs mainly during the production of melt rocks during impacts, and so is limited to a few percent of the target rocks.

Regional geochemical anomalies are probably not due to lateral heterogeneities produced during global differentiation of the magma ocean. This event appears to have been uniform and moon-wide, as is evidenced by the uniform isotopic and chemical characteristics of KREEP on a moon-wide basis. Other factors account for the various geochemical anomalies: (a) basin-forming processes, (b) early reworked mare lavas, (c) buried mare lavas as shown by the presence of dark-halo craters. Thinly buried mare units may make an important contribution to the existence of geochemical anomalies

[117]. Values for Fe [118], Mg [119], and Ti [120] have also been recovered from the gamma-ray data.

5.9 The Chemical Composition of the Highland Crust

Initial observation with low-powered telescopes revealed that the highlands were elevated, relative to the maria [121]. This led to analogies, both for density and composition, to the terrestrial continents. A crucial step was to resolve the nature of the large craters. If these were of volcanic origin, then lunar magmas would possess different properties than those on Earth. The resolution of the crater problem was accomplished effectively by Gilbert and Baldwin (Section 3.2), but the concept of widespread volcanism on the lunar highlands continued, finally influencing the selection of the Apollo 16 landing site. The terrestrial continent analogy suggested the possibility that the lunar highlands were of granitic composition [122, 123]. This concept was reinforced by two factors: (a) Detailed mapping of the highlands revealed the presence of light plains units of varying stratigraphic age, which would be consistent with deposition by a mechanism analogous to terrestrial ignimbrite eruptions. The highly viscous lavas required to generate such ash-flow deposits would necessarily be acidic, analogous to terrestrial dacites or rhyolites in composition [124]. (b) This concept was agreeable to those workers who wished to derive tektites from the Moon, since it provided an acidic source material. The distinctions between the composition of terrestrial rhyolites and tektites were ignored.

The first direct analysis of the lunar highland surface by Surveyor VII, on the rim of Tycho, revealed a totally different composition, similar to terrestrial high-alumina basalt [125], and widely different from granitic compositions. The first clue to the mineralogical nature of the highlands came from the discovery of anorthosite fragments in the Apollo 11 soil samples [126]. This immediately suggested a possible resolution to a major geochemical dilemma by providing a sink for europium. Thus began the "magma ocean" concept.

The next surprise was the discovery at the Apollo 12 site of the light gray fines (e.g., 12033) and rock sample 12013, both enriched to an extraordinary degree in large ion lithophile elements [127]. The evidence for an extreme degree of element fractionation, reminiscent of the concentrations observed in terrestrial pegmatites, was dramatically reinforced by the Apollo 14 sample return from Fra Mauro [128]. The existence of large areas of K-rich material (KREEPUTH) at the lunar surface, indicated by the gamma-ray orbital data, led to new concepts of the origin of the highland crust. Since the Fra Mauro site was on the Imbrium ejecta blanket, these unusual compositions focused attention on possible sources, either local or from within the Imbrium basin.

Attempts to explain the chemical composition of the crust with its high content of refractory elements led quickly to the development of heterogeneous accretion models [129]. The late addition of a layer rich in refractory elements at first appeared to pose fewer problems than those caused by melting and cooling of large volumes of the Moon, since this was required to happen at a very early stage of lunar history. The geochemical debate over homogeneous versus heterogeneous accretion, which led to some extremely high-alumina moons [130], was eventually resolved in favor of homogeneous models (or homogenization after accretion) [131]. The key evidence was the recognition that the ratios of volatile/refractory elements were similar in mare basalts (derived from the deep interior) and in the highland crust [132]. This linking of the highland chemistry with that of the source regions of the mare basalts provided a ready explanation for the europium anomalies and many other geochemical problems [74].

Meanwhile, the sampling problems persisted. How representative of the crust were the surface samples, and how might they be related to the Al/Si and Th values derived from the orbital geochemistry experiments? A solution to this problem was proposed by the Apollo soil survey [133], in which the proposition was advanced that the glass spherules formed during impact would be representative of the principal components of the highland crust. (Composition of the spherules could be rapidly determined by microprobe analysis.) The amount of mixing which has occurred and the tendency of impact melts to homogenize differing source rocks [30] render this approach less useful for distinguishing "primordial" rock types [45]. If these conclusions are valid, then there should be a prominent grouping of glass compositions, representing the average crust. The "highland basalt" composition (26% Al_2O_3) [133] probably meets this criterion. Other samples of granulitic breccias (e.g., 67955, 76230, 77017, 78155, 79215) [134] have bulk compositions close to that of the average highland crust.

5.9.1 Element Correlations

The observation that many of the refractory trace elements were correlated in lunar highland samples of differing composition, and from different landing sites [135, 136], is a key which enables estimates to be made for the abundances of many trace elements.These can be related via the gamma-ray thorium abundances to moon-wide compositions. By this means, estimates for average lunar highland surface compositions can be made.

These correlations among many distinctive elements in the highland samples (Fig. 5.26) have been instructive to geochemists [137]. The correlations depend on various factors such as similarity of geochemical behavior due to resemblances in ionic radius, valency or bond type which lead to conventional geochemical coherence [e.g., K/Rb, Th/U, Zr/Hf, REE (except

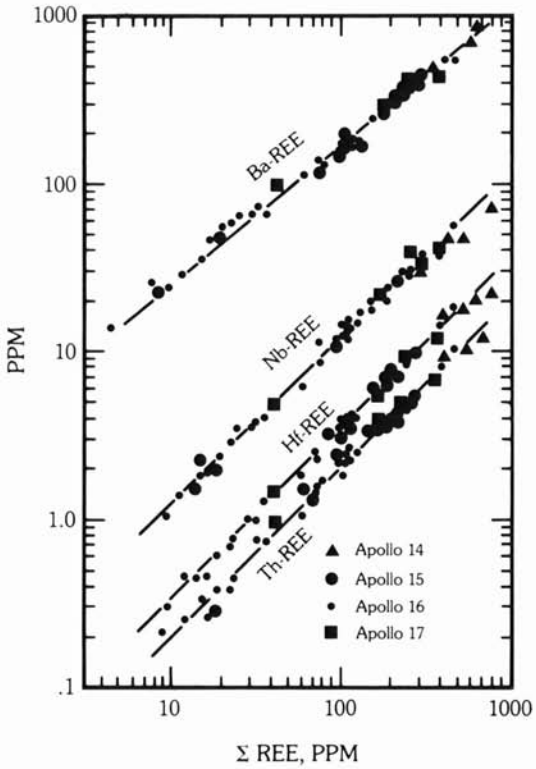

5.26 The close correlation observed between many involatile elements in the highland samples. In this diagram, the abundances of Ba, Nb, Hf, and Th are plotted against total REE abundances. Correlations with individual REE would be similar. Many other similar correlations exist. These shown here are selected to emphasize the correlations between elements of dissimilar geochemical behavior.

Eu), Ba/Rb, Rb/Cs, Fe/Mn], and concentration of incompatible elements into residual melts (e.g., K/U, Zr/Nb, K/Zr, K/La). This type of correlation needs to be treated with the understanding that it is not due to fundamental geochemical properties, but is accidental to some degree. The fact that these correlations are highly significant statistically indicates the degree of uniformity in crustal processes on the Moon. The close correlations between volatile and refractory elements (K/U, Ba/Rb, K/Zr, K/La) both in mare and highland samples indicates that both regions were originally homogeneous with respect to volatile and involatile elements. This is a primary piece of evidence for homogeneous accretion of the Moon, or homogenization following accretion.

Correlations resulting from mixing of different rock types during intense cratering of the highlands is a further process that will contribute to the observed close inter-element ratios in highland samples. The fact that the chemistry of the highland samples appears to be controlled by three end-member components (anorthosite, Mg-component and KREEP), and that the large ion lithophile element abundances are dominated by the KREEP component, lead us to expect simple element correlations.

Table 5.5 Highland crustal composition, compared with data from granulitic breccia 78155.

Oxide	wt.%	78155	Element	ppm	78155	Element	ppm	78155
SiO_2	45	45.6	La	5.3	4.0	U	0.24	0.28
TiO_2	0.56	0.3	Ce	12	10.2	Th	0.9	1.0
Al_2O_3	24.6	25.9	Pr	1.6	1.5	Th/U	3.8	3.6
FeO	6.6	5.8	Nd	7.4	6.3	K/U	2500	2320
MgO	6.8	6.3	Sm	2.0	1.81	Zr	63	54
CaO	15.8	15.2	Eu	1.0	0.87	Hf	1.4	1.49
Na_2O	0.45	0.3	Gd	2.3	2.3	Zr/Hf	45	36
K_2O	0.075	0.08	Tb	0.41	0.39	Nb	4.5	—
Cr_2O_3	0.10	0.10	Dy	2.6	2.6	Zr/Nb	14	—
			Ho	0.53	0.61	Ti	3350	—
Element	ppm		Er	1.51	1.69			
Cs	0.07	0.11	Tm	0.22	—	Cr	680	680
Rb	1.7	2.1	Yb	1.4	1.73	V	24	—
K	600	650	Lu	0.21	0.26	Sc	10	13
Ba	66	59				Ni	100	80
Sr	120	147	ΣREE	39.3	34.3	Co	15	14
			Eu/Eu^*	1.4	1.3	Fe%	5.13	4.51
			Y	13.4		Mg %	4.1	3.8

Data sources for 78155:

Warner, J. L., et al. (1977) *PLC 8:* 2057.
Wänke, H., et al. (1976) *PLC 7:* 3482.
Hubbard, N. J., et al. (1974) *PLC 5:* 1235.

The preservation of so many element correlations in highland rocks is thus a predictable consequence of mixing of a few components. The parallel nature of the REE patterns is only the most striking of these, since any igneous fractionation would change the slopes of the patterns. These correlations greatly facilitate the calculation of highland crustal abundances.

5.9.2 Highland Crustal Abundances

In this section a table of element abundances (Table 5.5) in the lunar highlands is presented. The method used is similar to that described previously ([137], pp. 249–253) and the details are not repeated here. The technique is to employ the orbital data to provide moon-wide averages, at least over the orbital tracks. Thus, the averages are not dominated by a specific region [138].

Al/Si and Mg/Si ratios from the orbital data for the highlands are 0.62 (± 0.10) and 0.24 (± 0.05), respectively. Concentrations of $Si0_2$ are relatively uniform at 45% in highland samples, yielding values of 24.6% Al_2O_3 and 8.6% MgO. A value of 6.6% FeO is obtained from the MgO/FeO relationship observed in the highland soils and breccias. This value compares with 6.9%

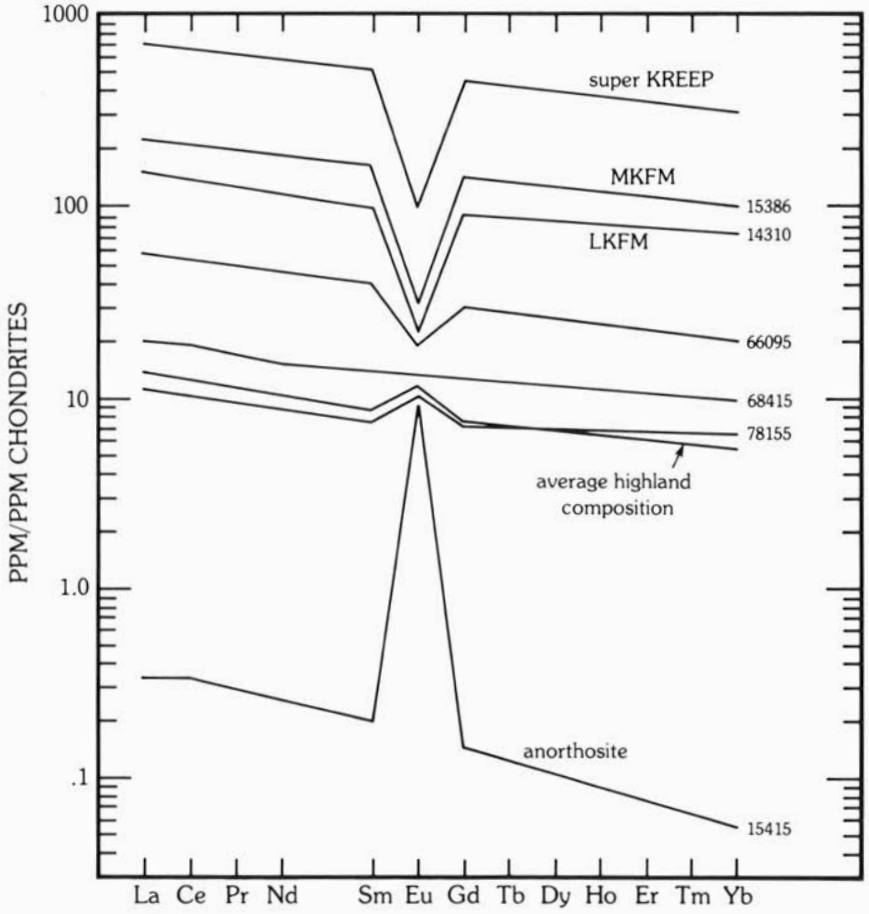

5.27 Rare-earth element abundances in various typical highland rock samples. Data from Table 5.3. Note that the average highland composition proposed in this book shows enrichment in europium, and is close in compostion to the granulitic breccia 78155.

FeO from the orbital data [118]. MgO orbital values average 6.8% [119], being lowered by the far-side highland values in comparison with the sample data. The orbital value is adopted here. From the Fe/Cr relationship, a figure of 0.10% Cr_2O_3 results. Allowing a typical lunar Na_2O abundance of 0.45%, the remaining major constituent is CaO, which yields, by difference, a value of 15.8%. This value is consistent with that observed in samples of this approximate composition and with the Ca/Al relationship. The Th value is 0.9 ppm [111, 112]. Using a Th/U value of 3.8, then U = 0.24 ppm; from the lunar K/U ratio of 2500, then the K abundance is 600 ppm [137] which is in

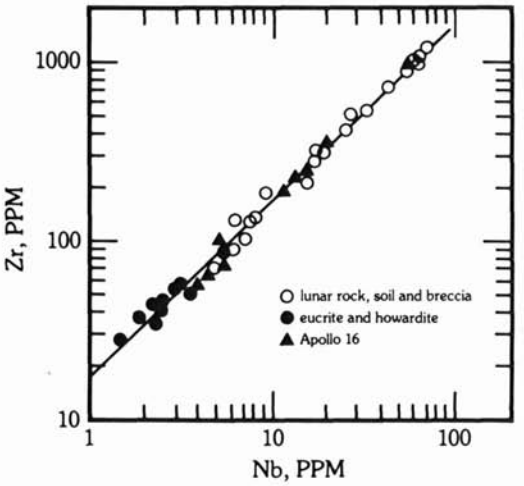

5.28 The correlation between zirconium and niobium for lunar samples and the howardite and eucrite groups of meteorites [140].

agreement with a recent orbital average estimate of 500 ppm [139]. Rubidium and cesium values are calculated from K/Rb = 350 and Rb/Cs = 24.

From the Th/REE correlation (Fig. 5.26) a total REE value of 39 ppm is obtained. Assuming that the La/Yb ratio is the same as for other highland rocks, REE values can be obtained from the data illustrated in Fig. 5.27, where the average pattern is compared with the other highland REE data. The pattern is rather close to that of "highland basalt" [137], consistent with the derivation of that well-known composition by overall mixing during impact events. A notable consequence is that the europium enrichment in the highland crust is pronounced ($Eu/Eu^* = 1.4$). Since the overall lunar REE pattern has no Eu anomaly (Chapter 8), the origin of this europium enrichment in the highlands is a major factor to be explained in theories of highland crustal formation.

Values for the other trace elements (Ba, Hf, Nb) may be derived from the data illustrated in Fig. 5.26. Values for Zr come from the well-marked Zr/Nb correlation (Fig. 5.28)[140]. Yttrium values are derived from the similarity of chondrite-normalized Y and Ho values. Cr/V and Cr/Sc ratios (Table 5.5) provide V and Sc values while Sr values are derived from Sr/Eu and Rb/Sr ratios.

The composition in Table 5.5 is considered to be representative of the overall highland crustal surface (as noted above), in the same manner as estimates of continental crustal composition are representative of the terrestrial crust. For comparison, the composition of the granulitic breccia 78155 is given in Table 5.5. The abundances of both major and trace elements in this sample are remarkably close to the average highland composition, derived from a differing set of criteria. The next step, extending these results to draw

conclusions about the composition of the total highland crust, is less readily taken. How representative is this surface composition to that of the bulk highland crust to depths of 60–80 km? How reliable are the geophysical estimates of crustal thickness? Does the crust vary laterally in chemistry and/or thickness? From what depth are samples brought to the surface by the large impacts which form the ringed basins? How much mixing and homogenization has resulted from these and smaller collisions? These questions have been debated throughout the text (see Chapters 2 and 3, especially), and they will be addressed again in Chapter 8. The overall evidence indicates that this composition is representative of the upper 30 km of crust at least. Probably it extends to the base of the crust, although this may be irregular due to mantle uplift during multi-ring basin formation.

The consequences of a more aluminous composition, which will lower the crustal density (Section 7.2), is that a thinner crust will accommodate the geophysical requirements; conversely, a less aluminous crust needs to be thicker. The crustal composition discussed here forms about ten percent of the lunar volume, so that the elemental concentrations comprise a significant fraction of their whole moon abundances (Section 8.4), in contrast to those of the mare basalts which comprise perhaps only 0.1% of the lunar volume.

5.10 Age and Isotopic Characteristics of the Highland Crust

5.10.1 The Oldest Ages

Few samples of the highland crust have avoided having their isotopic systems reset by the meteoritic bombardment. These include the black and white breccia 15455, of which the white portion yields an Rb-Sr age of 4.52 aeons, and the dunite (72417) (Fig. 5.29). How reliable are these old ages? All show some signs of disturbed isotopic systematics, with data points falling off the isochrons.

Redistribution of volatile elements such as Rb (Section 4.5.2) is particularly likely and may affect KREEP ages. Some debate exists over the effects of impact in resetting ages. Studies at the Ries Crater show that granite clasts shocked to 450 kbar have lost most (99%) of their radiogenic ^{40}Ar [141], hence the view that only melted rocks which have reset ages need reconsideration. Rb-Sr isochron ages of greater than 4.5 aeons have been obtained for troctolite 76535. Other methods give younger ages. For 76535, both Sm-Nd and Ar-Ar methods yield ages near 4.3 aeons, distinctly younger than the Rb-Sr age, but these may represent excavation ages from a deep hot crust. However, the initial $^{87}Sr/^{86}Sr$ ratios are close to BABI, and no pre-4.6 AE ages were obtained. Accordingly, these old ages are probably meaningful [142]. A summary of those samples which yield very old ages is given in Table 5.6 and

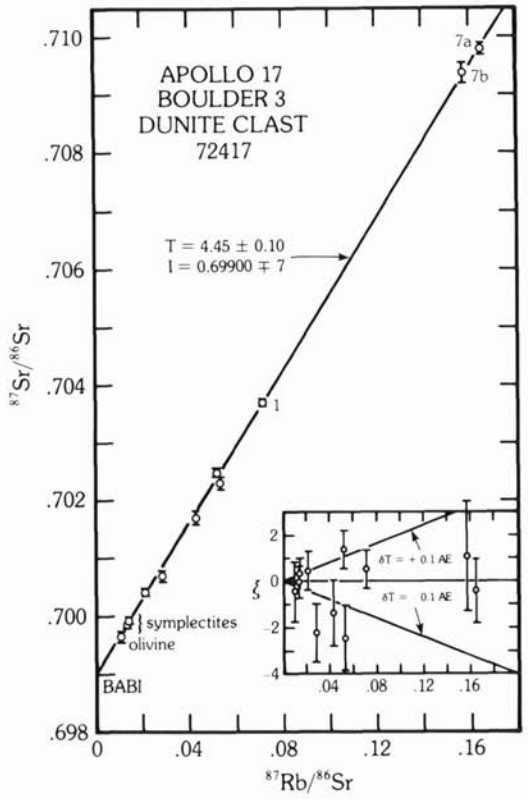

5.29a The oldest lunar rocks. Rb-Sr evolution diagram for mechanically separated samples of the dunite. The insert shows deviations ξ (in parts in 10^4) of the measured $^{87}Sr/^{86}Sr$ from the best-fit line. The present measured enrichment in $^{87}Sr/^{86}Sr$ is 1.4%. The initial $^{87}Sr/^{86}Sr$ of the dunite is essentially equal to BABI = 0.69898.[Papanastassiou, D. A., and Wasserburg, G. J. (1977) *PLC* 6: 1473.]

Fig. 5.30. Their significance is considerable. They provide additional evidence for crustal formation at times around 4.4 aeons. The principal conclusion is that the highlands crust is very old, dating back almost to the origin of the solar system.

The existence of such ancient lunar ages places very tight time constraints not only on the accretion of both Earth and Moon, but also on their possible relationship, fission origins and time of melting of the outer portions of the Moon. By 4.4 aeons, solid-liquid equilibria must have already acted to establish both the isotopic and chemical characteristics of the mare basalt source regions (Section 6.4) and the reciprocal nature of mantle and crustal geochemistry. Nevertheless, a solid crust in the sense that we observe it today may not have been in evidence. The existence of formed bodies of crustal rocks prior to 4.2 aeons is conjectural on account of the "stonewall" effect [143].

The age of the Earth and meteorites is usually given as 4.56 aeons. This age dates the time of fractionation of the U-Pb system from low values of

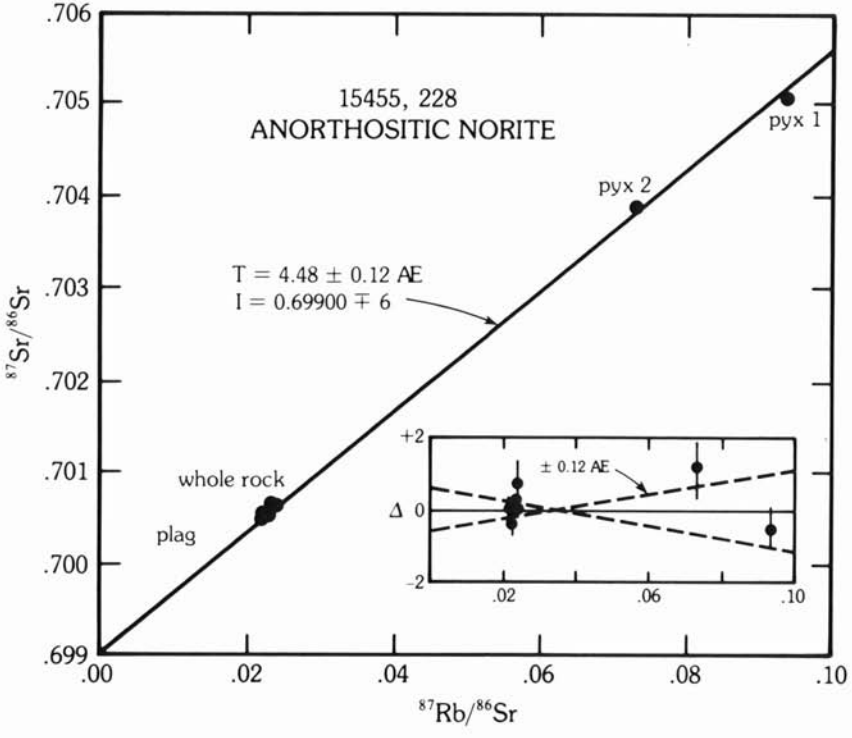

5.29b The oldest lunar rocks. An isochron age of 4.48 aeons for the anorthositic norite 15455, 228. (Courtesy L. E. Nyquist.)

Table 5.6 Old ages on highland crustal rocks.

Rock Sample		Age	Reference†
15455	Anorthositic gabbro (Rb-Sr)	4.48 ± 0.10	1
72417	Dunite (Rb-Sr)	4.45 ± 0.10	2
76535	Troctolite (Rb-Sr)	4.61 ± 0.07	3
77215	Norite (Rb-Sr, Sm-Nd)	4.4	4
78236	Norite (Sm-Nd)	4.49	7
Various anorthosites ($^{40}Ar/^{39}Ar$)		4.4 – 4.5	5,6

†References:

1. Nyquist, L. E., et al. (1979) Lunar Highlands Conf. Abstracts, 122.
2. Papanastassiou, D. A., and Wasserburg, G. J. (1975) *PLC 6:* 1467.
3. Papanastassiou, D. A., and Wasserburg, G. J. (1976) *PLC 7*: 2035.
4. Nakamura, N., et al. (1976) *PLC 7*: 2309.
5. Dominik, B., and Jessberger, E. (1978) *EPSL.* 38: 407.
6. Huneke, J. C., and Wasserburg, G. J. (1979) LPS X: 598.
7. Carlson, R. W., and Lugmair, G. W. (1979) Lunar Highlands Conf. Abstracts, 9.

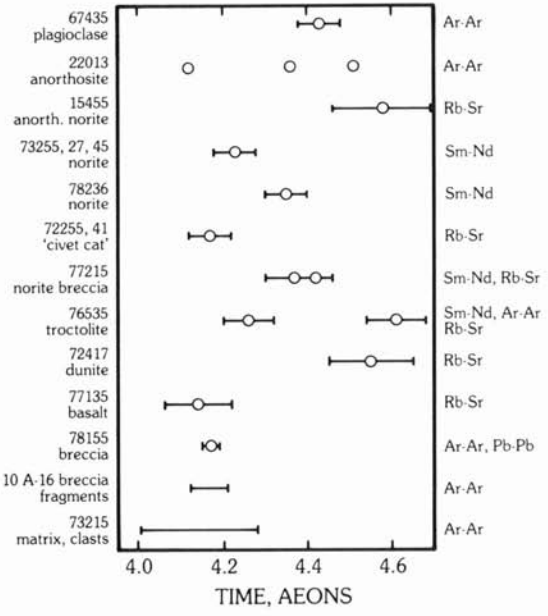

5.30 List of lunar highland samples with ages greater than 4.1 aeons. Multiple ages listed for single samples indicate discrepancies between data obtained from different radiometric systems, or multiple plateau ages from ^{40}Ar–^{39}Ar studies. The samples listed belong to the Mg-rich suite with the exception of 22013 (anorthosite), 77135 and the 73215 matrix clasts. [Carlson, R. W., and Lugmair, G. W. (1981) *EPSL.* *52*: 235. Courtesy G. W. Lugmair.]

μ ($^{238}U/^{204}Pb$) of the average solar system material (0.3) to primitive terrestrial values of about 7.5. Whether or not this fractionation occurred before, during, or after the accretion of the Earth, it *is* clear that it occurred close to the accretion event (within 20 ± 10 million years).

The following sequence of events thus had to occur within 150–200 million years of the general accretion of the solar system:

(a) Accretion of the Moon (from previously fractionated material not of solar nebula composition).
(b) Melting of at least the outer half and probably the whole Moon.
(c) Crystallization of the magma ocean to provide the old anorthosites, troctolites and dunites.
(d) Formation and isotopic closure of the source regions of the mare basalts.
(e) Invasion of the highland crust by the residual liquids from the crystallization of the magma ocean.

The next question to be addressed is the time at which early differentiation of the crust occurred. An age of 4.46 aeons for the time of the crustal differentiation is derived from the U-Pb-Th systematics [144] (Fig. 5.31). The Rb-Sr and Sm-Nd systematics combine to yield somewhat younger ages; however, crystallization of the magma ocean was apparently complete by 4.35 aeons. We note again the problems associated with determining this age from

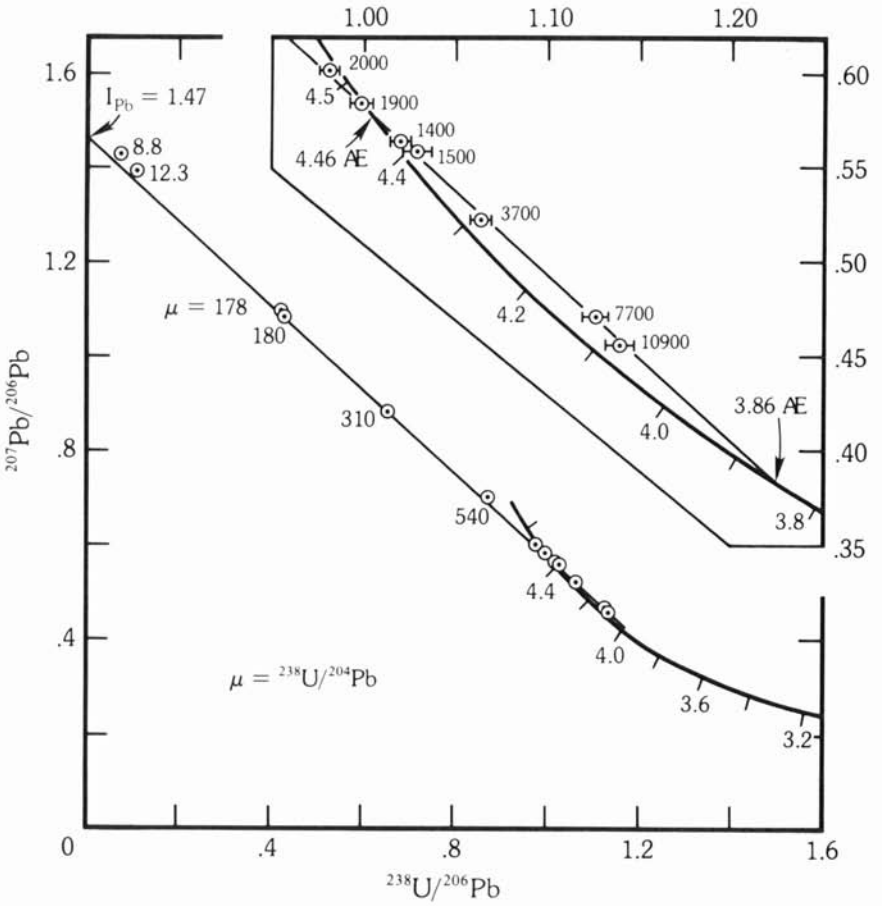

5.31 U-Pb evolution diagram for highland breccias. Inset shows data points near concordia curve with error bars. The measured value of $\mu = {}^{238}U/{}^{204}Pb$ is given for each sample. Of 13 data points, 10 lie precisely on a line intersecting concordia curve at 4460 m.y. and 3860 m.y. The upper intersection represents the time of early lunar differentiation and crust formation. The lower intersection corresponds to a time of intense bombardment, which has reset the ages. Samples whose data points do not plot precisely on the line may have impact ages slightly different from 3860 m.y. The bombardment affected almost all lunar highland rocks, causing severe U/Pb fractionation in the breccias. This is reflected by the linear distribution of the data points on the graph and the strong correlation of μ values with position of the data points [144]. (Courtesy G. J. Wasserburg.)

highland crustal rocks, in which the systematics may be reset down to 4.2 aeons or to younger times by the meteoritic bombardment.

5.10.2 The 4.2 Aeon Ages

A number of highland samples have ages of about 4.2 aeons. An extensive investigation of Apollo 16 breccias carried out by Maurer et al. [145] established three age groups based on $^{40}Ar/^{39}Ar$ using new decay constants; 48 soil samples from the 2–4 mm fines collected near North Ray crater (50 million years old) were investigated. The oldest group had ages from 4.06–4.15 aeons and were all anorthositic. These are regarded as coming from impact craters up to a few hundred kilometers in diameter, which excavated an upper anorthositic layer. This might, however, represent the Kant Plateau anorthositic layer recognized by high Al/Si ratios (Section 5.8) (most probably primary Nectaris ejecta) and so date the Nectaris event itself. The second group had ages from 3.83 to 3.96 aeons and were noritic anorthosite and anorthositic norite breccias. These showed a higher degree of annealing (melted matrix) and contained one totally melted KREEP basalt. This group was considered to be connected with the Nectaris basin-forming event, which in this model had sampled deeply enough to excavate deep-seated KREEP. Most ages in this group are from 3.83 to 3.96 aeons. Their interpretation gives an age for the Nectaris event of 3.92 aeons, supporting the multi-impact cataclysm model in which Nectaris and other major basins were formed within a 0.1 aeon time span. This interpretation is model dependent. The older ages might well be due to the Nectaris event. If they are not, it might reasonably be inquired which event is in fact represented by them. The third group was composed of much younger breccias (< 2.5 aeons). Only one of the 48 samples fell outside the three groups; its age was 3.55 aeons and it is thought possibly to have come from Theophilus (100 km diameter), which is within three crater diameters of the Apollo 16 site. Rb-Sr dates on a suite of pristine anorthosites yielded ages of 4.17 ± 0.20 aeons (2σ) with an initial ratio of 0.69906 ± 2, which is within the error limits of LUNI (0.69903), as defined by the purest anorthosites [146]. These samples, which contain high Sr and low Rb concentrations, are the best candidates for preserving primitive $^{87}Sr/^{86}Sr$ ratios. A "pristine" lherzolite yields an Sm-Nd isochron of 4.18 aeons [147]. Several questions are raised by these and similar data and various interpretations are possible. For example:

(a) Crystallization of the lunar highland crust lasted until about 4.2 aeons.
(b) Crystallization of the main magma ocean was complete at 4.4 aeons, but some of these samples are the products of later intrusions into the crust.
(c) The isotopic systems remained open until about 4.2 aeons due to high temperatures within the crust. Thus, the 4.2 aeon ages could either represent excavation ages, or the time at which the temperature became low enough to close the isotopic systems.
(d) The ages are reset by the bombardment.

Many of the ages are $^{40}Ar/^{39}Ar$ ages, and it is generally considered that these were reset during large cratering or basin events, with opinions differing as to whether the age distribution is dominated by the large basin impacts [148, 149, 150] or during formation of medium-sized craters [151]. Argon loss or retention may occur as a result of (a) heating or melting during crater formation, (b) annealing in a hot ejecta blanket, either in a short time at high temperatures or over a long period at lower temperatures, (c) uplift and cooling following a major basin impact (this only works for large impact basins where the depth of excavation is many kilometers) and (d) crystallization from either a primary igneous or meteorite impact melt [148]. Few highland samples appear to belong to this igneous category. Both 14310 and 68415 are impact melts.

There are several arguments in favor of the resetting of argon ages by big basin impacts rather than by small craters. There are many examples of rocks which are identified as coming from young lunar impact craters, such as North Ray, Camelot or Cone. There are no examples where any significant resetting of the ^{40}Ar-^{39}Ar ages has occurred as a result of the formation of these kilometer-sized craters [148].

Examples exist of a few highland rocks which have been reset at times younger than 3.8 aeons. These include 14318, 61016 and 63335 which yield ages of 3.7 aeons. The anorthosite 60015, which has a glass coating, gives a well-defined age of 3.50 aeons [150], which cannot be due to a basin-forming event. Since the number of large craters younger than 3.0 aeons is small (about 15), the chances of finding rocks reset by these events (e.g., by Copernicus or Tycho) are likewise small.

Table 5.7 Calculated temperatures and heating times required to produce 70% argon loss from lunar anorthosites.

Temperature θ (°C)	Heating time† τ (years)	Conduction length* a	Depth§ d (km)
720	1	4(m)	24
560	10^2	40	19
450	10^4	400	15
370	10^6	4(km)	12
300	10^8	40	10
270	$5 \cdot 10^8$	90	9

† The time required to produce 70% argon loss is calculated by extrapolating laboratory diffusion data assuming an activation energy of 50 (kcal mole^{-1}K^{-1}).

* $a = (2\kappa\tau)^{1/2}$ is the depth from which significant heat loss can occur (e.g., from an ejecta blanket in time τ). Calculated using $\kappa = 10^{-5}$ km^2 year^{-1}.

§ $d = \theta/(d\theta/dz)$ is the depth below the surface at which time the ambient temperature equals θ. Calculated assuming $(d\theta/dz) = 30°C\ km^{-1}$.

Turner, G. (1977) *PCE* 10:181.

The high frequency of $^{40}Ar/^{39}Ar$ ages of 3.8 aeons in the lunar highlands may be due to resetting by excavation from depths below the 350° C isotherm. Although heating during the basin-forming process may be minor and the ejecta blankets are cool, rather than hot, nevertheless, much melt is produced in these events.

Table 5.7 shows the time needed to lose 70% of argon for various temperatures and inferred depths of burial. It must be recognized, however, in contrast to terrestrial examples, that multiple impact histories are involved. Even though the amount of melt, and thus igneous appearing rocks with reset ages may be small in each event, the cumulative total due to the extended bombardment history explains the rarity of ages older than about 4.2 aeons.

5.10.3 Basin Ages and the Lunar Cataclysm

This topic has many implications for lunar history, with diverse conclusions being reached from isotopic and cratering studies. A principal difficulty is to identify samples as resulting from particular basin-forming collisions. This is becoming more difficult as we understand the complexities of large collisions, the likely temperatures in ejecta blankets, and the relative roles of secondary and primary ejecta. A recent survey of basin ages has been given in *Basaltic Volcanism on the Terrestrial Planets* (Chapter 7 [152]).

Nectaris Basin

There is considerable controversy over the age of this basin. The Descartes site, sampled at Apollo 16, is only 60 km from the outer rim of the Nectaris basin, and accordingly, primary ejecta from that basin must be present at depth. The Cayley plains are too young to be Nectarian, but the hilly Descartes Formation might represent primary ejecta. If so, two possibilities exist for sampling. North Ray crater may have excavated deeply enough to sample it. Alternatively, samples from stations 4 and 5 on Stone Mountain may be of Nectaris ejecta (see Section 5.8 on Kant Plateau). A Nectaris age of 4.2 aeons was assigned by Schaeffer and Husain [150] from analyses of Apollo 16 site material. The work reported earlier by Maurer et al. [145] is relevant here. They considered that the older (> 4.06 aeons) ages represented medium-sized impacts. The large number of 3.83–3.96 aeon ages were thought to come from a basin-sized impact which dug deeply enough to penetrate a conjectured upper crustal anorthosite layer, and excavate KREEP rich material. This was considered to be the Nectaris event, and hence these data provide an age of 3.92 aeons for Nectaris. This interpretation is dependent on our models of the highland crust. A reasonable case can be made that the anorthositic Kant Plateau is primary Nectaris ejecta. Accordingly, the anorthositic samples with 4.06 aeon ages might be derived from this region and so date the Nectaris event. At least two other possibilities exist.

Imbrium secondaries might have plowed up Nectarian ejecta, or the site is dominated by primary Imbrium ejecta [20]. An unknown contribution from Serenitatis primaries or secondaries may be present.

Serenitatis Basin

Various age estimates from the Apollo 17 site converge on 3.86 aeons as a probable age for this basin excavation. However, this estimate has not gone unchallenged. The highland samples collected at the Apollo 17 site are dominated by poikilitic, impact-produced melt breccias, not necessarily Serenitatis ejecta, but possibly deeper uplifted material.

A separate class of rocks are identified as aphanitic (crypto-crystalline—too fine grained to be readily visible). These light-colored rocks occur at Boulder 1 at Station 2 (73215, 73235, 73255), and have different chemistry, clast populations and petrography, compared to the more common impact melts, and are thought to come from shallower depths. Wood [153] suggested that they came from deep within the basin and were average crustal samples. Dence [154] suggested that the average crust was of low-K Fra Mauro composition, which is unlikely, particularly since granulitic breccias such as 78155, matching estimates of highland crustal compositions from the Apollo 16 site, are present. Spudis and Ryder [155] suggest that samples from smaller impacts such as Littrow (30-km diameter, 50 km from the landing site) and Vitruvius (30-km diameter, 80 km from the landing site) are possible candidates. They suggest that the Taurus-Littrow highlands are not dominated solely by Serenitatis ejecta, but rather have a complex multiple-impact history involving other basins.

Imbrium Basin

This is usually dated from the Apollo 14 site, where most of the KREEP-rich melt rocks have ages of 3.82 aeons (e.g., 14310, 14073, 14276, 14001). The general interpretation of 14310 as an impact melt has lent credence to this as dating the age of the Imbrium event. Basaltic clasts within the Apollo 14 breccias have ages of 3.86–3.88 aeons. There appears to be a general consensus about this age for a number of reasons. The oldest ages from the mare basalts are only just younger (and indeed 10003 is older!) so that there is some agreement between the geochronologists and the geologists on this interpretation. The possibility that the Apollo 14 samples are local material, merely disturbed by the Imbrium event [30], seems less likely. The Apollo 14 site at Fra Mauro is only 550 km from the main Imbrium rim and the material there must have a high component of primary ejecta from Imbrium. How much of this material was melted and reset, and how much of the ejecta blanket was cold is a matter of debate. The presence of thermal effects and of local magnetic fields is taken to indicate the presence of local pools of melt within the ejecta blanket. The problems of Cayley-type plains and the importance of

secondary ejecta should not be over-emphasised at the Apollo 14 site, close to the Imbrium basin rim.

The Lunar Cataclysm

One interpretation of the age data given here could support the concept that Nectaris and the post-Nectarian basins all formed within about 100 million years. There are, as noted earlier (Section 3.14), many pre-Nectarian basins, and the occurrence of several large collisions in such a period is not suggestive of a spike in the cratering flux and depends heavily on interpretation of individual samples. The principal philosophical support is the agreement about the Imbrium age, dated at 3.82 aeons. This is based on the analyses of the melt rocks at the Apollo 14 site and the assumption that these date the Imbrium event. The South Serenitatis basin event has a possible age of 3.86 aeons. The Nectaris basin may have an age of 3.92 aeons, although the older ages of 4.1 aeons seem equally likely to date the Nectaris event [150]. There are sufficient uncertainties in the interpretation of the age data and in the assignments to specific basins to make the cataclysm a non-unique interpretation. Even on the most conservative assumption, the cataclysm does not appear to be remarkable. Between Imbrium and Nectaris, only the formation of twelve multi-ring basins occurred. Imbrium was followed by Orientale, but Nectaris was preceded by 29 basins (Appendix IV, Table 3.1).

5.11 Evolution of the Highland Crust

The processes which formed the highland crust are in principle rather simple, but the details are complex, as is typical of most geological processes, recalling the statement of Urey that "Nature has a great capacity to produce most surprising results within the limitations of the basic laws of physical science." The anorthosite component is derived from flotation of plagioclase during crystallization of the magma ocean. The Mg-rich component is derived principally from trapped cumulus liquids with some probable later intrusions, while the KREEP component represents the final residual melt from the magma ocean which invades the highland crust. This scenario is complicated by the details of crystallization of the magma ocean and by the repeated infalling of large projectiles, which continued well beyond the crystallization of the magma ocean at about 4.4 aeons. The detailed processes responsible for the evolution of the highland crust are now considered.

5.11.1 The Magma Ocean

There is a considerable amount of evidence in support of the concept of large scale lunar differentiation. Geochemical balance problems provide one argument. The lunar highland crust is generally considered to be at least 60

km thick and contains perhaps 25% Al_2O_3. Reasonable lunar compositions do not exceed 6% Al_2O_3 so that the amount of aluminum in the highland crust is about 40% of the total lunar budget. Potassium, uranium and thorium are concentrated near the lunar surface by two orders of magnitude in excess of their lunar abundances. Europium is concentrated in the highland feldspathic crust to about the same degree as aluminum, and is depleted in the source regions of the mare basalts. Upper limits for the U content are set by heat flow as well as by overall cosmic abundance arguments. The isotopic data (Pb, Sm-Nd, and Rb-Sr) all point toward large-scale early differentiation. The Sm-Nd systematics of KREEP, which are uniform from all landing sites, imply a moon-wide event. In all these debates, an integrated approach is required involving geophysical models for crustal structure and thickness, and geochemical models which integrate orbital and sample data. The mere existence of a single differentiated rock sample does not, of course, imply moon-wide differentiation nor justify the existence of magma oceans. No one proposes that lunar "granites" are widespread or demand more than trivial amounts of parent material. It is the combination of the whole set of evidence which requires moon-wide differentiation.

The geochemical evidence does not specify the physical state of the initial differentiation. It does necessitate the operation of crystal-liquid fractionation on a moon-wide scale so that, for example, 50% of the europium and a similar amount of the potassium content of the bulk moon now reside in the lunar highland crust, which comprises about ten percent of the lunar volume. This may be carried out either by an extended sequence of small melting episodes, or by a magma ocean. For simplicity, the concept of a single magma ocean is adopted throughout the text since the geochemical evidence demands that most of the Moon was involved in a crystal-liquid fractionation sequence.

This differentiation must be completed quickly, in planetary terms. The time constraints on this process are discussed in Section 5.11.2. Less than 200 million years are available, and even less time (100 million years) if the accretion of the Moon takes 10^8 years. It is thus tempting to associate the differentiation and the thermal energy required with the lunar accretionary process. In contrast, the melting and eruption of the mare basalts does not require a massive energy source. They comprise about 0.1% of the lunar volume so that the amount of heat necessary to form them by partial melting in the lunar interior is over three orders of magnitude less than that required for the initial differentiation. Although various questions have been raised about the possible existence of the magma ocean, the alternatives are even less attractive and "the one time existence of a magma ocean is a reasonable conclusion"[156].

The question of the initial depth of the magma ocean is relevant here. Estimates have ranged from 200 km [157] to whole-moon melting [158].

Estimates of 800 km (85% of the lunar volume) [74], consistent with models of internal structure, were proposed at an early stage. The possible presence of a discontinuity at 400–480 km is not uniquely specified by the seismic data (Section 7.6.1) and is not considered to be a reasonable constraint. The requirement for concentration of elements into the lunar crust requires minimal depths of 500 km [159, 160], but more realistic depths exceed 800–1000 km [161]. If a lunar core is present, as is argued in Sections 7.6.2 and 8.4, then whole moon melting is effectively demanded. The geochemical necessity for massive near-surface concentration of elements by crystal-liquid fractionation is most readily accommodated by whole moon melting. It should be noted here that effectively all mare basalts have negative europium anomalies (Section 6.3.3) so that a massive removal of that element into the crust has occurred.

The possibility that mare basalts are derived by partial melting mainly from depths of 400–500 km lends support to the concept of whole-moon melting. The mare basalt source regions crystallize following prior crystallization of olivine, orthopyroxene and plagioclase (as is shown by the ubiquitous Eu depletion in the basalts). No evidence of the presence of garnet appears in the REE patterns of the mare basalts, indicating that Ca and Al were not present at depth in sufficient amounts to crystallize garnet as would be the case for undifferentiated lunar material. Probable convective overturning and sinking of dense cumulates forming late in the crystallization sequence has occurred. Very large volumes of olivine and orthopyroxene, which crystallized earlier, must be present at greater depths. It is thus a reasonable assumption that the Moon was melted to depths considerably in excess of 400–500 km. In summary, the evidence which requires effectively whole-moon differentiation and hence a "magma ocean" includes (a) the presence of a feldspathic crust comprising 10% of lunar volume, (b) complementary highland and mare basalt Eu anomalies and general geochemical characteristics, (c) enrichment of incompatible elements in the crust, (d) the isotopic uniformity of KREEP, and (e) the isotopic evidence for early differentiation of mare basalt source regions, completed by about 4.4 aeons.

5.11.2 How Long did the Early Highland Crust Take to Evolve?

There is a considerable body of evidence which suggests that lunar differentiation occurred as early as 4.47 aeons [144]. One interpretation of the isotopic data is that early lunar magmatism involving highly fractionated sources continued for at least 200 million years [156]. As long as the bombardment of the highlands continued, with projectiles capable of excavating craters and basins greater than 150 km in diameter, it is reasonable to expect continued reworking of the highland crust.

Further insights into this question are gained from calculations about the time taken for the magma ocean to solidify [162]. The time required depends on the thickness of the crust which develops, since heat loss is then controlled by conduction through the solid crust. Early estimates forbade a molten Moon by giving timescales for conductive cooling that exceeded the age of the solar system. Later estimates swung to the other extreme when the importance of loss of heat by convective processes began to be realized. Estimates for the solidification time of a 200-km thick magma ocean are now about 10^7–10^8 years, one or two orders of magnitude lower than the original estimates. Various unknown factors beset these calculations. The thickness and rate of growth of the crust is uncertain, and since this is occurring (from the isotopic evidence) at about 4.4 aeons, a heavy bombardment was continually breaking up the crust. The diameter of planetesimals following planetary condensation

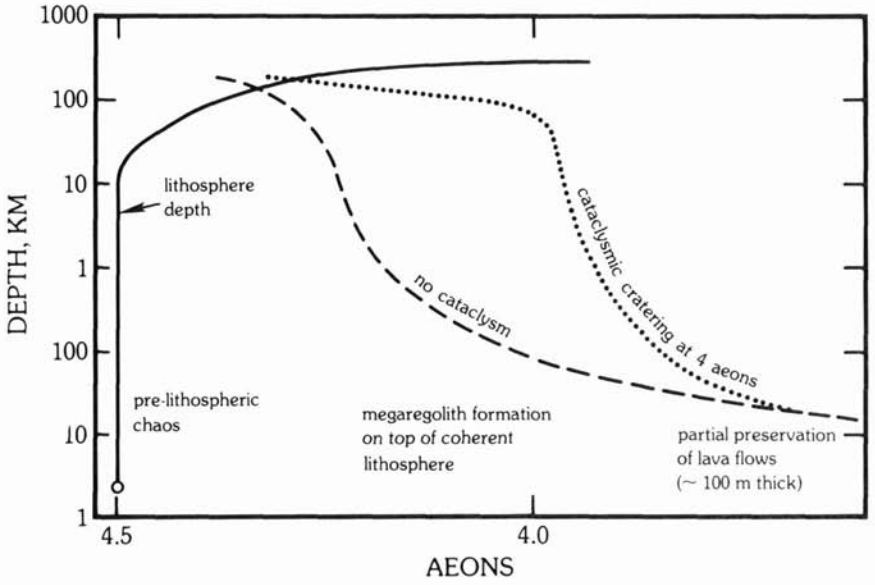

5.32 The relationship between cratering history and the growth of the lunar crust, according to Hartmann [96]. The competition between formation of coherent lithosphere (magma ocean solidification in absence of cratering, solid curve) and pulverization of lithospheric layers (dotted and dashed curves). In first 10^8 yr. or so (before cross-over of curves) cratering would be so intense that any lithospheric crust would be 100% penetrated on a timescale short compared to the solidification time. Later, solid lithosphere layers could form at the bottom of a megaregolith tens of kilometers (10^2 km?) deep, probably partially welded into coherent breccia. Plausibly thick lava flows on the surface would avoid complete pulverization only after about 3.8 to 4.2 aeons ago.

has been estimated to be about 10 km [163]. These will punch through the growing crust, and hence promote radiative cooling. If no crust is present, heat loss by radiation will cause the magma ocean to crystallize in a few decades [164, 165]! Accordingly, the meteoritic flux rate is an important controlling factor on cooling rates. The isotopic data (see Section 6.5) show that the source regions of the mare basalts were closed by 4.4 aeons (i.e., crystallized and cooled to temperatures below which no isotopic redistribution occurs). At this time, the surface crust was still being rapidly destroyed by the meteorite bombardment (the so-called stonewall effect [166, 167]) (Fig. 5.32). Any rock which crystallized at depths of 100 km at 4.5 aeons would be destroyed rapidly. The intense early cratering would inhibit formation of any coherent igneous rock, and so the highlands probably began as a megaregolith tens of kilometers deep [166]. Plagioclase would have to comprise ~80% of the crust if it were to float [157] (melt density = 2.83 gm/cm^3); accordingly, plagioclase would dominate the early crust. Before plagioclase can crystallize, at least 50% of the olivine must have crystallized and the temperature must have dropped by 400° C [165]. Thus, a solid conducting crust will not grow until the temperature drops below about 1150° C. This will be continually broken up by the raining planetesimals down to ages of about 4.2 aeons, long after the deeper parts have frozen. Accordingly, there is little problem with heat loss, since a solid crust, through which heat can only be lost by conduction, will not be established until after much of the crystallization of the magma ocean is completed.

The evidence is consistent with models which call for rapid crystallization of the crust before 4.3 aeons, breakup of this crust by projectiles to about 4.2 aeons, and resetting of ages down to 3.80 aeons by the large basin-forming impacts.

5.11.3 Crystallization History of the Lunar Crust

A possible sequence of events is as follows: Crystallization of bulk moon composition begins in the magma ocean. Olivine crystallizes until the olivine-plagioclase peritectic line is reached at which point plagioclase begins to crystallize. Calcium-rich plagioclase (anorthosite) will float in the dry lunar magma [168] although it would sink in a terrestrial wet magma. Thus, plagioclase floats to begin the formation of the highland crust. It is very uniform in composition (Section 5.4.1). Some intercumulus liquid is trapped at this point, and differentiates to low Mg/(Mg + Fe) values, typical of the anorthosites. The composition of the liquid where the plagioclase appears is that of low-K Fra Mauro basalt (with about 10–15 ppm Sm = 40–60 times chondritic REE values or 18–26 times bulk moon compositions). Crystallization continues with clinopyroxene joining the crystallization sequence. Feldspar cumulates continue to accrete. The difference between this well-ordered

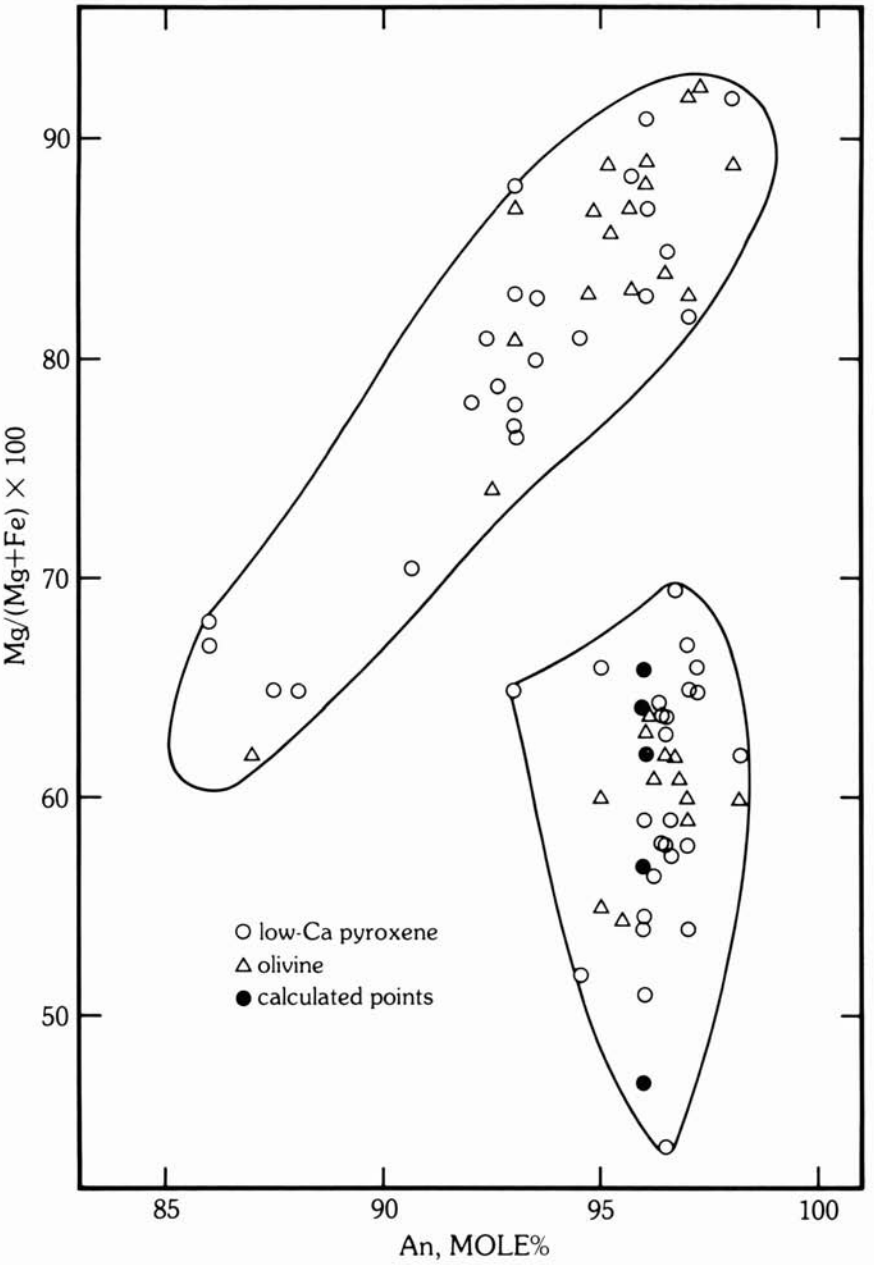

5.33 The relation between the anorthite content of plagioclase and the Mg number in co-existing mafic minerals in lunar highland samples. Similar trends are shown in the banded zone of the terrestrial Stillwater intrusion, except that the gap between the lunar trends is filled [169]. (Courtesy Linda Raedeke and Stuart McCallum.)

crystallization sequence and the actual situation is that there is a continuing infall of planetesimals of whole moon composition since the siderophile element content is low, excluding a meteoritic component. These remix, remelt, add heat, and generally create an extremely complex picture in detail. In some areas, the already solidified crust is remelted, and recrystallizes. Longhi [156] has described such scenarios. No rocks survive in the near-surface environment until the crust reaches a thickness of 1–10 km, with this stage being as late as 4.2 aeons or even younger [166]. The so-called stonewall effect operates until that time. Although the surface of the Moon is in turmoil, crystallization can proceed more quietly at depth and the zoned cumulate source regions, from which the mare basalts would subsequently be derived, escape the bombardment. Thus, the isotopic systematics of the mare basalt source regions are likely to exhibit more regularities than those in the battered and reworked highland crust. The impacting bodies may induce convective overturn in the magma ocean, and cause rafts of dense zones of accumulating crystals (e.g., ilmenite-rich zones later to be the source regions for the high-Ti basalts) to sink to the bottom of the magma ocean.

The most direct terrestrial analogue to the lunar highlands appears to be the Stillwater Intrusion [169], although useful constraints come from the study of other layered intrusions such as the Skaergaard [170]. Particular insights have come from the concept of cumulus and intercumulus models for crystallization involving trapped liquids. None of the terrestrial examples remotely approaches the scale of the lunar magma ocean, and differences between lunar and terrestrial oxidation states affect the behavior of elements such as Fe and Cr. The absence of water on the Moon is another major difference affecting many properties. The most significant of these appears to be the demonstration that plagioclase (anorthite) will float in anhydrous magmas parental to the lunar crust [168]. An important contribution from the Stillwater studies has been the demonstration that two apparently diverse fractionation trends can develop during crystallization of a single magma. Such trends were observed in the lunar highland samples (Fig. 5.33)[171, 172], which draws attention to a steep decrease in $Mg/(Mg + Fe)$ while the An content of the plagioclase remained effectively constant. This behavior is the reverse of that observed in terrestrial fractional crystallization, where the An content of feldspar should decrease with decreasing $Mg/(Mg + Fe)$. The same two trends have been observed in the Stillwater crystallization sequence [169]. In this example, only one magma is involved, since widely separated samples possess the same initial Nd isotopic ratios [173]. Sm-Nd data are lacking in the anorthosites at present. The explanation for the two trends in the Stillwater is as follows: the vertical trends of $Mg/(Mg + Fe)$ with relatively constant An content are ascribed to the crystallization of intercumulus liquid trapped in a plagioclase rich crystal mush. The abundance of plagioclase buffers the An composition (in the "middle" BZ). The other conventional trend, in the upper

and lower "banded" zones of the Stillwater, is the result of normal fractional crystallization, with resulting decrease of Mg/(Mg + Fe) and An content (Fig. 5.33).

The same effects on the Moon are shown by the vertical trend exhibited by anorthosites, noritic anorthosites and troctolitic anorthosites (the Mg suite) from the Apollo 15 and 16 missions. The noritic troctolites of Apollo 15 and 17 show the effect of conventional fractional crystallization. Various granulitic impactites fall between the two trends [174]. The major remaining questions focus on whether one magma or two are involved on the Moon. In the case of the Stillwater Intrusion, these trends have developed during the crystallization of one magma. The question is partly semantic, partly on whether the "gap" in the lunar plot (Fig. 5.33) is real or will be filled in by later data, and partly depends on trace element evidence.

The dunite (74215), which plots on the evolved trend, resembles the anorthositic suite. The complexity of magma ocean crystallization, the continuing bombardment, the trapping of intercumulus liquids all contribute to masking the overall simplicity of the crystallization patterns. The initial $^{87}Sr/^{86}Sr$ ratios of the anorthosites may be slightly older. All this constitutes evidence for prior crystallization of anorthosites.

Insights can be gained from Sc/Sm and Ti/Sm relationships among the anorthosite and the Mg rich suites (Fig. 5.34). The former rocks are products of direct crystallization of the magma ocean, involving removal of olivine and pyroxene crystallization before reaching plagioclase saturation. The anorthosites and Mg-suite are clearly separated on Ti/Sm and Sc/Sm plots. In both cases, the anorthosites plot nearer to chondritic (and whole moon) ratios. Titanium, Sm (= REE) and Sc are all refractory elements and have chondritic ratios in the bulk Moon. The depletion in Ti in the Mg suite indicates that ilmenite has been removed, while the Sc depletion indicates removal of pyroxene. Ilmenite is not, however, a liquidus phase in the Mg suite. This paradox can be explained by the mixing of a primitive component, with high Mg/(Mg + Fe) values, and a differentiated component, from which ilmenite has already been removed. Mafic minerals are not abundant in the anorthosites, but there are some mafic members of the Mg suite (61224, 67667) which have Ti/Sm and Sc/Sm ratios more like the anorthosites. The dunite has near chondritic values for these ratios so that it is an equivocal member of the Mg suite.

Trace element evidence in olivines and plagioclases is consistent with differing crystallization histories for the two groups. Thus, the plagioclases from the anorthosites show a very restricted range in composition [175], but those from other rock types have a wide range in values, which is indicative of an origin either as separate events, perhaps in small intrusions, or by mixing. Strontium shows a positive correlation with sodium, the reverse of that expected, but explicable if other minerals (e.g., olivine or orthopyroxene) are

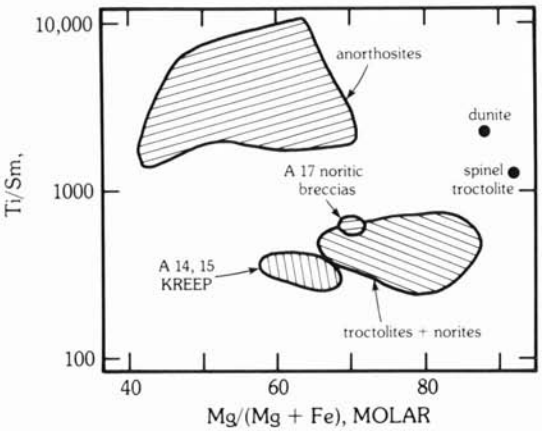

5.34a The relationship between Mg number and Ti/Sm ratios in lunar highland rocks. Figure shows the difference between the anorthosites which have Ti/Sm in the chondritic range, and the rocks of the Mg suite (troctolites and norites). The latter are characterized by high Mg numbers (indicative of a primitive undifferentiated composition) and low Ti/Sm ratios (Sm serves as an index for the other rare-earth and incompatible elements). The Mg suite rocks and KREEP have similar Ti/Sm ratios, indicative of a highly fractionated source. This combination of primitive and fractionated chemical characteristics is typical of KREEP and the Mg suite. It is here interpreted as evidence for mixing of primitive and late stage material during the raining bombardment of the highland crust (cf. Fig. 5.32). (Courtesy G. A. McKay.)

crystallizing simultaneously. All lunar plagioclases, including those from mare basalts, lie on this trend. The uniformity of the trace element contents of plagioclase from the anorthosites is consistent with a common origin, and hence supportive of the magma ocean concept.

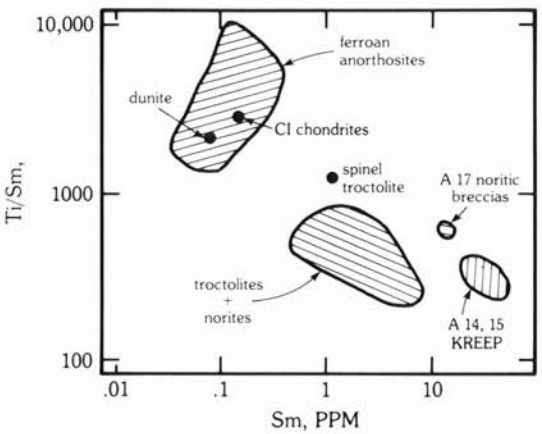

5.34b The relationship between Sm abundances (representative of REE and incompatible elements generally) and the Ti/Sm ratio (cf. Fig. 34a). Note that the dunite plots among the anorthosites, and both have C1 type abundances. The troctolites and norites of the Mg suite show the highly fractionated geochemical characteristics of KREEP, with marked depletion in Ti interpreted as being due to prior removal of ilmenite. This is not petrologically feasible because of the primitive unfractionated major element compositions and Mg numbers. A mixing scenario is is preferred to explain the geochemical paradoxes in these two diagrams. (Courtesy G. A. McKay.)

Similar relationships are noted for the trace element content of olivine. Olivines from anorthosites have consistently lower contents of minor elements than those from other rock types [176], except for Ca and Mn, although such olivines have high Fe contents, with Fo values ranging from 66 down to 45. Olivines from other rocks show a higher and more variable concentration of these elements (Al, P, Ti, Cr). Chromium is notably low in olivines from anorthosites and rarely exceeds 50 ppm. In the Mg-rich rocks, Cr is typically about five times higher, consistent with the more primitive nature of portions of the Mg suite.

The complexity of these crystallization sequences in detail have resulted in many models, in particular to account for the high Mg suite. Remelting of early basic cumulates would provide high Mg/(Mg + Fe) [177], but not the highly fractionated REE patterns. Contamination of solid rock by KREEP does not explain why the anorthosites are not contaminated. The Mg suite shows many of the characteristics of a differentiated suite, as is well displayed in the An versus Mg/(Mg + Fe) diagram.

A viable but complex hypothesis appears to be magma mixing [178]. The unfractionated nature of the major elements (Mg/Mg + Fe) is due to a primitive magma, while the addition of a relatively small amount of highly fractionated residual liquid from the magma ocean dominates the trace element characteristics (Fig. 5.35). One problem is that very little primitive magma is available when the residual liquid stage is reached. Rare-earth element patterns will be flatter than KREEP due to dilution with "chondritic" patterns, although the KREEP abundances are large enough to swamp most of this effect.

Another scenario is that many of the rocks of the Mg suite have crystallized subsequent to the main magma ocean crystallization as small intrusions within the crust, thus explaining many of their trace element characteristics [26, 56, 97, 99]. The data are not yet capable of distinguishing between these alternatives, but it is judged here that the mixing scenarios, induced by the effects both of the bombardment and the pervasive infiltration of late differentiated liquids into the crust is the more reasonable scenario.

The origin of KREEP has been commented upon several times in this chapter. There is an extensive debate on this subject (e.g., [179–183]). Two important facts need to be considered. First, extremely high concentrations of the incompatible elements are present (Section 5.4.3) with the concentrations of the REE up to 700 times chondritic abundances [78]. The second is that the Sm-Nd isotopic systematics [73] are uniform on a moon-wide basis (Fig. 5.36). The Nd isotopic evolution in KREEP is complementary to that of the high-Ti basalts (Section 6.4) (Fig. 5.37). Variations in Rb-Sr isotopic systematics are probably due to differential movement of volatile Rb in KREEP breccias during impacts (Section 5.5).

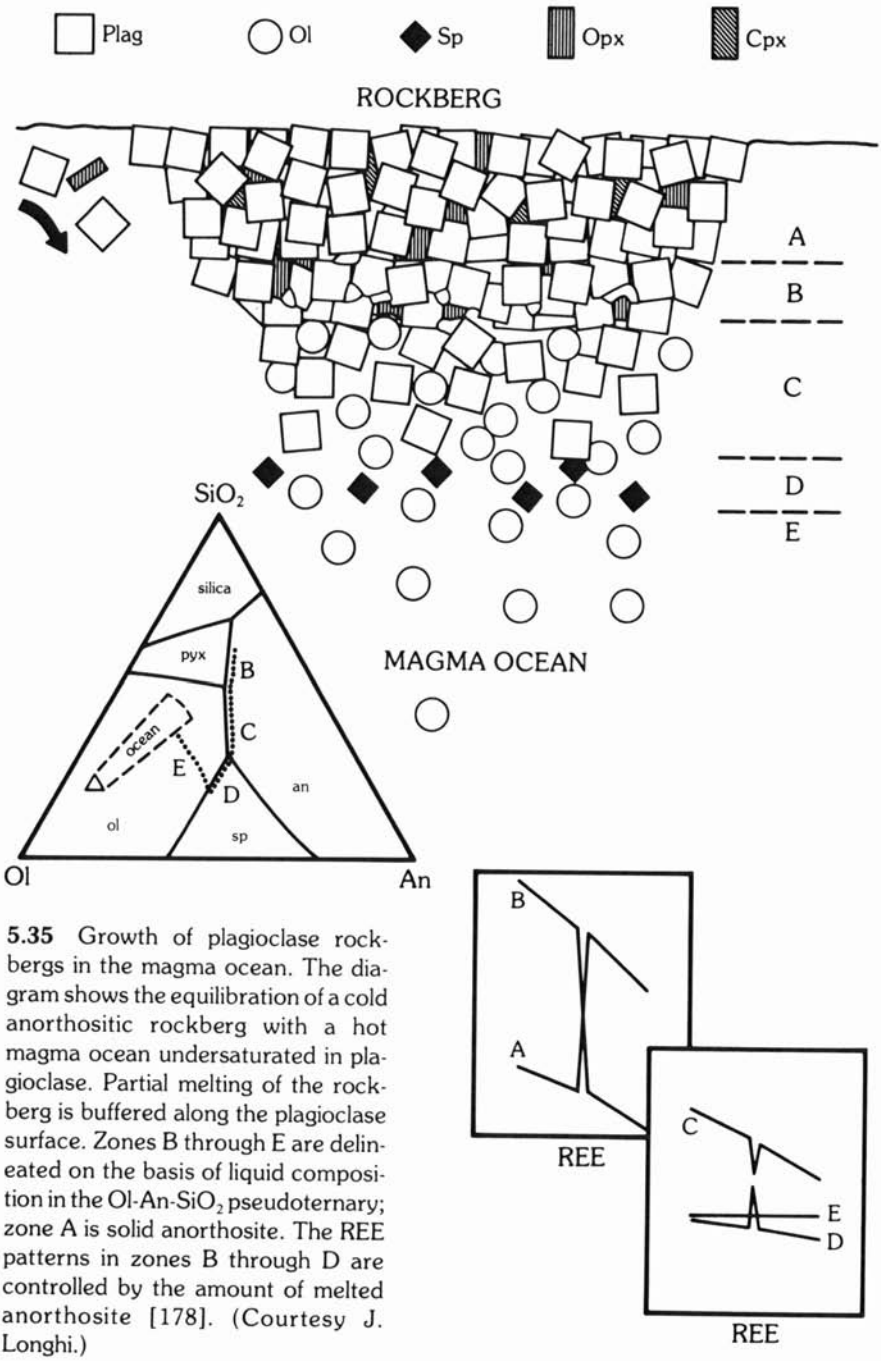

5.35 Growth of plagioclase rockbergs in the magma ocean. The diagram shows the equilibration of a cold anorthositic rockberg with a hot magma ocean undersaturated in plagioclase. Partial melting of the rockberg is buffered along the plagioclase surface. Zones B through E are delineated on the basis of liquid composition in the Ol-An-SiO_2 pseudoternary; zone A is solid anorthosite. The REE patterns in zones B through D are controlled by the amount of melted anorthosite [178]. (Courtesy J. Longhi.)

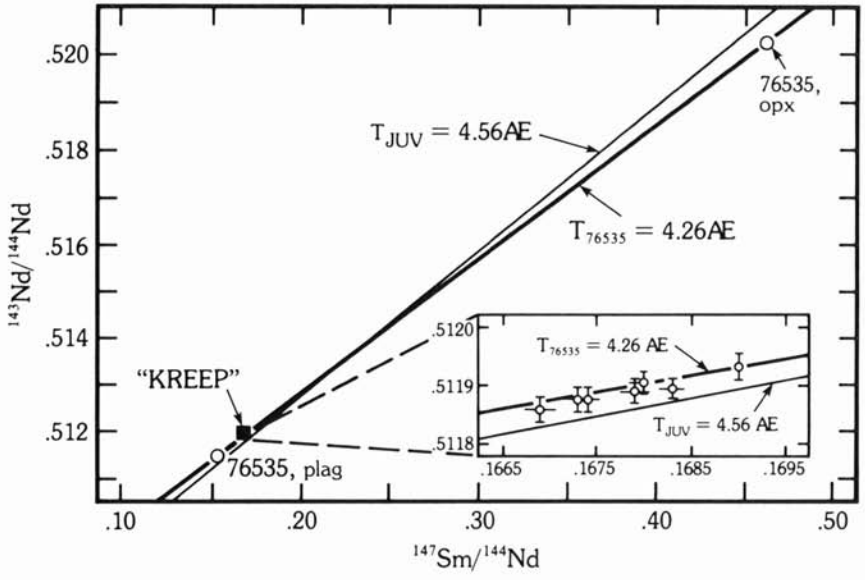

5.36 Samarium-neodymium systematics of "KREEP" samples from different Apollo sites. The Sm-Nd evolution diagram indicates the remarkably close clustering of Sm-Nd data of KREEP samples. Resolution of the points from the 4.56 AE reference isochron for Juvinas and the rough alignment along the 4.26 AE reference isochron obtained from troctolite 76535 suggests a close relationship between the Sm/Nd system of KREEP and other lower crustal materials [73]. (Courtesy G. W. Lugmair.)

A basic premise of the model adopted here is that KREEP originates as the final melt residuum following crystallization of the magma ocean. The volume may be about one or two percent. This low density iron-rich and trace-element-rich residual melt (4.4 aeons) invades the crust [184] where it is mixed in by the continuing bombardment with the later products of magma ocean crystallization.

5.12 The Crust of the Earth

There is a primary division into oceanic and continental crusts. The oceanic crust is young (< 200 m.y.), comprised primarily of basalt and is recycled into the mantle. It may serve as a model for conditions in the earliest Archean. The continental crust, in contrast, is old and complex, but has grown throughout geological time. The oldest rocks have ages of 3.8 aeons, postdating the decline in the massive planetesimal bombardment. Is there any sign of a primitive crust analogous to that of the moon? There is no isotopic or

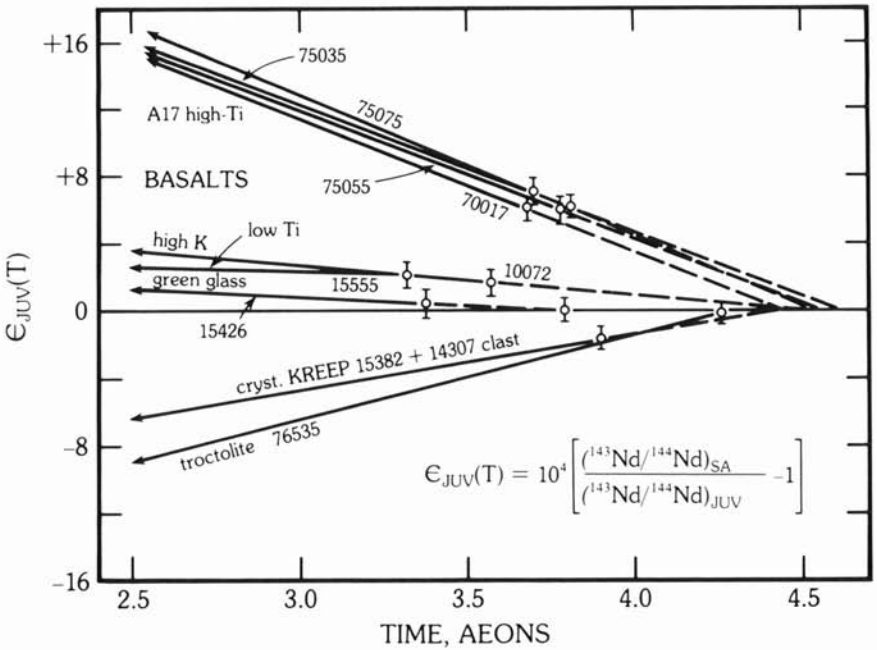

5.37 Differentiated ^{143}Nd evolution for highland samples (KREEP and troctolite) and mare basalts [73]. This diagram clearly shows the early differentiation of the Moon and the development of separate source reservoirs for mare basalts. The time of the early differentiation is not well resolved by the Sm-Nd systematics, except that it is early.

chemical evidence of the existence of such a crust. The principal information comes from Rb-Sr and Sm-Nd isotopic systematics, which indicate derivation of the present crust from primitive mantle, and the absence of recycled material of continental composition [185].

The composition of the upper continental crust, is approximately that of granodiorite [186]. There is too high a content of the radioactive heat producing elements, K, U, and Th in the accessible upper crust for this composition to persist to depths in excess of 10–15 km. The composition of the whole crust, down to the Mohorovičić discontinuity at 40 km is thus model dependent, as is that of the inaccessible lower crust. A reasonably close approximation to the bulk composition is provided by that of the voluminous silica-rich island arc volcanic rocks. These are derived, at subducting plate boundaries, from the mantle and represent the only reasonable present-day source of igneous rocks, both voluminous and silica-rich, to be viable candidates for additions to the continental crust. There is a considerable body of geological evidence indicating that the latter stages of continental growth involved lateral accretion of

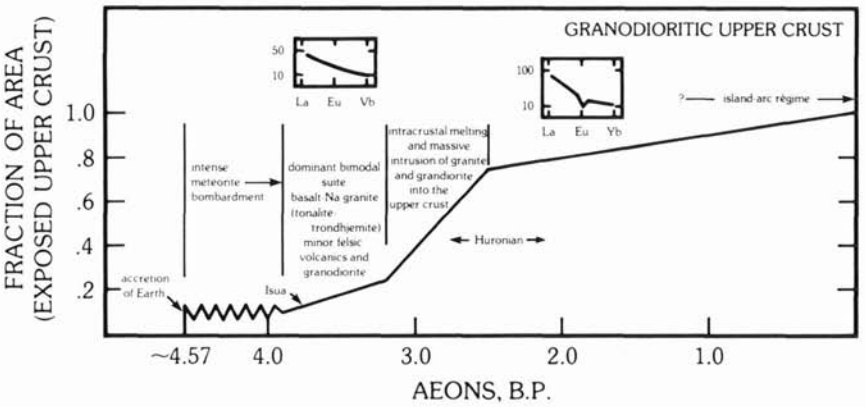

5.38 Model for the evolution of the terrestrial continental crust during geological time. Principal events of crustal evolution are indicated, as well as average REE patterns for the *upper* crust, as derived from sedimentary rock data [186].

island-arcs. However this model is only valid so long as the present-day plate-tectonic regime was operating. There is a growing body of isotopic evidence, principally from the Sm-Nd system, which indicates that a massive increase in the volume of continental material occurred in the period between 3.0 and 2.5 aeons, at the close of the Archean [187].

Figure 5.38 shows a recent attempt to model the growth rate of the crust. The largely episodic nature of this event in the late Archean raises several questions. Although the island-arc model is valid back to beyond 1.0 aeon, it is probably not an appropriate model for the massive late Archean additions to the continents. The Archean crustal composition is not very different to that of the present day total crust, except that it may be higher in Ni and Cr. Within about 200 m.y. of the massive episodic additions from the mantle, large scale intra-crustal partial melting produced the granodioritic upper crust, leaving a depleted lower crust. The ubiquitous depletion in the rare earth element, Eu, observed in upper crustal sedimentary rocks, was produced by this process. This relative concentration is due to differences in ionic size and valency from those of common mantle cations, so that the most "incompatible" elements (e.g., Cs, Rb, K) are the most strongly concentrated in the crust. About 30% of the total mantle budget of these elements have been so concentrated in the continental crust. This accordingly sets a lower limit on the volume of the mantle which has been involved. The extraction of these elements has led to the formation of "depleted" mantle. The geochemical characteristics of Mid-Ocean-Ridge basalts (MORB), which exhibit relative depletion of light REE, K, Rb, etc. as well as the isotopic systematics (particularly Sm-Nd) indicate that they are derived from such regions.

The thermal regime responsible for the evolution of the terrestrial crust may be briefly commented upon. Heat production in the early Archean was at least three times its present value. Whether the surface heat loss was substantially greater is unknown. At present 50% of the surface heat loss occurs at mid-ocean ridge (spreading plate boundaries) [188]. Either faster plate movement or many more plates are needed in the Archean. The continental growth model outlined here is consistent with a steady temperature buildup in the mantle (heat production exceeding heat loss) until about 3.0 aeons, when massive mantle melting and production of continental crust ensues. This event transfers substantial quantities of K, U, and Th into the crust. Intra-crustal melting, producing granodiorite, occurs within a few hundred million years of this event. The massive increase in continental volume changes the tectonic style, and initates the present regime of linear style tectonics and subduction zones. About 80% of continental volume is thus emplaced by about 2.5 aeons, and the upper continental crust has not changed in composition since that time.

It can thus be seen that there are great differences in the origin and evolution of the two planetary crusts with which we are most familiar. The lunar crust, although greatly complicated by the details of its crystallization history and the raining bombardment, results essentially from an early planetary-wide melting episode. The *upper* continental crust of the Earth is the product of at least three successive partial melting events from the mantle and lower crust.

5.13 Other Planetary Crusts

No chemical data are available for the Mercurian crust (Section 2.5), but the preservation of the record of an early intense bombardment indicates that crustal formation was completed well before 4.0 aeons. The reflectance spectra indicate a silicate surface much resembling that of the Apollo 16 soils [189], possibly indicating a composition containing less than about 5% FeO. The evidence for early differentiation and lack of global expansion reinforce the similar situation observed on the Moon.

The resemblance between the reflectance spectra of the lunar highlands and of Mercury may mean that the crust of the planet is of anorthositic gabbro composition on the average. The remote-sensing data are integrated over the whole planetary surface, and resolution of individual areas, for example the smooth plains, is not possible. No spectra typical of mare basalts have been observed [189]. Both the similarities and differences between Mercury and and the Moon are important constraints for our understanding of early solar system history.

Most of the details of the Martian crust have been discussed in Section 2.6. The evolution of the crust appears to have continued, with the eruption of basaltic lavas, until relatively recently, as indicated by the young age of Olympus Mons. The question of the elevation of the Tharsis plateau is dealt with in Section 7.6.3; whether this plateau is due to uplift or to superposition of a series of lavas is uncertain.

A comprehensive review of the Venusian crust is given by Phillips et al. [190]. The geology of Venus has been described in Section 2.7 and little can be added here. The Venera gamma-ray data indicate K/U ratios of 10^4 and abundances comparable with those in terrestrial granites (see Section 4.13).

Many details of the surface are not yet clear, e.g., the circular features on the Median Plains may be impact craters or volcanic features [191]. The age of the surface features (Section 2.7) is uncertain, but if these circular features are craters, then the plains are very old. Accordingly, the operation of plate tectonic processes at present is unlikely. The continental masses (Ishtar and Aphrodite) present major puzzles, possibly indicative of an early period of crustal evolution (see Section 7.6.3). A principal conclusion is that in many respects Venus is dissimilar to the Earth, a fact of great significance for planetary formation (Chapter 9).

Little compositional evidence is available for the surface crusts of the satellites of the outer planets, and debate, for example over the surface of Io, is too speculative for much discussion here. The grooved terrains, exhibited by Ganymede and Callisto, provide some new insights into planetary crustal evolution. The former provides an excellent example.

Ganymede, the third of the four Galilean satellites of Jupiter, with a radius of 2638 km, is a little larger than Mercury. Areas of an older cratered crust are separated by younger grooved terrain. The most reasonable interpretation is that the older crust has been split, and new material injected from below (192).

Ganymede has a density of 1.99 gm/cm^3, consistent with a silicate-ice mixture. Expansion on such a planet can occur by the following mechanism. A mixture of silicate and ice accretes. The ice deep within the planet undergoes polymorphic change to higher density forms. These have densities ranging from 1.16 to 1.66 gm/cm^3. The initial planetary crust is heavily cratered at times earlier than 4000 million years. Heating on a longer time scale due to the radioactive elements K, U and Th present in the silicates causes melting in the ice in the interior. The water migrates outward.

The change from high density ice to lower density water provides an expansion of the planet of up to 5–7%. The water refreezes near the surface in the low density Ice I polymorph, after disrupting the older frozen crust. Thus we find some evidence for minor expansion in Ganymede. This is explicable on the known properties of ice and it is not necessary to invoke any more mysterious mechanism (192).

References and Notes

1. Lyell, C. (1830) *Principles of Geology*, Vol. 1, John Murray. Lyell commented (p. 82) that a race of intelligent amphibia would have arrived much sooner at a proper understanding of geological processes than land-dwelling species. The truth of this comment was fully appreciated with the development of the plate tectonic hypothesis.
2. Windley, B. W. (1977) *The Evolving Continents*, Wiley.
3. *New Yorker*. May 11, 1981, p. 2.
4. Haines, E. L., and Metzger, A. E. (1980) *PLC 11*: 689; Bielefeld, M. J., et al. (1976) *PLC 7*: 2661.
5. Metzger, A. E., et al. (1977) *PLC 8*: 978.
6. Davis, P. A. (1980) *JGR*. 85: 3209.
7. Bills, B.G., and Ferrari, A. J. (1977) *JGR*. 82: 1306.
8. Thurber, C. H., and Solomon, S. C. (1978) *PLC 9*: 3481.
9. Kaula, W. M., et al. (1972) *PLC 3*: 2189.
10. Phillips, R. J., and Lambeck, K. (1980) *Rev. Geophys. Space Phys.* 18: 27.
11. Airy, G. B. (1855) *Phil. Trans. Roy. Soc. London* B145: 101.
12. Pratt, J. H. (1855) *Phil. Trans. Roy. Soc. London* B145: 53.
13. Lingenfelter, R. E., and Schubert, G. (1973) *Moon*. 7: 172.
14. Aggarwal, H. R., and Oberbeck, V. R. (1979) *PLC*. 10: 2689.
15. Thompson, T. W., et al. (1979) *Moon Planets*. 21: 319; (1980) *Lunar Highlands Crust*, p. 175; (1981) *Icarus*. 46: 201.
16. See Section 5.10.3.
17. Wolfe, E. W., and Bailey, N. G. (1972) *PLC 3*: 15.
18. Mattingly, T. K., and El-Baz, F. (1973) *PCL 4*: 55.
19. Spudis, P. D., and Ryder, G. (1980) *Multi-ring Basins*, p. 86.
20. Wilhelms, D. E. (1980) Apollo 16 Workshop, 10; (1979) LPS X: 1251.
21. Hawke, B. R., and Head, J. W. (1980) *Multi-ring Basins*, p. 36.
22. Stöffler, D., et al. (1980) *Lunar Highlands Crust*, p. 51; Stöffler, D., et al. (1979) *PLC 10*: 639.
23. McKinley, J. P., et al. (1981) LPS XII: 691.
24. Norman, M. D. (1981) LPS XII: 776.
25. a) Poikilitic textures comprise large host crystals enclosing many smaller crystals of other phases.
    b) Ophitic textures comprise elongated feldspar crystals embedded in pyroxene or olivine.
    Both terms are good examples of jargon.
26. James, O. B. (1980) *PLC 11*: 365.
27. Stewart, D. B. (1975) LS VI: 774.
28. Warner, J. L., et al. (1977) *PLC 8*: 2051.
29. Stöffler, D., et al. (1979) LPS X: 1177.
30. Grieve, R. A. F. (1980) *Lunar Highlands Crust*, p. 187.
31. Miller, D. S., and Wagner, G. A. (1979) *EPSL*. 43: 351.
32. Blanchard, D. P., and Budahn, J. R. (1979) *PLC 10*: 803.
33. James, O. B., and McGee, J. J. (1980) *PLC 11*: 67.
34. Ryder, G., and Taylor, G. J. (1976) *PLC 7*: 1741.
35. Ryder, G. (1980) *PLC 10*: 575.
36. Vaniman, D. T., and Papike, J. J. (1979) *GRL*. 5: 429.
37. *Basaltic Volcanism* (1981) Section 1.2.10.
38. Irving, A. J. (1975) *PLC 7*: 363.
39. Prinz, M., and Keil, K. (1977) PCE 10: 215.

40. Meyer, C. E. (1977) PCE 10: 506.
41. Warren, P. H., and Wasson, J. T. (1977) *PLC 8*: 2215; (1978) *PLC 9*: 185.
42. Norman, M. D., and Ryder, G. (1979) *PLC 10*: 531.
43. Phinney, W. C., and Simonds, C. H. (1977) *Impact Cratering*, p. 771.
44. Grieve, R. A. F., et al. (1977) *Impact Cratering*, p. 791; Floran, R. J., et al. (1981) *JGR*. In press.
45. Meyer, C. (1978) *PLC 9*: 1551.
46. Reid, A. M., et al. (1977) *PLC 8*: 2321.
47. Taylor, S. R., and Bence, A. E. (1975) *PLC 6*: 1121; Taylor, S. R. (1976) *PLC 6*: 3461.
48. Wänke, H., et al. (1977) *PLC 8*: 2237.
49. Ryder, G. (1979) *PLC 10*: 561.
50. Haskin, L. A. (1979) Lunar Highlands Crust Abstracts, 49.
51. The ratio Eu/Eu* is a measure of the depletion or enrichment of europium relative to the neighboring rare-earth elements, samarium and gadolinium. Eu is the measured elemental abundance in the sample; Eu* is the theoretical concentration for no Eu anomaly, and is calculated by assuming a smooth REE pattern in the region Sm-Eu-Gd. Values of Eu/Eu* less then 0.95 indicate depletion, and values of greater than 1.05, enrichment of europium relative to the neighboring REE.
52. Ryder, G. (1979) *PLC 10*: 560.
53. Wänke, H., et al. (1977) *PLC 8*: 2191.
54. McKay, G. A., et al. (1978) *PLC 9*: 661.
55. Garrison, J. R., and Taylor, L. A. (1980) *Lunar Highlands Crust*, p. 395.
56. Wasson, J. T., et al. (1977) *PLC 8*: 2237.
57. The simpler term "Anorthosite" is preferred to usages such as Ferroan Anorthosite, with its slightly horsey overtones. Although it is useful to note that the accompanying minerals have high Fe/Mg ratios consistent with crystallization from a magma ocean, the prefix appears to be unnecessary. Smith, J. V., and Steele, I. M. (1976) *Amer. Mineral.* 61: 1074.
58. James, O. B. (1980) *PLC 11*: 365.
59. Norman, M D., and Ryder, G. (1979) *PLC 10*: 531.
60. Papanastassiou, D. A., and Wasserburg, G. J. (1972) *EPSL*. 17: 52; (1975) *PLC 6*: 1467.
61. Schaeffer, O. A., and Husain, L. (1974) *PLC 5*: 1541.
62. Lugmair, G. W., et al. (1976) *PLC 7*: 2009.
63. Papanastassiou, D. A., and Wasserburg, G. J. (1976) *PLC 7*: 2035.
64. Dowty, E., et al. (1974) *EPSL*. 24: 15.
65. Prinz, M., and Keil, K. (1977) PCE 10: 215.
66. Laul, J. C., and Schmitt, R. A. (1975) *PLC 6*: 1231.
67. Dymek, R. F., et al. (1975) *PLC 6*:301.
68. Taylor, G. J., et al. (1979) *Lunar Highlands Crust*, p. 166.
69. Roedder, E., and Weiblen, P. W. (1970) *PLC 1*: 801.
70. Glass, B. P. (1976) LS VII: 296.
71. Arnold, J. R. (1972) *Apollo 15 PSR*, p. 16-1.
72. Hawke, B. R., and Head, J. W. (1978) *PLC 9*: 3285.
73. Lugmair, G. W., and Carlson, R. W. (1978) *PLC 9*: 689; (1978) *EPSL*. 39: 349; (1979) *EPSL*. 45: 123.
74. Taylor, S. R., and Jakes, P. (1974) *PLC 5*: 1287.
75. Taylor, S. R. (1975) *Lunar Science: A Post-Apollo View*, Pergamon, Fig. 7.2.
76. Warren, P. H., and Wasson, J. T. (1979) *Rev. Geophys. Space Phys.* 17: 73.
77. Meyer, C. (1977) PCE 10: 239.

78. Nyquist, L. E., et al. (1977) LS VIII: 738.
79. Walker, D., et al. (1972) *PLC 3*: 797; Hess, P. C., et al. (1977) *PLC 8*: 2357.
80. Irving, A. J. (1975) *PLC 6*: p. 363.
81. Ryder, G. J., and Spudis, P. D. (1980) *Lunar Highlands Crust*, p. 353.
82. Ryder, G., and Taylor, G. J. (1976) *PLC 7*: 1741.
83. Charette, M. P., et al. (1977) *PLC 8*: 1049.
84. Metzger, A. E., et al. (1979) *PLC 10*: 1701.
85. McKay, G. A., and Weill, D. F. (1977) *PLC 8*: 2339.
86. Jovanovic, S., and Reed, G. W. (1974) *PLC 5*: 1685.
87. Taylor, L. A., et al. (1974) *PLC 5*: 743.
88. Nunes, P. D., and Tatsumoto, M. (1973) *Science*. 182: 916.
89. Taylor, L. A., and Burton, J. C. (1976) *Meteoritics*. 11: 225.
90. Cirlin, E. H., and Housley, R. M. (1980) *PLC 11*: 349.
91. Cirlin, E. H., and Housley, R. M. (1981) *PLC 12*: 529.
92. Hunter, R. H., and Taylor, L. A. (1981) LPS XII: 488.
93. Gros, J., et al. (1976) *PLC 7*: 2403.
94. Hertogen, J., et al. (1977) *PLC 8*: 17.
95. Janssens, M. J., et al. (1978) *PLC 9*: 1537.
96. Hartmann, W. K. (1980) *Lunar Highlands Crust,* p. 155.
97. Warren, P. H., and Wasson, J. T. (1977) *PLC 8*: 2215; (1978) *PLC 9*: 185; (1979) *PLC 10*: 583; (1980) *PLC 11*: 431.
98. Norman, M. D., and Ryder, G. (1979) *PLC 10*: 531.
99. Warren, P. H., and Wasson, J. T. (1980) *PLC 11*: 431.
100. James, O. B. (1973) USGS Prof. Paper 841.
101. Delano, J. W., and Ringwood, A. E. (1978) *PLC 9*: 111.
102. Grieve, R. A. F. (1980) *Lunar Highlands Crust*, p. 189.
103. Ryder, G., et al. (1980) *PLC 11*: 471.
104. Taylor, L. A., et al. (1976) *PLC 7*: 837.
105. Norman, M. D., and Ryder, G. (1979) *PLC 11*: 531.
106. Wolf, R., et al. (1979) *PLC 10*: 2107.
107. Adler, I., et al. (1972) NASA SP-289, 17-1; (1972) NASA SP-315, 19-1.
108. Arnold, J. R., et al. (1972) NASA SP-289, 16-1; (1972) NASA SP-315, 18-1.
109. Adler, I., and Trombka, J. I. (1977) PCE 10: 17.
110. Haines, E. L., et al. (1976) IEEE Trans. Geoscience Electronics GE 15: 141.
111. Metzger, A. E., et al. (1977) *PLC 8*: 969.
112. Haines, E. L., et al. (1978) *PLC 9*: 2985.
113. Hawke, B. R., et al. (1981) LPS XII: 415.
114. Haskin, L. A. (1979) Lunar Highlands Crust Abstracts, 49.
115. Andre, C. G., and El-Baz, F. (1981) *PLC 12*: 767; Andre, C. G., et al. (1979) *PLC*: 1739.
116. Andre, C. G. (1981) *Multi-ring Basins*, p. 1.
117. Hawke, B. R., and Spudis, P. D. (1980) *Lunar Highlands Crust*, p. 467.
118. Haines, E. L., and Metzger, A. E. (1980) *PLC 11*: 689.
119. Bielefield, M. J., et al. (1976) *PLC 7*: 2661.
120. Metzger, A. E., and Parker, R. E. (1979) *EPSL*. 45: 155. The average Ti value quoted (0.8% Ti) demands a very large Fra Mauro or KREEP component and is probably about twice the correct value. They suspect an "unidentified systematic offset."
121. Galilei, G. (1610) *Nuncius Siderus*, Padua.
122. O'Keefe, J. A., and Cameron, W. S. (1962) *Icarus*. 1: 271.
123. Walter, L. S. (1965) *Ann. N.Y. Acad. Sci.* 123: 367.
124. O'Keefe, J. A., et al. (1967) *Science*. 155: 77.
125. Jackson, E. D., and Wilshire, H. (1968) *JGR*. 73: 7621.

126. Wood, J. A. (1970) *PLC 1*: 965.
127. LSPET (1970) *Science:* 2697.
128. LSPET (1971) *Science*. 173: 681.
129. Gast, P. W. (1972) *Moon*. 5: 121.
130. E.g., Anderson, D. L. (1973) *EPSL*. 18: 301.
131. Brett, P. R. (1973) *GCA*. 37: 2697.
132. Duncan, A. R., et al. (1973) *PLC 4*: 1097.
133. Reid, A. M., et al. (1974) *Moon*. 9: 141.
134. Warner, J. L., et al. (1977) *PLC 8*: 2051.
135. Wänke, H., et al. (1975) *PLC 4*: 1461.
136. Taylor, S. R., et al. (1973) *GCA*. 37: 2665.
137. See Taylor, S. R. (1975) *Lunar Science: A Post-Apollo View*, p. 245–249 for an extended discussion of the significance of inter-element correlations.
138. Spudis, P. D., and Hawke, B. R. (1981) LPS XII: 1028.
139. Parker, R. E., et al. (1980) LPS XII: 811.
140. Duncan, A. R., et al. (1973) *PLC 4*: 1108.
141. Bogard, D. D., et al. (1981) LPS XII: 92.
142. James, O. B., and Hörz, F. (1980) Apollo 16 Workshop, 20.
143. Hartmann, W. K. (1975) *Icarus*. 24: 181; (1980) *Lunar Highlands Crust*, p. 155.
144. Oberli, F., et al. (1978) LPS IX: 832; LPS X: 940.
145. Maurer, P., et al. (1978) *GCA*. 42: 1687.
146. Nyquist, L. E., pers. comm., 1981.
147. Carlson, R. W., et al. (1976) LPS XII: 126. The lherzolite has 58% olivine, 21% plagioclase, 15% orthopyroxene and 5% diopside.
148. Turner, G. (1977) PCE 10: 179.
149. Jessberger, E. K., et al. (1974) *PLC 5*: 1419.
150. Schaeffer, O. A., and Husain, L. (1974) *PLC 5*: 1541.
151. Kirsten, T., and Horn, P. (1974) *PLC 5*: 1451.
152. *Basaltic Volcanism* (1981) Chapter 7.
153. Wood, J. A. (1975) *Moon*. 14: 505.
154. Dence, M. R., et al. (1976) *PLC 7*: 1821.
155. Spudis, P. D., and Ryder, G. (1980) *Multi-ring Basins*, p. 86.
156. Longhi, J. (1980) *PLC 11*: 289.
157. Solomon, S. C., and Chaiken, J. (1976) *PLC 7*: 3229.
158. Binder, A. B. (1976) *Moon*. 16: 159.
159. Taylor, S. R. (1978) *PLC 9*: 15.
160. Herbert, F., et al. (1977) *PLC 8*: 573; (1978) *PLC 9*: 249.
161. Brown, G. M. (1978) in *Origin of the Solar System* (ed., S. F. Dermott), Wiley, p. 897.
162. Minear, J. W. (1980) *PLC 11*: 1941.
163. Goldreich, P., and Ward, W. R. (1973) *Astrophys. J.* 183: 1051. See also Section 9.2. See also Wetherill, G. W. (1981) *Ann. Rev. Astron. Astrophys.* 18: 77.
164. Herbert, F., et al. (1977) *PLC 8*: 573.
165. Solomon, S. C., and Longhi, J. (1977) *PLC 8*: 583.
166. Hartmann, W. K. (1980) *Lunar Highlands Crust*, p. 166.
167. The term is appropriate enough, with its Civil War connotations. Formed bodies of troops were destroyed by the Stonewall tactics of Jackson just as the crystallizing lunar crust was destroyed by the meteorite bombardment.
168. Walker, D., and Hays, J. F. (1977) *Geology*. 5: 425.
169. Raedeke, L., and McCallum, I. S. (1980) *Lunar Highlands Crust*, p. 133; McCallum, I. S., et al. (1981) LPS XII: 676; Steele, I. M., et al. (1981) LPS XII: 1034.
170. Wager, L. R., and Brown, G. M. (1967) *Layered Igneous Intrusions*, Oliver and Boyd.

171. Steele, I. M., and Smith, J. V. (1973) *PLC 4*: 419.
172. Roedder, E., and Weiblen, P. W. (1974) *PLC 5*: 303.
173. DePaolo, D. J., and Wasserburg, G. J. (1979) *GCA*. 43: 999.
174. Bickel, C. E., and Warner, J. L. (1978) *PLC 9*: 1629.
175. Steele, I. M., et al. (1980) *PLC 11*: 571.
176. Smith, J. V., et al. (1980) *PLC 11*: 555.
177. Norman, M. D., and Ryder, G. (1980) *PLC 11*: 317.
178. Longhi, J., and Boudreau, A. E. (1979) *PLC 10*: 2085.
179. Weill, D. F., and McKay, G. A. (1975) *PLC 6*: 2427.
180. McKay, G. A. (1978) *PLC 9*: 661.
181. Warren, P. H., and Wasson, J. T. (1979) *Rev. Geophys. Space Phys.* 17: 73.
182. Gromet, L. P., et al. (1981) LPS XII: 368.
183. Hess, P. C., et al. (1981) LPS XII: 442.
184. Palme, H., and Wänke, H. (1975) *PLC 6*: 1179; Shirley, D. N. (1981) LPS XII: 979.
185. Moorbath, S. (1978) *Phil. Trans. Roy. Soc.* A288: 401.
186. Taylor, S. R., and McLennan, S. M. (1981) *Phil. Trans. Roy. Soc.* A301: 381.
187. McCulloch, M. T., and Wasserburg, G. J. (1978) *Science*. 200: 1003.
188. Pollack, H. N. (1981) pers. comm.
189. McCord, T. B., and Clark, R. N. (1979) *JGR*. 84: 7664; *Basaltic Volcanism* (1981) Section 2.2.3.
190. Phillips, R. J., et al. (1981) *Science*. 212: 879.
191. Campbell, D. B., and Burns, B. A. (1980) *JGR*. 85: 8271.
192. Squyres, S. W. (1980) *GRL*. 7: 593.